

1-1-2017

The Effect Of Oil Palm Phenolics (opp) On Pancreatic Ductal Adenocarcinoma (pdac) In Transgenic Mouse Model

Nurul Huda Razalli
Wayne State University,

Follow this and additional works at: https://digitalcommons.wayne.edu/oa_dissertations



Part of the [Nutrition Commons](#)

Recommended Citation

Razalli, Nurul Huda, "The Effect Of Oil Palm Phenolics (opp) On Pancreatic Ductal Adenocarcinoma (pdac) In Transgenic Mouse Model" (2017). *Wayne State University Dissertations*. 1737.
https://digitalcommons.wayne.edu/oa_dissertations/1737

This Open Access Dissertation is brought to you for free and open access by DigitalCommons@WayneState. It has been accepted for inclusion in Wayne State University Dissertations by an authorized administrator of DigitalCommons@WayneState.

**THE EFFECT OF OIL PALM PHENOLICS (OPP) ON PANCREATIC DUCTAL
ADENOCARCINOMA (PDAC) IN TRANSGENIC MOUSE MODEL**

by

NURUL HUDA RAZALLI

DISSERTATION

Submitted to the Graduate School

of Wayne State University,

Detroit, Michigan

in partial fulfillment of the requirements

for the degree of

DOCTOR OF PHILOSOPHY

2017

MAJOR: NUTRITION AND FOOD SCIENCE

Approved By:

Advisor

Date

© COPYRIGHT BY
NURUL HUDA RAZALLI
2017
All Rights Reserved

DEDICATION

**To my family,
especially my parents; thank you for always believing in me.**

ACKNOWLEDGMENTS

Praise be to God, The Most Gracious, The Most Merciful for all His favors and bounties. Firstly, I would like to express my sincere gratitude to my advisor Dr. Smiti Gupta for being an excellent mentor to me. Her guidance, patience and motivation have helped me in many ways in completing this work. Besides my advisor, I would like to thank my committee members: Dr. Pramod Khosla, Dr. Ahmad Heydari and Dr. Robert Arking for their encouragement and constructive comments. My special thanks go to the past and present members of Gupta Lab: Dr. Nadia Saadat, Dr. Arvind Goja, Dr. Andreea Geamanu, Lichchavee Rajasinghe, Yan Wu, Shilpa Vemuri, Vindhyaja Srirajavatsavai, Harshini Pindiprolu, Inaam Abdul Karim, Soniya Katekar and Klair Urbin for stimulating discussions and helpful hands. Thank you for cheering me up every time and I will always remember all the great memories we have created together. I thank the Ministry of Higher Education Malaysia (MOHE) and my employer, Universiti Kebangsaan Malaysia for assisting me financially, also for all the helps offered throughout my studies. To the Malaysian and Indonesian families that I have known well for years by now, thank you for the continuous love and emotional support. I am thankful to have a second family away from home. Finally, I would like to thank my biggest supporters: my family members especially my dad, Razalli Jantan and my mom, Rokiah Ismail, my sisters Syazana Razalli and Nurul Ain Razalli, and my brother Muhammad Syafiq Razalli for their unconditional love, tireless prayers and endless support for me in whatever I do.

TABLE OF CONTENTS

Dedication	ii
Acknowledgements	iii
List of Tables	vi
List of Figures	vii
List of Abbreviations	x
Chapter 1 Introduction	13
1.1 Pancreatic cancer	13
1.2 The biology of Pancreatic Ductal Adenocarcinoma (PDAC).....	14
1.3 Clinical presentation and diagnosis	16
1.4 Treatment strategies and prognosis.....	17
1.5 Phytochemicals in cancer therapy: Oil Palm Phenolics (OPP).....	19
1.6 KPC transgenic mice as <i>in vivo</i> model to study PDAC	21
1.7 Hypothesis and specific aims.....	21
Chapter 2 Methodology	23
2.1 Animals	23
2.2 Experimental conditions and protocols.....	23
2.3 Experimental diets	24
2.4 Experimental procedures	24
2.5 MRI scans	28
2.6 Histological analyses	28
2.7 Gene expression analyses	30
2.8 Urine metabolomic analysis.....	32

2.9 Statistical analyses	34
Chapter 3 Results	35
3.1 Body weight and diet intake	35
3.2 Effect of OPP on tumor and cyst growth	39
3.3 Toxicity analysis of OPP in non-PDAC controls	44
3.4 Effect of OPP on Pancreatic Intraepithelial Neoplasia (PanIN) progression.....	47
3.5 Immunohistochemical analysis of selected tumor markers: S100P and SMAD4	53
3.6 Gene expression analysis of selected tumor markers: MMP9, Notch1 and CCND1 ...	56
3.7 Exploration of urinary ¹ H NMR metabolomic profiles of different groups	64
3.8 Identification and quantification of differential metabolites	72
3.9 Regression analysis	77
3.10 Metabolic pathway analyses following dietary OPP intervention	83
Chapter 4 Discussion	90
References	102
Abstract	113
Autobiographical Statement	115

LIST OF TABLES

Table 1: Composition of experimental diets 27

Table 2: PDAC progression of experimental animals 40

Table 3: Profiled metabolites based on urinary ¹H NMR with fold change differences of metabolite concentration between groups 73

Table 4: Significant pathways related to Notch1 expression with dietary intervention identified by MetaboAnalyst 3.0 86

Table 5: Significant pathways related to MMP9 expression with dietary intervention identified by MetaboAnalyst 3.0 87

Table 6: Significant pathways related to total PanIN count with dietary intervention identified by MetaboAnalyst 3.0 88

LIST OF FIGURES

Fig. 1: Representative structure of the three isomers of caffeoylshikimic acid	20
Fig. 2: Study design and experimental conditions	26
Fig. 3: Flow diagram of the study.....	36
Fig. 4: Mean body weight	37
Fig. 5: Mean daily diet intake	38
Fig. 6: Representative transverse T2-weighted MRI of KC mouse abdomen at week1 and week 5	41
Fig. 7: Representative transverse abdominal T2-weighted MRI of KG mouse that responded to chemotherapy drug at week1 and week 5	41
Fig. 8: Representative transverse T2-weighted MRI of KP mouse abdomen at week1 and week 5	41
Fig. 9: Representative transverse T2-weighted MRI of KPG mouse abdomen at week1 and week 5.....	41
Fig. 10: Effect of dietary OPP on tumor and cyst growth.	43
Fig. 11: Histological analysis of H & E stained fore stomach in control mice fed with regular diet and 5% OPP diet	45
Fig. 12: Histological analysis of H & E stained pancreatic tissue in control mice fed with regular diet and 5% OPP diet	46
Fig. 13: Representative pancreatic H&E of the three PanIN grades in KPC mice.	49
Fig. 14: Effect of dietary OPP and/or gemcitabine on total PanIN lesion count.	50
Fig. 15: Effect of dietary OPP and/or gemcitabine on different PanIN grades.	52
Fig. 16: Immunohistochemical analysis of the tumor promoter, S100P expression.	54
Fig. 17: Immunohistochemical analysis of the tumor suppressor, SMAD4 expression.	55
Fig. 18: Notch1 regulation by OPP treatment.....	57
Fig. 19: MMP9 regulation by OPP treatment.	59

Fig. 20: CCND1 regulation by OPP treatment.	60
Fig. 21: Multivariate analysis of KC and CC groups utilizing the unsupervised method, PCA. ...	63
Fig. 22: Multivariate analysis of KC and CC groups utilizing the supervised method, PLS-DA. .	64
Fig. 23: Multivariate analysis of KC group at baseline and endpoint utilizing the unsupervised method, PCA.....	66
Fig. 24: Multivariate analysis of KC group at baseline and endpoint utilizing the supervised method, OPLS-DA.....	67
Fig. 25: Multivariate analysis of KC and KP groups utilizing the unsupervised method, PCA.....	69
Fig. 26: Multivariate analysis of KC and KP groups utilizing the supervised method, PLS-DA. .	70
Fig. 27: Multivariate analysis of PDAC groups utilizing the unsupervised method, PCA.	71
Fig. 28: Urinary metabolites associated with non-PDAC controls.....	74
Fig. 29: Urinary metabolite associated with PDAC progression.....	75
Fig. 30: Urinary metabolites associated with OPP treatment.	76
Fig. 31: OPLS regression of total PDAC lesion, PanIN count with urinary ¹ H NMR profiles of the four PDAC experimental groups at end point.....	78
Fig. 32: OPLS regression of PanIN-3 lesion count with urinary ¹ H NMR profiles of the four PDAC experimental groups at end point.	79
Fig. 33: OPLS regression of Notch1 expression at end point.....	80
Fig. 34: OPLS regression of MMP9 expression at endpoint.	81
Fig. 35: OPLS regression of CCND1 expression.	82
Fig. 36: MetaboAnalyst 3.0 output illustrating the most predominant metabolic pathways correspond to OPLS regression between urinary metabolomic profiles and Notch1 expression...	86
Fig. 37: MetaboAnalyst 3.0 output illustrating the most predominant metabolic pathways correspond to OPLS regression between urinary metabolomic profiles and MMP9 expression. ...	87
Fig. 38: MetaboAnalyst 3.0 output illustrating the most predominant metabolic pathways correspond to OPLS regression between urinary metabolomic profiles and total PanIN lesion count.....	88

Fig. 39: The role of taurine in taurine and hypotaurine metabolism (KEGG database).....89

Fig. 40: Schematic diagram outlining the molecular targets and *in vivo* effect of OPP and OPP-gemcitabine combination in transgenic mouse model of PDAC 100

Fig. 41: Gemcitabine cellular metabolism and main mechanisms of action 101

LIST OF ABBREVIATIONS

ΔC_T	Delta (normalized) cycle threshold value
$^1\text{H NMR}$	Proton nuclear magnetic resonance spectroscopy
ANOVA	Analysis of one way variance
Bcl-2	B-Cell CLL/Lymphoma 2
CA 19-9	Carbohydrate antigen 19-9
CCND1	Cyclin-D1
CDK	Cyclin-dependent kinases
CDKN2A	Cyclin-dependent kinase inhibitor 2A
cDNA	Complimentary deoxyribonucleic acid
CT	Computerized tomography
C_T	Cycle threshold
dFdCDP	Gemcitabine diphosphate
dFdCMP	Gemcitabine monophosphate
dFdCTP	Gemcitabine triphosphate
dFdU	2',2'-difluoro-2'-deoxyuridine
dFdUMP	2',2'-difluoro-2'-deoxyuridine monophosphate
DNA	Deoxyribonucleic acid
dNTP	nucleotide triphosphate
DPC4	Deleted in pancreatic cancer, locus 4
ECGC	Epigallocatechin gallate
EGF	Epidermal growth factor
FID	Free induction decay
H&E	Haematoxylin and eosin

hNT	Human nucleoside transporter
IgG	Immunoglobulin G antigen
IHC	Immunohistochemistry
KEGG	Kyoto Encyclopedia of Genes and Genomes database
KPC	Kras ^{LSL.G12D/+} ; p53 ^{R172H/+} ; PdxCre ^{tg/+}
<i>K-ras</i>	V-Ki-ras2 Kirsten rat sarcoma
MMP9	Matrix metalloproteinase-9
MRI	Magnetic resonance imaging
mRNA	Messenger ribonucleic acid
NF- κ B	Nuclear factor kappa-light-chain-enhancer of activated β cell
Notch1	Notch homolog 1
NTC	Non-template control
OPLS	Orthogonal projections to latent structures regression
OPLS-DA	Orthogonal partial least squares discriminant analysis
OPP	Oil palm phenolics
PanIN	Pancreatic intraepithelial neoplasm
PCA	Principle component analysis
PDAC	Pancreatic ductal adenocarcinoma
PLS-DA	Partial least square discriminant analysis
qRT-PCR	Quantitative real-time polymerase chain reaction
RNA	Ribonucleic acid
S100P	S100 calcium binding protein P
SMAD4	Contraction of Sma and Mad (Mothers against decapentaplegic)
TGF	Transforming growth factor

TNM	Tumor-node-metastasis
VIP	Variable of projection

CHAPTER 1 INTRODUCTION

1.1 Pancreatic cancer

Pancreatic cancer is a condition in which malignant cells are found in pancreatic tissues. The pancreas is a 6-inch organ located deep in the abdomen behind the stomach with four general regions namely the head, neck body and tail. It is made up of two functional components, the exocrine and endocrine pancreas. Pancreatic acinar cells play the exocrine function by secreting digestive enzymes which are being released into a system of small ducts that lead to the main pancreatic duct. In the digestive system, pancreatic duct and bile duct are connected together releasing both pancreatic enzymes and bile into the duodenum to aid in the digestion of fats, proteins and carbohydrates. The second functional component of the pancreas is composed of small islands of cells called the islets of Langerhans. This endocrine pancreas produces hormones, mainly insulin and glucagon into the bloodstream in order to maintain the normal level of blood glucose in the body.

According to the most recent data on cancer mortality in the United States, pancreatic cancer is being ranked as the fourth leading cause of cancer-related deaths in this country[1]. Majority of pancreatic cancer cases (95%) emerge from the exocrine part of the pancreas with the most common type involving the exocrine part is pancreatic ductal adenocarcinoma (PDAC), while the remaining 5% of pancreatic cancer cases are related to endocrine pancreas[2]. Although the percentage of incidences for pancreatic cancer is the lowest among other digestive systems related cancers, it remains as one of the most fatal malignancies with only eight percent of five year survival rate. The American Cancer Society estimated that in 2016, 53070 of new cases of pancreatic cancer would be diagnosed and almost 42000 of deaths are expected due to

this disease[1]. Some of the factors that contribute to the high mortality rate include late diagnosis, early metastasis of tumors and poor response to treatments [3].

1.2 The biology of Pancreatic Ductal Adenocarcinoma (PDAC)

The cause of PDAC has been widely researched and documented to be resulted from the accumulation of genetic mutations and alterations. The consequences from these genetic changes consist of over expression of oncogenes, inactivation of tumor suppressor genes and also growth factors and their receptors being highly expressed[4,5]. In more than 95% of PDAC cases, *K-ras* mutations appeared as the most common of oncogene mutations. *K-ras* is a proto-oncogene which encodes guanine nucleotide-binding protein. It plays an important role in normal cell growth and differentiation[6,7]. Point mutations of *K-ras* oncogene in codon 12, 13 or 61 activates an abnormal increase in membrane-bound ras proteins causing an alteration of the signal transduction pathway across the membrane leading to an abnormal, uncontrolled cell growth of tumor[7]. *K-ras* mutations are believed to be involved in the early stage of pancreatic carcinogenesis[5]. P53 is a tumor suppressor gene located on the short arm of chromosome 17 that encodes a 53 kDa nuclear phosphoprotein which plays role in the negative regulation of cell growth and proliferation. This important tumor suppressor gene is known to be inactivated in pancreatic cancer[8]. Mutations of p53 gene have been reported to exist in 40-70% of pancreatic adenocarcinoma cases and it is suggested that its inactivation contributes to carcinogenesis through the inhibition of apoptosis. In contrast to *K-ras* oncogene, it is still inconclusive whether aberration of p53 involves in the early or late event in pancreatic cancer[5]. Additionally, alterations in CDKN2A and DPC4/SMAD4 tumor suppressor genes are also generally seen in PDAC[9,10].

In tumor progression, the role of growth factors and their receptors is highly significant[11]. Together with genetic mutations of *K-ras* and p53, over expression of growth factors such as EGF, TGF alpha, TGF beta 1-3 and also factor receptors including EGF receptor, c-erbB-2, c-c-erbB-3, TGF beta receptor I-III is also exist in several kinds of gastrointestinal cancers[12]. These anomalies often trigger the tumor growth and enhance the metastatic ability of pancreatic cancer cells that may lead to poor prognosis following treatments of this disease[5].

The growth of tumor in PDAC arises from the ductal epithelium and progresses from pre-malignant lesion to fully invasive cancer[2]. Pancreatic intraepithelial neoplasia (PanIN) is a well known precursor lesion type that can lead to this invasive adenocarcinoma. PanINs are proliferations of the smaller pancreatic ducts that can be viewed microscopically and its classification represents step by step morphological alterations that happen in the pancreatic ductal epithelium. A normal pancreatic duct is characterized by low cuboidal, non-mucinous cells in a single layer formation. Low-grade PanINs (PanIN-1a and PanIN-1b) are characterized by the change from a cuboidal duct epithelium to elongated cells and by the abundant accumulation of mucin. PanIN-1a lesion is made up of columnar shape cells with the presence of mucin production. PanIN-1b lesion is somewhat identical to PanIN-1a except for its architectural difference. PanIN-1b has a papillary, micropapillary or basally pseudostratified architecture. As the lesions advance from PanIN-1 to PanIN-2, some nuclear abnormalities have emerged which can be viewed under a microscope. The architectural make up of mucinous epithelial lesion of PanIN-2 can either be flat or papillary. Some of the nuclear alterations that can be seen in PanIN-2 lesion include loss of polarity, nuclear crowding, enlarged nuclei, pseudo-stratification and hyperchromatism. PanIN-3 lesion is a pre-invasive form of adenocarcinoma (carcinoma in situ). It is architecturally papillary or micropapillary, however, they may also appeared flat. This lesion

may form budding into the pancreatic lumen with the observance of severe nuclear atypia and some abnormal mitosis[13,14].

1.3 Clinical presentation and diagnosis

The clinical presentation of the early stages of PDAC can hardly be seen. Symptoms presented by PDAC are not exclusive and differ depending on the location of tumor as well as the stage of the disease. Although the etiology of pancreatic cancer remains unknown, several risk factors have been suggested such as male gender, black race, meat and fat consumption, cigarette smoking, pancreatic ductal hyperplasia and chronic pancreatitis. Since the majority of tumors develop in the head of the pancreas, obstructive cholestasis is normally manifested. Rarely, a pancreatic tumor may also cause gastrointestinal bleeding or duodenal obstruction while obstruction of the pancreatic duct by tumor may lead to pancreatitis. PDAC generally causes abdominal discomfort, nausea and dull, deep upper abdominal pain. For most patients, systemic manifestations of this disease include anorexia, unexplained weight loss and asthenia. Other less common manifestations include deep and superficial venous thrombosis, increased abdominal girth, panniculitis, gastric-outlet obstruction and depression. Upon physical examination, jaundice, temporal wasting, hepatomegaly and ascites may be observed. Patients may also have mild liver-function test abnormalities, hyperglycemia and anemia[2,15].

Commonly, contrast-enhanced computerized tomography (CT) is sufficient to help in the diagnosis of pancreatic cancer. Other imaging tests use to diagnose this disease include ultrasound and magnetic resonance imaging (MRI). Some other diagnostic tools that are also useful are endoscopic ultrasonography and endoscopic retrograde cholangiopancreatography (ERCP). In terms of serum biomarker, CA 19-9 is the most commonly used biomarker that has demonstrated clinical usefulness for therapeutic monitoring and early detection of recurrent

event of pancreatic cancer despite its limitation of not being a solely specific biomarker for this disease[16,17]. Recently, few researchers have identified Survivin, an inhibitor of apoptosis that is known to be overexpressed in PDAC as a new potential serum biomarker for this lethal disease[18,19]. According to the most recent edition of the American Joint Committee on Cancer, pancreatic cancer is staged based on tumor-node-metastasis (TNM) classification. TNM information of tumor grade, nodal status and distant metastases is being integrated in assigning the stages of pancreatic cancer (stage 0 to IV). Stage 0 is marked by the presence of carcinoma in situ while in stage I, tumor is confined to the pancreas. Once the tumor has grown beyond the pancreas, assignment to stage II or stage III will be given depending on the involvement or non-involvement of major blood vessels or nerves respectively. The final stage of the disease, stage IV, is characterized by the spreading of tumor beyond the pancreas to distant sites commonly to the liver, lungs and peritoneum[20].

1.4 Treatment strategies and prognosis

Treatment plans for PDAC are limited and mainly determined by the location of the pancreatic tumor. The only treatment that is considered curative is through surgical resection of the tumor. Unfortunately, this option is only limited to the early stages of PDAC, mostly stage I cases and some of cases involving stage II[3,21]. Even in early PDAC stages cases, only 20% of PDAC cases can be intervened surgically. In the majority of cases, the removal of tumor through surgical procedure is not possible or the use of surgical techniques alone as curative strategy is less beneficial[21]. Some of the most common operative procedures are cephalic pancreatoduodenectomy also known as the Whipple procedure and distal subtotal pancreatectomy depending on the location of the tumor. The Whipple procedure is commonly the procedure of choice for tumors presence in the head or uncinata process while the latter is

performed when the tumor is located the body or tail of the pancreas. In some cases, the treatment of PDAC may involve total removal of the pancreas or pancreatectomy. Observations from several randomized clinical trials have demonstrated that a more extensive surgical resection does not improve survival due to the increase risk of postoperative morbidity[2]. This poor prognosis is contributed by several factors including large tumor size, high tumor grade, lymph-node metastases and high level of CA 19-9 that continue to elevate persistently in postoperative setting[22,23].

Despite being the only possible curative treatment for PDAC, prognosis following total resection of tumor alone in early-stage patients is somewhat disappointing[2]. Data from several studies have shown that adjuvant therapy through postoperative administration of chemotherapy with either leucovorin and fluorouracil or gemcitabine improves overall survival[24–26]. In addition, the combination of gemcitabine with fluorouracil given as continuous infusion and radiation therapy has also shown an increase in overall survival with a median survival of 20 to 22 months[2,23]. Hence, the use of gemcitabine alone or gemcitabine in combination with fluruouracil-based chemoradiation postoperatively can be acknowledged as the standard of care for the management of early-stage pancreatic cancer. Interestingly, the emerging use of preoperative (neoadjuvant) gemcitabine-based chemoradiation treatment has also been demonstrated to be at least as effective as postoperative (adjuvant) treatment in patients with resectable pancreatic cancer[27]. As the disease progresses to becoming locally and systemically advanced, tumor is no longer resectable. In these cases, treatment is palliative with median overall survival ranges from 9 to 10 months. Treatment options diverge from chemotherapy alone to combination of treatment with chemoradiation therapy and chemotherapy. Data from several randomized trials have established that chemoradiation therapy is better than radiation

therapy alone[28,29]. Gemcitabine, a genotoxic drug has been the treatment of choice for pancreatic cancer particularly for patients with nonresectable pancreatic cancer. It is the current standard therapy that is known to extend survival by a matter of weeks[30]. Several clinical trials have tested the effect of using few new agents in combination with gemcitabine but the reported outcomes were not much better. The use of erlotinib as part of combinatorial therapy with gemcitabine is so far the only agent that showed a small yet significant increase in survival among patients diagnosed with advanced pancreatic cancer. However, this combination is reported to have more toxicity compared to the use of erlotinib alone[32]. Thus far, gemcitabine regimen or its combination with platinum agent, erlotinib or fluropyrimidine is being practiced as the treatment approach for advanced pancreatic cancer patients[31,32].

1.5 Phytochemicals in cancer therapy: Oil Palm Phenolics (OPP)

In the hope to combat cancers, researchers are now trying a newer approach through the use of naturally occurring substances from plants called phytochemicals. Phenolic phytochemicals are plant secondary metabolites playing major role in plant defense mechanisms. In the recent years, phenolics have started to draw researchers' attention for their positive impacts on health. Variety of phytochemicals have been demonstrated to have anticancer properties including curcumin, garcinol[33,34], lycopene[35,36], resveratrol[37], epigallocatechin gallate (ECGC)[38] and genistein[39,40].

Oil palm (*Elaeis guineensis*) is a high oil plant from the family of *Arecaceae*, is mainly used for extraction of edible oils from its fruits. Successful recovery from the aqueous by-products following palm oil production has identified a water soluble complex rich in phenolics and organic acids collectively referred as Oil Palm Phenolics (OPP)[41]. Major components of OPP include three isomers of caffeoylshikimic acid (3-,4- and 5-caffeoylshikimic acids),

protocatechuic acid and p-hydroxybenzoic acid with the three caffeoylshikimic acid isomers contribute majorly to the total phenolics content of OPP. The representative chemical structure of 3-,4- and 5-caffeoylshikimic acids is shown in Fig. 1[42,43].

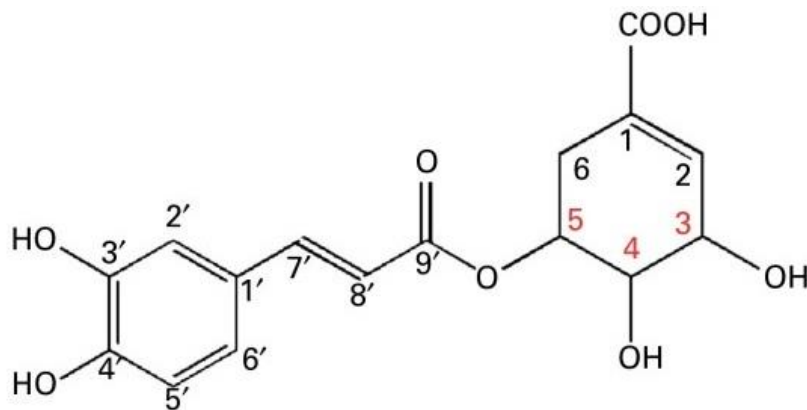


Fig. 1 Representative structure of the three isomers of caffeoylshikimic acid [43]

OPP has been shown to exhibit antioxidant properties and was reported to display positive outcomes in various *in vivo* studies on both non-PDAC and chronic diseases models such as cardiac arrhythmia, atherosclerosis and diabetes without any signs of toxicity[43–47]. The antiproliferative effects of OPP were also documented in several types of cancers including myeloma and lung carcinoma[45]. In our laboratory, we have recently studied the antitumor activities of OPP using two pancreatic cancer cell lines, PANC-1 and BxPC-3. The antitumor effects that we observed from this *in vitro* study demonstrate the potential use of OPP as a treatment modality for PDAC, thus necessitate a further investigation using a clinically relevant animal model[48].

1.6 KPC transgenic mice as *in vivo* model to study PDAC

The generation of $Kras^{LSL.G12D/+}$; $p53^{R172H/+}$; $PdxCre^{tg/+}$ or KPC transgenic mouse model is achieved by crossing mice with a conditional activated Kras allele ($Kras^{LSL.G12D}$) to transgenic strain that expresses Cre recombinase in pancreatic lineages ($PdxCre^{tg}$). This will generate a conditionally express mutant allele of the Li-Fraumeni human ortholog, $p53^{R172H}$. Through interbreeding with $PdxCre^{tg}$ transgenic animals, activation of both the $Kras^{LSL.G12D}$ and the $p53^{R172H}$ happens in tissue progenitor cells of the developing mouse pancreas. The development of advanced PDAC in KPC mice happens at an early age and this model has many features similar to pancreatic cancer in human. This model developed the full range of PanIN lesion that ultimately progresses to pancreatic carcinoma formation. Similar to what is commonly observed in humans, majority of KPC mice have metastases to the liver and lungs. Moreover, some comorbidities that are associated with human PDAC including cachexia, jaundice and ascites also occur in this KPC mouse model[30,49].

1.7 Hypothesis and specific aims

Our recent work on the anticancer effect of OPP *in vitro* had highlighted successful outcome of OPP in inhibiting pancreatic cancer cells proliferation and growth also in inducing cell cycle arrest and apoptosis especially on PANC-1 which is a *K-ras* mutated cell line[48]. This has led us to hypothesize that OPP would produce a similar effects in PDAC model. Thus, we conducted an animal model investigation with the objective to explore the *in vivo* effect of dietary OPP in transgenic mouse model of PDAC. The following specific aims were proposed to meet the hypothesis that OPP will display therapeutic effects against PDAC in transgenic mice and it will have synergistic effect with chemotherapy drug, gemcitabine when used in combination.

Specific Aim 1: To evaluate disease progression of Pancreatic Ductal Adenocarcinoma (PDAC) and *in vivo* tumor response following dietary Oil Palm Phenolics (OPP) therapy.

- a) To monitor tumor and cyst growth using MRI technique
- b) To evaluate possible toxicity of dietary OPP by microscopic assessment

Specific Aim 2: To investigate mouse pancreatic tissue for antitumor activity of OPP by histology and gene expression.

- a) To conduct histological assessment of PDAC precursor lesions and markers
- b) To perform gene expression analysis of selected tumorigenesis markers following OPP treatment

Specific Aim 3: To conduct urinary metabolomic investigation of KPC transgenic mice following dietary OPP intervention.

- a) To examine the differences in ^1H NMR urinary metabolomic profiles with OPP treatment using multivariate data analysis
- b) To perform target analysis in identification and quantification of differential metabolites

CHAPTER 2 METHODOLOGY

2.1 Animals

Forty male, triple mutant, KPC ($Kras^{LSL.G12D/+}$; $p53^{R172H/+}$; $PdxCre^{tg/+}$) transgenic mice at the age between 6-8 weeks old were obtained from Van Andel Institute (Grand Rapids, MI, USA) for this study. To confirm their genotypes, PCR genotyping of genomic DNA was conducted prior to shipment of animals. Thirty mice that developed pancreatic cancer by KPC mutation were used for experimental treatments and ten mice with non-mutated KPC from the same litter served as control. Each animal was housed in an individual cage at Wayne State University Division of Laboratory Animal Resources (DLAR) facility under standard conditions as approved by the Wayne State University Animal Investigation Committee (AIC). All animals were kept in the same room with alternating 12 hours light alternating with 12 hours darkness under normal humidity and at room temperature.

2.2 Experimental conditions and protocols

The study design and experimental conditions are presented in Figure 2. The protocol for this study was approved by Wayne State University IACUC (approval number: A 3310-01). Upon arrival at the facility, all animals were allowed to acclimatize for one week prior to the start of the experiment. Following acclimatization period, KPC mutant mice (n=30) and non-PDAC control non-mutant mice (n=10) were weighed and randomly distributed into 4 and 2 experimental groups respectively where the diet was changed to custom made diets (5% OPP or isocaloric control diets) with weekly administration of gemcitabine drug or saline as placebo. Thirty mutant mice were randomly grouped into 4 different experimental conditions: KC (n=8) (control diet), KP (n=8) (OPP diet), KG (n=8) (gemcitabine), KPG (n=6) (OPP diet + gemcitabine) while ten littermates without mutations serving as non-PDAC controls were

assigned into 2 groups: CC (n=5) (control diet) and CP (n=5) (OPP diet). Ad libitum supply of diet and water was available throughout the 6 weeks of study. Body weight and diet intake of the animals were measured twice weekly. Cage bedding, diets and water were replaced every week and their health were monitored regularly. Criteria for early euthanization included 20% weight loss or abdominal distention with respiratory distress.

2.3 Experimental diets

OPP for this study was provided by Malaysian Palm Oil Board (Kajang, Malaysia) at the stock concentration of 1500 mg/ml gallic acid equivalents (GE). Both the 5% OPP and the standard purified diets were formulated and produced by Dyets Inc. (Bethlehem, PA). Composition of both diets is shown in Table 1.

2.4 Experimental procedures

All mice were provided with their respective diets for 6 weeks. Body weight, diet and water intake were recorded twice weekly throughout the study duration. Chemotherapy injections from 100mg/5ml gemcitabine stock were delivered intraperitoneally to KG and KPG groups (5ul/g body weight) once-weekly (Week 1-5) while groups with no chemotherapy treatment were given placebo injections of saline (0.85% NaCl). To confirm the presence of pancreatic cancer and for disease progression monitoring purpose, MRI scans were conducted at week 1 and 5. Urine samples were collected once a week on weeks 2, 4 and 6 for urinary metabolomic profiling. Animals were transferred to suspender cages for 24 hours to allow for urine sample collection from the bottom of the cages. Upon collection, urine samples were centrifuged at 5000 rpm for removal of debris followed by addition of sodium azide (0.01%) to prevent microbial growth. Urine samples collected were then measured, aliquoted and stored at -80°C until further use. Upon completion of the study at Week 6, all animals were kept fasted

overnight then euthanized under 80mg/ml Ketamine-20mg/ml Xylazine anesthesia (5ul/g body weight) by exsanguination and major organs removal prior to harvesting all major organs (pancreas, liver, fore stomach, spleen, kidneys, heart and testes) including tumors. A part of tissue from the harvested organs was fixed in 10% neutral buffered formalin to be used for histological analyses while the remaining part was flash-frozen in liquid nitrogen then stored at -80°C until ready to be used for gene expression analyses.

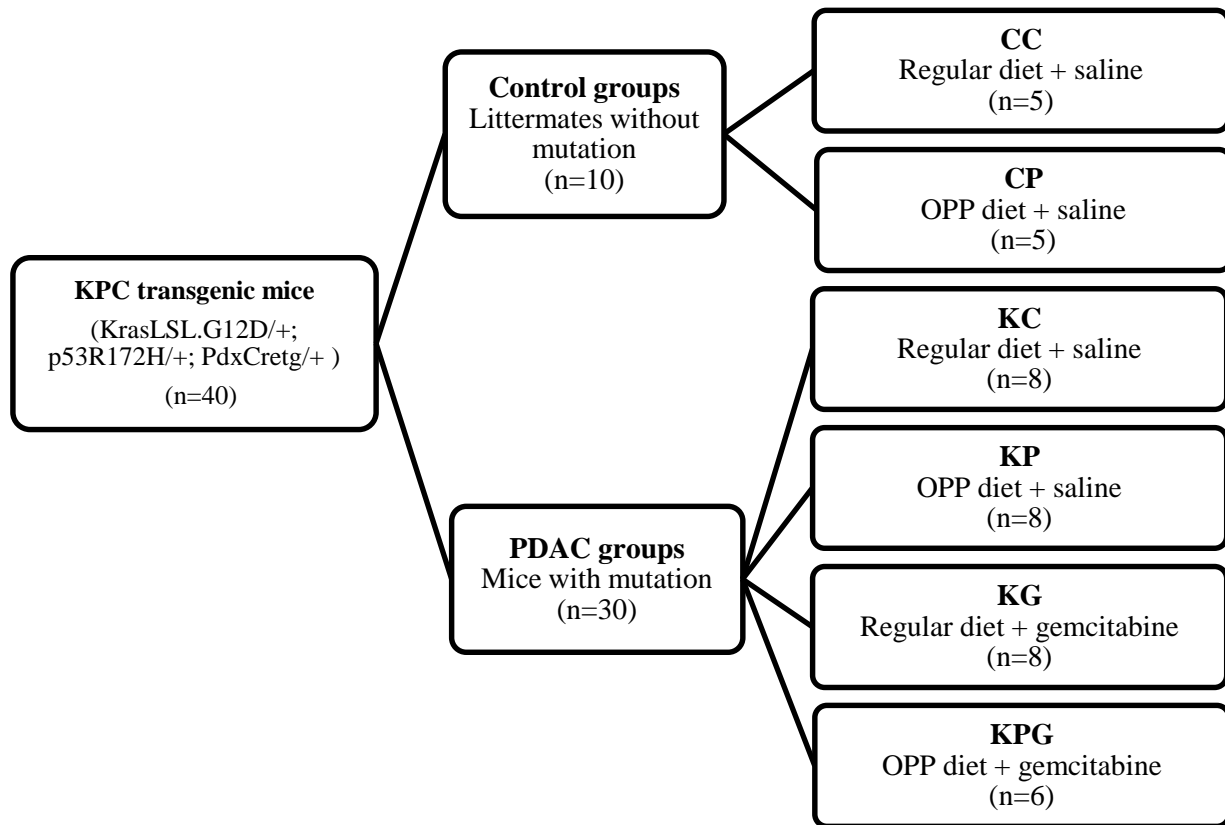


Fig. 2 Study design and experimental conditions

Control groups

CC: Control mouse, standard purified diet.

CP: Control mouse, 5% OPP diet.

Experimental groups

KC: Pancreatic cancer mouse, standard purified diet + no drug treatment.

KP: Pancreatic cancer mouse, 5% OPP diet + no drug treatment.

KG: Pancreatic cancer mouse, standard purified diet + gemcitabine drug treatment.

KPG: Pancreatic cancer mouse, 5% OPP diet + gemcitabine drug treatment.

5% OPP added diet				Regular purified diet			
Ingredient	kcal/g	grams/ kg	kcal/kg	Ingredient	kcal/g	grams/ kg	kcal/kg
Casein	3.58	200	716	Casein, High Nitrogen	3.58	200	716
L-Cystein	4	3	12	L-Cystein	4	3	12
Sucrose	4	100	400	Sucrose	4	100	400
Cornstarch	3.6	347.5	1251.0	Cornstarch	3.6	397.5	1431.0
Dyetrose	3.8	132	501.6	Dyetrose	3.8	132	501.6
Soybean Oil	9	70	630	Soybean Oil	9	70	630
t-Butyl hydroquinone	0	0.014	0	t-Butyl hydroquinone	0	0.014	0
Cellulose	0	50	0	Cellulose	0	50	0
Mineral Mix #210025	0.88	35	30.8	Mineral Mix #210025	0.88	35	30.8
Vitamin Mix #310025	3.87	10	38.7	Vitamin Mix #310025	3.87	10	38.7
Choline Bitartrate	0	2.5	0	Choline Bitartrate	0	2.5	0
OPP	0	50	0				

Table 1 Composition of experimental diets

2.5 MRI scans

The progression of PDAC in the experimental animals was tracked by tumor and cyst growth using MRI technique. MRI scans were carried out at two time points, at week 1 and week 5 of the study. Prior to MRI scans, all animals were anesthetized by Ketamine-Xylazine mixture administered through intraperitoneal injection at 5ul/g body weight. Eye lubricant was also applied to prevent corneal desiccation while under anesthesia. MRI scans were conducted on Bruker ClinScan 7.0T scanner (Karlsruhe, Germany). T2-weighted images were acquired from each animal in both coronal and transverse orientations. Tumors and cysts were indentified and measured for volumes by a trained personell of the MRI facility. Following MRI, animals were allowed to recover from anesthesia on a heating pad before returning to the animal facility.

2.6 Histological analyses

2.6.1 Toxicity analysis

Toxicity study was carried out by comparing forestomach and pancreatic tissues H&E stained slides of the control animals receiving standard diet (CC) and 5% OPP diet (CP). Harvested forestomach and pancreatic tissues from the two control groups were immediately fixed in 10% neutral buffered formalin for 24 hours, and then stored in 70% ethanol to prevent excess drying of tissue specimens. Specimens were sent to the pathology laboratory at Michigan State University for paraffin section preparation and H&E staining. First, specimens were embedded in paraffin wax followed by sectioning into 4-5 micron thin slices. Sections were mounted onto albumin coated slides, deparaffinized, hydrated and stained with hematoxylin & eosin (H&E). Each prepared H&E slide was later examined under the light microscope (Nikon Eclipse 80i) for hispatological changes.

2.6.2 Histology of PanIN lesions

Formalin fixed pancreatic tissues of animals in PDAC experimental groups (KC, KG, KP and KPG) were prepared for H&E staining as described above. Observation under the light microscope (Nikon Eclipse 80i) was then conducted on the prepared slides. Pancreatic intraepithelial Neoplasia (PanIN) lesions were identified and graded microscopically into PanIN-1, PanIN-2 and PanIN-3 based on morphology and criteria set by reference [13]. Lesions observed microscopically were counted for total number and also based on lesion grades, under the supervision of Dr. Doina David, pathologist from Wayne State University School of Medicine.

2.6.3 Immunohistochemistry

Pancreatic tissues of animals in PDAC experimental groups (KC, KG, KP and KPG) were analyzed for expression of tumor promoter (S100P) and tumor suppressor (SMAD4) genes. IHC slides were prepared at pathology laboratory at Michigan State University. Formalin fixed pancreatic specimens embedded in paraffin wax were sectioned into 4-5 micron thin slices. Slices were then deparaffinized with xylene and rehydrated with ethanol followed by pH adjustment in Tris Buffer Saline solution with pH 7.4. Epitope retrieval was performed with Citrate Plus pH 6.0 buffer using a rice steamer for 30 minutes followed by incubation at 25°C for 10 minutes. Endogenous peroxidase was then blocked by 3% hydrogen peroxide treatment for 10 minutes. For non specific protein blocking, 5% normal normal goat serum in phosphate-buffered saline (PBS) was applied for 30 minutes then incubated with Avidin/Biotin blocking system for 5 minutes each. The slides were incubated with primary antibodies for S100P and SMAD4 for 30 minutes in blocking solutions using rabbit polyclonal anti-S100P at 1:200 dilution and rabbit monoclonal anti-SMAD4 at 1:100 dilution (Abcam, Cambridge, Massachusetts, USA)

respectively followed by incubation with biotinylated rabbit anti-goat secondary IgG for 30 minutes (Vector Labs, Burlingame, California, USA). This was followed by incubation of slides with RTU Vectastain Elite ABC reagent for 30 minutes. Finally, slides were developed with Vector Nova red peroxidase chromogen and counterstained with haematoxylin, washed and dehydrated with ethanol, cleared with xylene and mounted. Observation for assessment of gene expression was carried out under the light microscope (Nikon Eclipse 80i).

2.7 Gene expression analyses

2.7.1 RNA isolation

Total RNA extraction of pancreatic tissues was performed with a commercial kit (RNeasy Mini Kit, Qiagen Valencia, California, USA) according to the manufacturer's instructions. Briefly, 30mg each of frozen pancreatic tissues were homogenized in trizol reagent provided. Homogenates were then kept at room temperature for 5 minutes followed by vigorous shaking after the addition of 140 uL of chloroform. Samples were kept at room temperature for 3 minutes prior to centrifugation for 15 minutes at 12,000 rcf at 4°C. The upper aqueous phase was collected and 525ul of 100% ethanol was added. The mixture was placed in a mini spin column and centrifuged at 10,000 rpm for 15 seconds discarding the flow-through. 700 uL of buffer RWT was added into columns and centrifuged at 10,000 rpm for 15 seconds. This was followed by double wash with 500 uL of buffer RPE, centrifuged at 10,000 rpm for 15 seconds and 2 minutes respectively. Spin columns were then transferred to new collection tubes and RNA samples were eluted with 40uL of RNase-free water followed by 1 minute centrifugation at 10,000 rpm. Isolated RNA samples were quantified and checked for purity using the Nanodrop spectrophotometer (Wilmington, Delaware, USA) prior to reverse transcription step for PCR.

2.7.1 Reverse transcription and qRT-PCR

Reverse transcription for cDNA synthesis was performed using miScript II RT Kit (Qiagen GmbH, Hilden, Germany) in 20ul reaction consisted of 4ul 5x miScript HiFlex Buffer, 2ul miScript Nucleics Mix, 2ul miScript Reverse Transcriptase Mix, 11ul RNase-free water and 1ul of template RNA (equal concentrations of 1000 ng/ul for all samples). Reverse transcription process was carried out in Eppendorf mastercycler realplex 4 (Eppendorf, Hauppauge, New York, USA) at the following temperatures; 37°C for 60 minutes, 95°C for 5 minutes and was kept at 4°C until retrieve for immediate use for qRT-PCR analysis or transferred to a -20°C freezer.

Three molecular markers (Notch1, CCND1, MMP9), involved in tumor progression were tested in a final reaction volume of 25ul that consisted of 12.5ul QuantiTect SYBR Green PCR Master Mix, 2.5ul of QuantiTect primer assay (Qiagen GmbH, Hilden, Germany), 9.5ul RNase-free water and 2ul of cDNA (equal concentrations of 10ng/ul for all samples). qRT-PCR was carried out on the Eppendorf mastercycler realplex 4 instrument (Eppendorf, Hauppauge, NY) in a 96-well plate (Agilent Technologies) with the following program; initial activation at 95°C for 15 minutes, 40 repeats of 3-step cycling: denaturation at 95°C for 15 seconds, annealing at 55°C for 30 seconds and extension at 60°C for 30 seconds. Each marker was analyzed in triplicate with single non-template control (NTC). Statistical significance for mRNA expression was obtained by comparing the ΔC_T values normalized against β -actin of treatment groups (KP, KG and KPG) to the untreated PDAC group (KC).

2.8 Urine metabolomic analysis

2.8.1 Sample preparation and ^1H NMR spectroscopic acquisition

Frozen urine samples were thawed and diluted 1:4 with Deuterium oxide (D_2O). 640ul of each diluted urine sample was mixed with 60ul of 1:9 D_2O diluted reference buffer solution containing 5mM DSS (disodium-2, 2-dimethyl 2-silapentane-5-sulphonate) and 10mM imidazole (Sigma-Aldrich, Mississauga, Ontario, Canada) to make the final volume of 700ul. Samples were mixed by vortexing and then transferred into 5mm NMR tubes immediately before NMR acquisition. ^1H NMR spectra of the prepared samples were acquired at 25°C using tnoesy pulse sequence with 4-second acquisition time, a sweep width of 6009 Hz and 32K data points on a Varian 500 MHz spectrometer equipped with AutoX probe and VNMRJ software. Settings and pulse sequence used were in accordance to that of CHENOMX software -1D version requirements. A total of 64 scans were collected out for every NMR spectrum to allow for optimum intensity build up and noise (random signals without information) reduction.

2.8.2 NMR spectra pre-processing and multivariate data analysis

The acquired NMR spectra in the form of free induction decay (FID) files were processed using ACD/Spec software (Advanced Chemistry Development Inc., Toronto, Ontario, Canada). FID files were fourier transformed to convert the spectra from the time domain to the frequency domain. The converted spectra were baseline corrected, autophased and binned into 1000 bins. The table of integrals from spectra pre-processing was then imported into Excel and used for multivariate data analysis using SIMCA-P+ software (version 13, Umetrics, Sweeden). Preceding further analysis, some regions of the spectrum including those corresponding to water, DSS and imidazole were excluded. Data were also Pareto-scaled prior to the subsequent model generations. Using SIMCA-P+ software, both multivariate pattern recognition techniques,

unsupervised (principal component analysis, PCA) and supervised (partial least-squares discriminant analysis, PLS-DA and orthogonal partial least-squares discriminant analysis, OPLS-DA) were employed to the data in order to discriminate sample spectra of different experimental groups. The unsupervised method, PCA provides a basic overview for initial exploration of the data which aim at revealing the arrangement of the data (spectra) without any class information given to the software. A desirable outcome of PCA is a score plot which reveals patterns and clusters that can be related to different treatment groups while the loading plot generated from the score plot explains the variables (spectral regions) that contribute to the clustering. For the supervised methods, PLS-DA and OPLS-DA, class information is included in the analysis. This often improves the transparency and interpretability of the model. Additionally, regression analysis using orthogonal projections to latent structures (OPLS) was also conducted on several investigated variables. Regression analysis enables the evaluation of the relationship between urinary metabolite profiles with the variables investigated independently of the metabolomic profiles.

2.8.3 Metabolite target analysis

Identification and quantification of metabolites responsible for separation in PCA, PLS-DA and OPLS-DA score plots were carried out using Chenomx NMR Suite software (Chenomx Inc., Edmonton, Canada) utilizing a targeted profiling approach. Metabolites were identified and measured for their concentrations by fitting the spectral peaks found for each compound in the compound library. Statistical tests were conducted to assess the differences in metabolite concentrations between groups followed by the exploration of possible metabolic pathways involved using KEGG database and MetaboAnalyst software. MetaboAnalyst software utilizes pathway enrichment analysis and pathway topology analysis to translate metabolic trends into

defined pathways relevant to the study while KEGG provides the molecular wiring diagrams of interaction and relations between pathways in biological system.

2.9 Statistical analyses

Statistical tests were performed using IBM SPSS Statistics 23 software with statistical significance level of 0.05 ($p < 0.05$).

CHAPTER 3 RESULTS

A total of 40 KPC transgenic mice were used for this study. Animals with positive KPC mutation (n=30) and littermates without mutation, served as non-PDAC controls (n=10) were randomly assigned to a 6-week dietary intervention to investigate the *in-vivo* effect of OPP on PDAC. At endpoint (week 6), all control animals both fed with regular or 5% OPP diet (CC and CP groups), completed the treatment (100%). For PDAC experimental groups, each group had lost at least one animal before the termination of the study due to death or conditions that demanded an early euthanization. Greater than 80% of animals completed this study in the untreated, KC (87%), OPP fed, KP (87%) and combination of OPP diet with gemcitabine drug treatment, KPG groups (83%), while a lower percentage of animals in the gemcitabine treated group, KG completed the treatment (75%; Fig. 3).

3.1 Body weight and diet intake

No significant differences were observed between groups at baseline (week 1) and endpoint (week 6) with respect to mean body weight (Fig. 4). For diet intake, data from week 2 were used as baseline instead of week 1 to allow for initial fluctuation in diet intake due to changing from the facility standard chow diet to experimental diets. Similarly, the means of daily intake were not found to be significant between groups at both baseline and endpoint (Fig. 5).

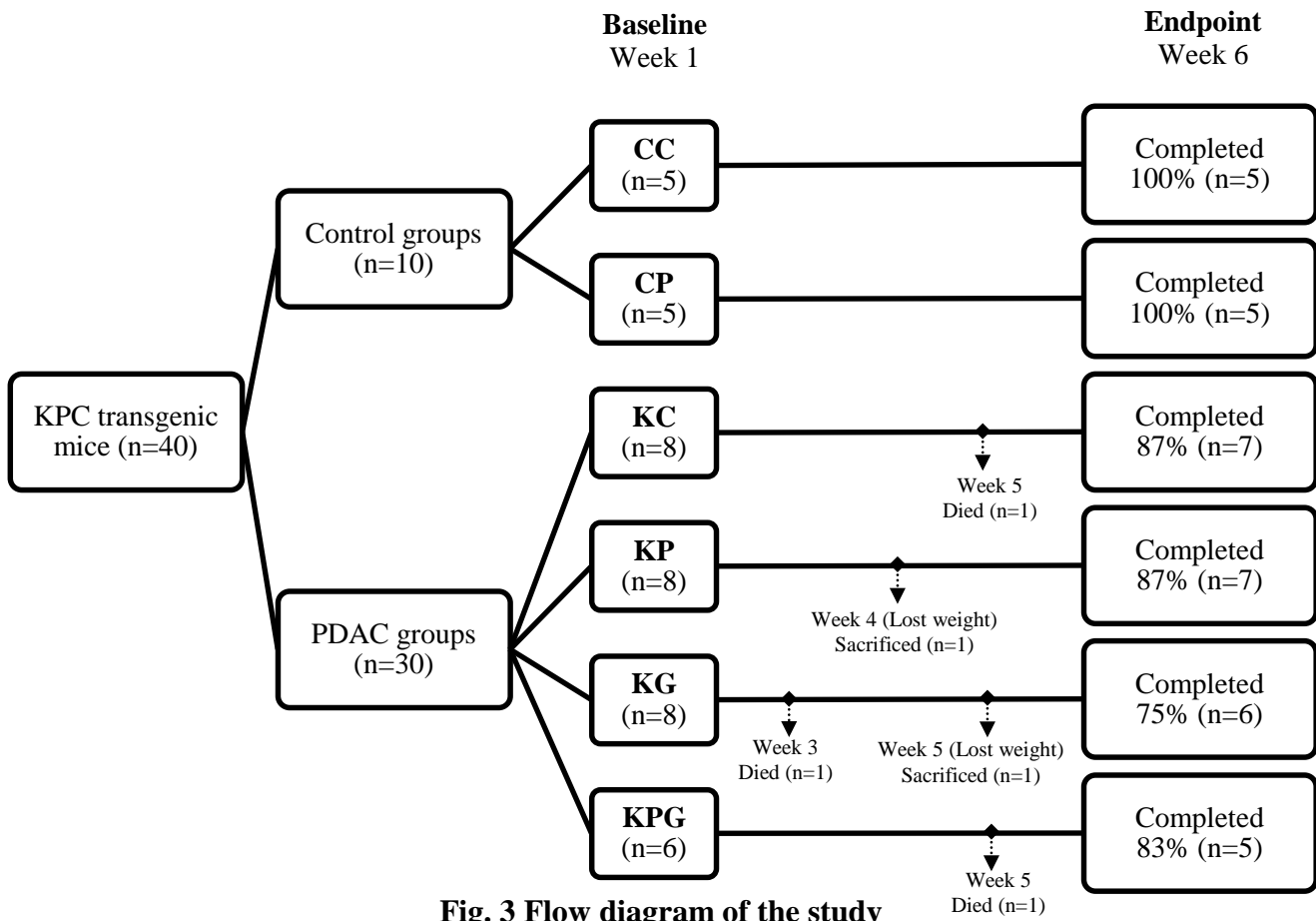


Fig. 3 Flow diagram of the study

Control groups

CC: Control mouse, standard purified diet.

CP: Control mouse, 5% OPP diet.

Experimental groups

KC: Pancreatic cancer mouse, standard purified diet + no drug treatment.

KP: Pancreatic cancer mouse, 5% OPP diet + no drug treatment.

KG: Pancreatic cancer mouse, standard purified diet + gemcitabine drug treatment.

KPG: Pancreatic cancer mouse, 5% OPP diet + gemcitabine drug treatment.

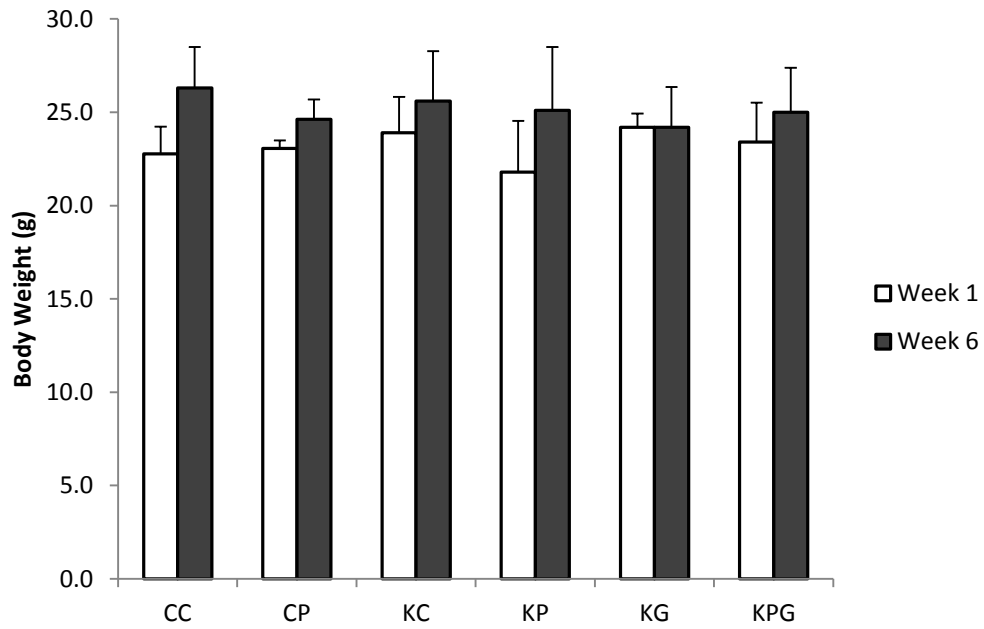


Fig. 4 Mean body weight. Comparison of mean body weight in KPC mice fed diets (regular/OPP) and treated with or without gemcitabine at baseline (week 1) and endpoint (week 6). Data are expressed as mean \pm SD. No significant differences between groups observed ($p>0.05$).

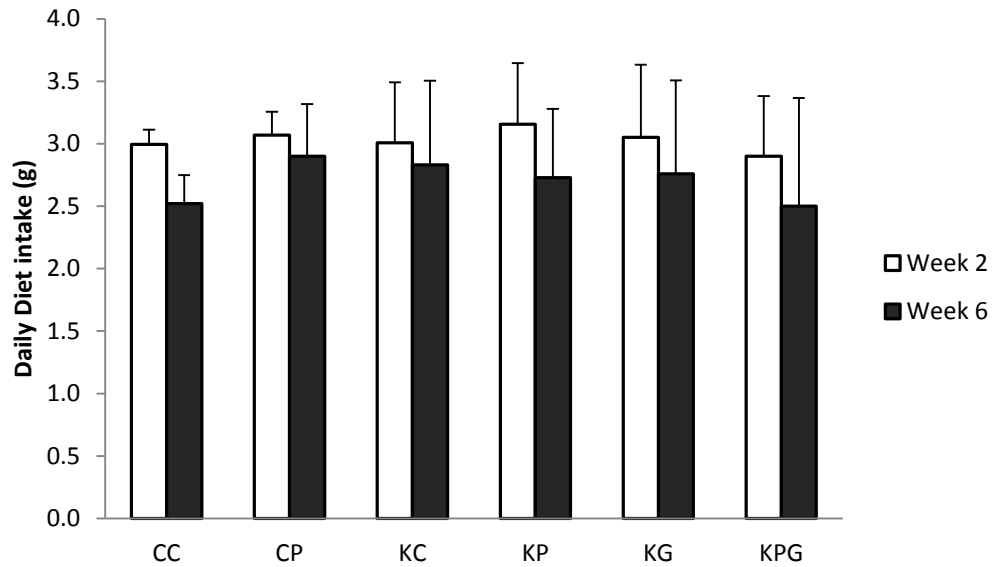


Fig. 5 Mean daily diet intake. Comparison of mean daily diet intake in KPC mice fed diets (regular/OPP) and treated with or without gemcitabine at baseline (week 2) and endpoint (week 6). Data are expressed as mean \pm SD. No significant differences between groups observed ($p>0.05$).

Specific Aim 1: To evaluate disease progression of Pancreatic Ductal Adenocarcinoma (PDAC) and in vivo tumor response following dietary Oil Palm Phenolics (OPP) intervention.

3.2 Effect of OPP on tumor and cyst growth

To identify the effect of dietary OPP treatment on PDAC progression, T2-weighted abdominal magnetic resonance imaging (MRI) was conducted on each animal at week 1 with subsequent follow up scans at week 5. Table 2 summarizes the changes in tumor and cyst volume in the four PDAC experimental groups (KC, KG, KP and KPG).

In PDAC group without treatment (KC), 85% of the observed tumors increased in size. Out of the eight tumors monitored, more than half of the tumors grew larger which none decreased in size. In KG group, it was found that not all animals receiving gemcitabine drug responded to the treatment with only 1 tumor had a reduction in tumor volume following chemotherapy drug treatment. 43% of tumors of the animals treated with dietary OPP (KP), showed an increase in tumor volume. However, KP group had more tumors that decreased in size following the dietary treatment compared to KG group. Remarkably, in the group receiving both dietary OPP and gemcitabine drug treatment (KPG), only 14% of the observed tumors was found to increase in size. Only one out of seven tumors continued to grow while the growth of the remaining tumors was arrested.

With respect to cysts, more than half of the cysts in KC group increased in size (80%), while KG and KP groups had 67% and 75% of cysts increased in size respectively. Equivalently interesting to the data for tumors, the growth of all cysts in KPG group was arrested, none of the cysts increased in size. Figs. 6-9 provide the representative images of the MRI scans showing the effect of different treatments on tumor and cyst growth.

	KC	KG	KP	KPG
Tumors				
Total number of tumors observed	8	6	7	7
Number increased in size	6	3	3	1
Number unchanged in size	2	2	1	2
Number decreased in size	-	1	3	4
% tumors increased in size	85%	50%	43%	14%
Cysts				
Total number of cysts observed	5	3	4	3
Number increased in size	4	2	3	-
Number unchanged in size	1	-	-	1
Number decreased in size	-	1	1	2
% cysts increased in size	80%	67%	75%	0%

Table 2 PDAC progression of experimental animals. Tracking of PDAC progression by monitoring the changes in tumor and cyst volumes at week 1 and week 5 using MRI.

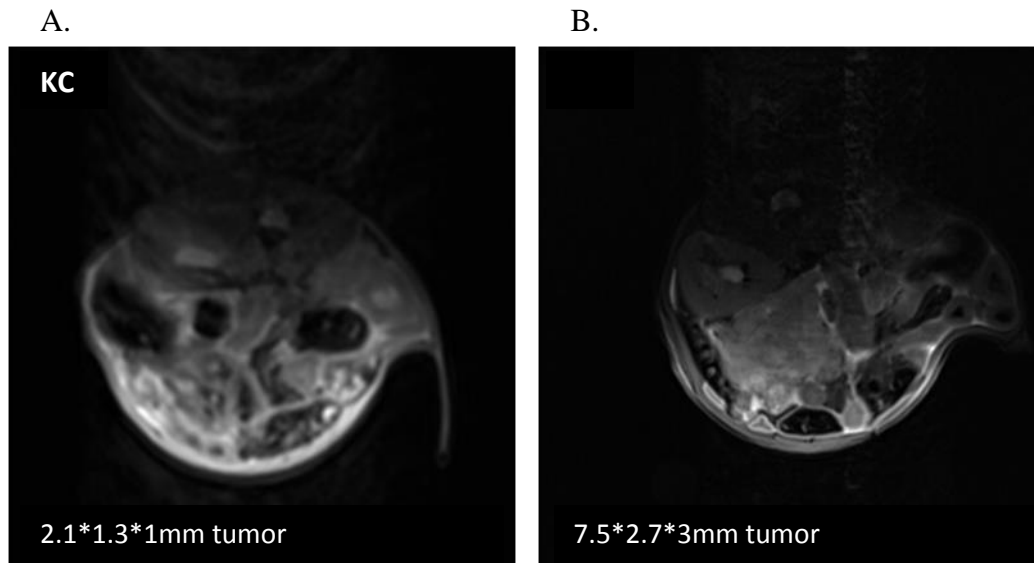


Fig. 6 Representative transverse T2-weighted MRI of KC mouse abdomen at week 1 (A), and follow up abdominal MRI scan at week 5 (B). MRI image showing an increase in tumor volume at endpoint.

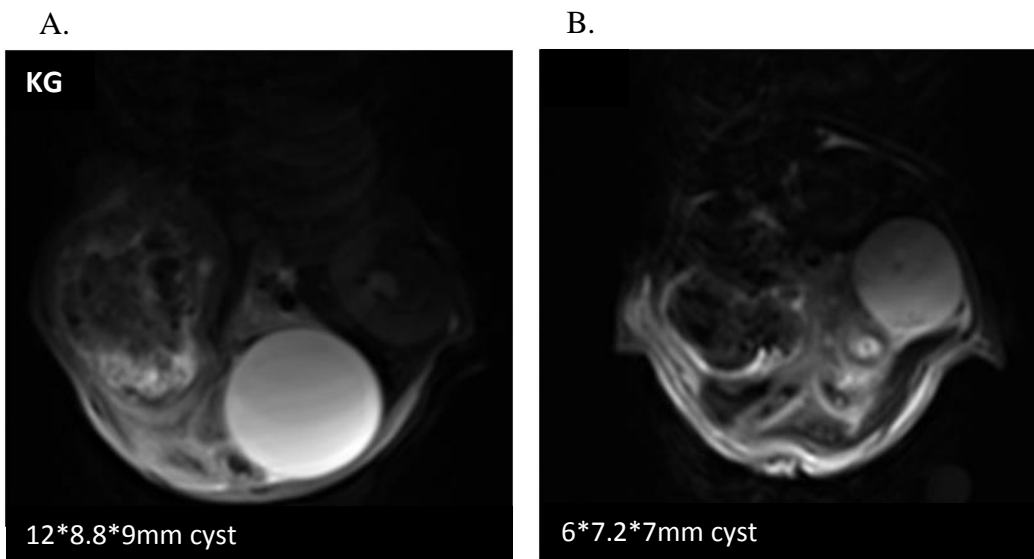


Fig. 7 Representative transverse abdominal T2-weighted MRI of KG mouse that responded to chemotherapy drug at week 1 (A), and follow up abdominal MRI scan at week 5 (B). MRI image showing a decrease in cyst volume at endpoint.

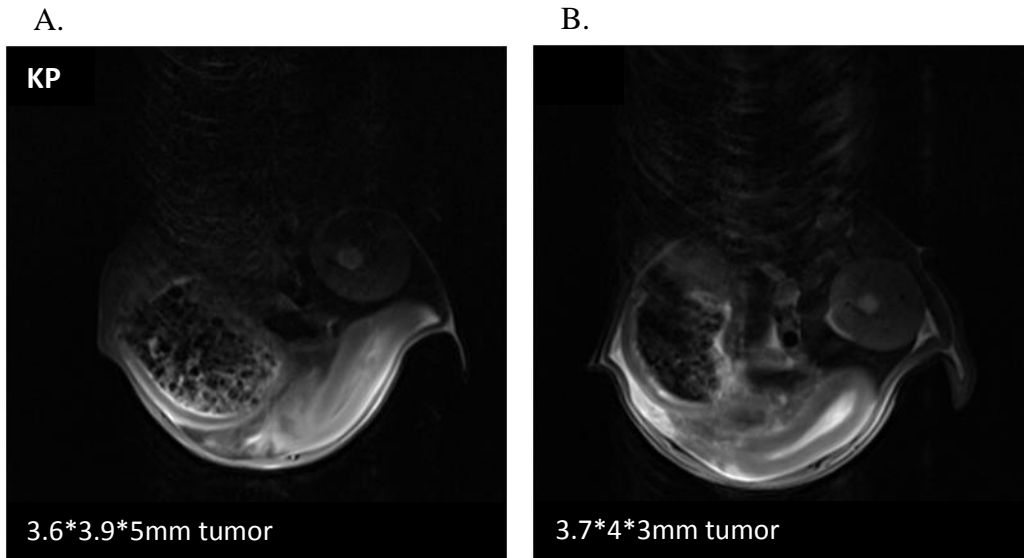


Fig. 8 Representative transverse T2-weighted MRI of KP mouse abdomen at week 1 (A), and follow up abdominal MRI scan at week 5 (B). MRI image showing a decrease in tumor volume at endpoint.

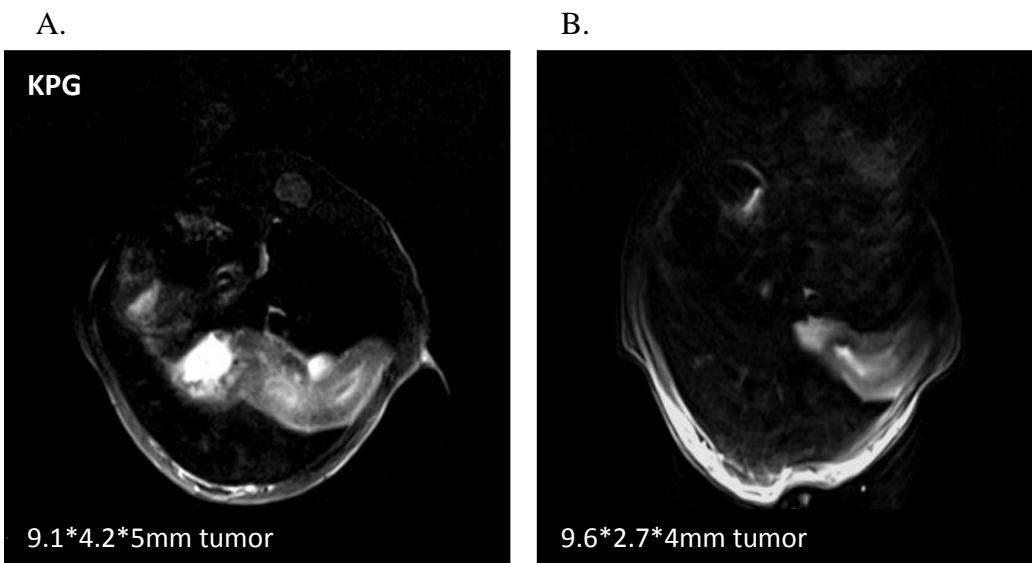


Fig. 9 Representative transverse T2-weighted MRI of KPG mouse abdomen at week 1 (A), and follow up abdominal MRI scan at week 5 (B). MRI image showing a decrease in tumor volume at endpoint.

Taking both data of tumor and cyst growth together, the untreated group had a 77% increase of both tumors and cysts in size. Either treatment with gemcitabine or dietary OPP alone produced a comparable effect in arresting the growth of half of tumors and cysts, both by 55%. The most striking result to emerge from this data is that the combinatorial treatment of dietary OPP and gemcitabine drug showed a synergistic effect in slowing the progression of PDAC with less than 10% of tumors and cysts increasing in size from week 1 and week 5 of the study (Fig. 10).

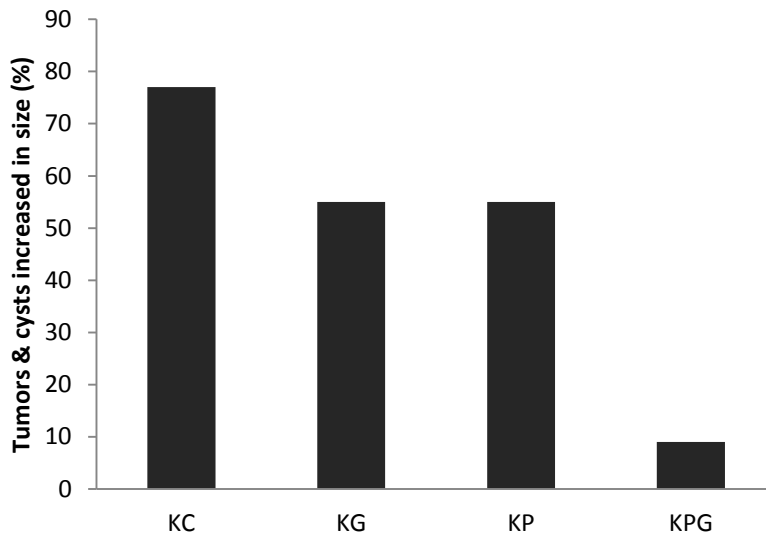


Fig. 10 Effect of dietary OPP on tumor and cyst growth. Data are expressed as percentage of tumors and cysts that increased in size following a 6-week treatment as monitored by MRI.

3.3 Toxicity analysis of OPP in non-PDAC controls

In order to exclude any possibilities of toxicity caused by dietary OPP consumed at 5% level, fore stomach and pancreatic tissues of non-PDAC control mice fed with OPP (CP) were examined microscopically and compared with the normal histoarchitecture of control mice receiving regular diet (CC).

Following six weeks of oral administration of OPP, histologic analysis in regular diet fed and OPP fed mice exhibited a normal fore stomach histoarchitecture. Epithelial hyperplasia or thickening of the fore stomach lining, hyperkeratosis, ulceration and inflammation associated with toxicity was not observed microscopically (Fig. 11). In pancreatic tissue, the similar presentation of normal histological structure of pancreas was observed in both CC and CP groups. Normal microscopic structure of pancreatic islets (endocrine glands) and also acinar cells (exocrine region) can be appreciated in control animals fed OPP, demonstrating no signs of toxicity of dietary OPP administered at 5% level (Fig. 12).

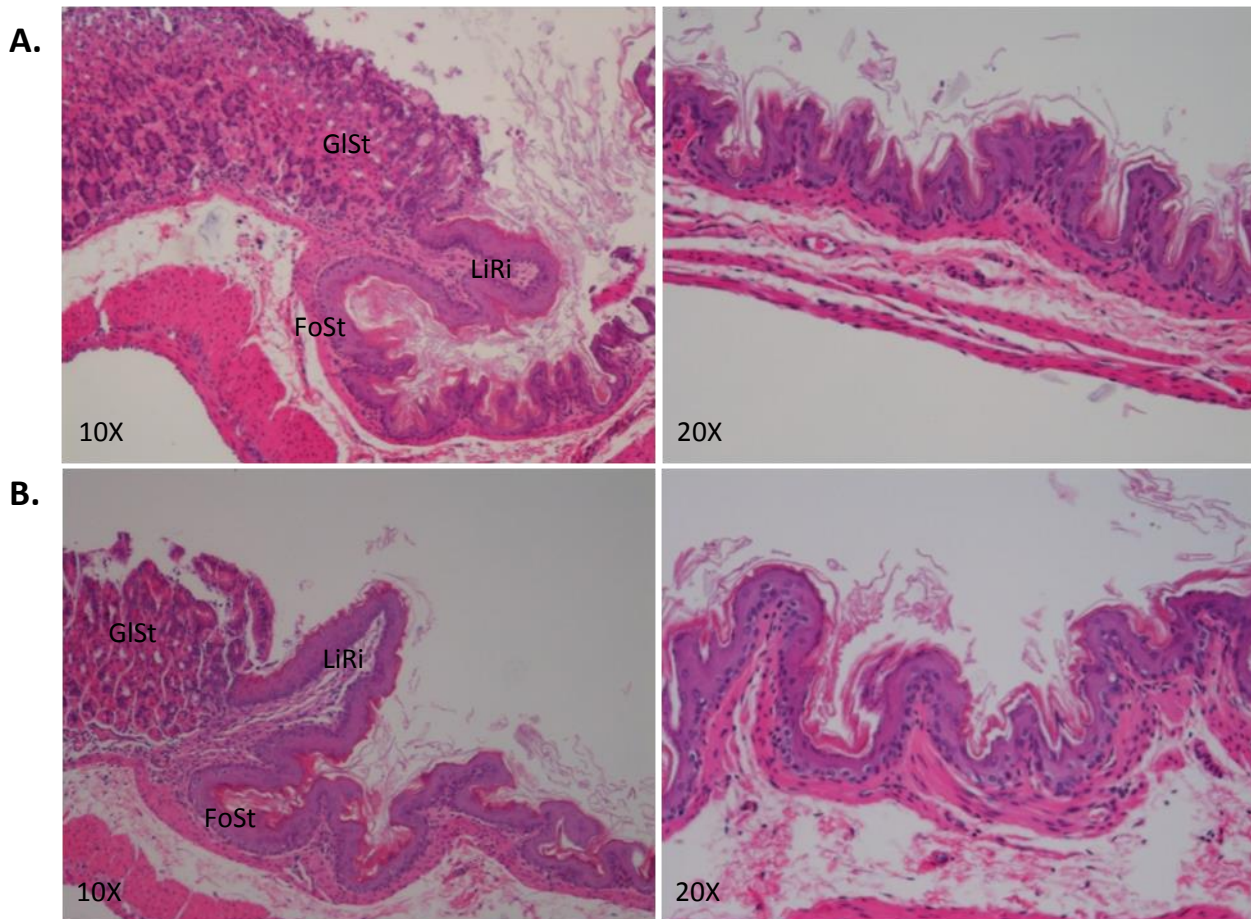


Fig. 11 Histological analysis of H&E stained fore stomach in control mice fed regular diet, CC (A), and 5% OPP diet, CP (B). Histological sections on left panel focusing on glandular stomach separated by the limiting ridge from of the fore stomach. Right panel showing similar normal fore stomach histoarchitecture in CP animal (below) compared to CC (above) indicating no signs of toxicity from 5% OPP administered. GISt = Glandular stomach, LiRi = Limiting ridge, FoSt = Fore stomach.

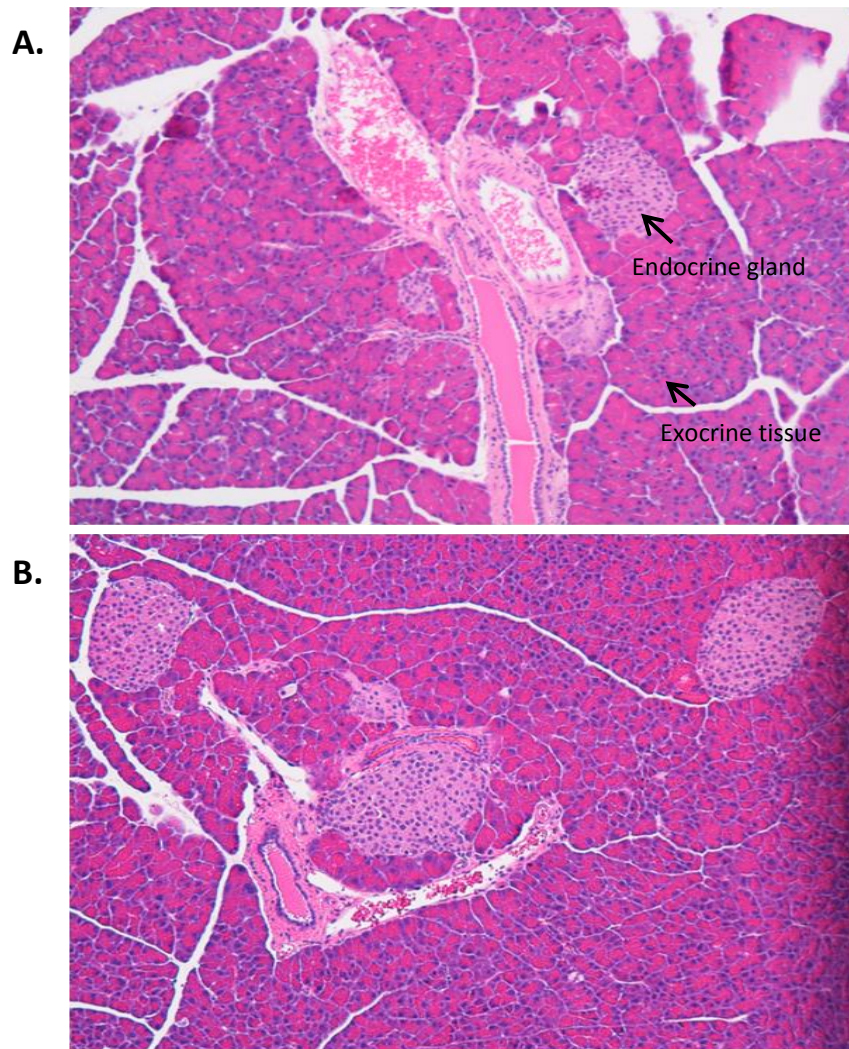


Fig. 12 Histological analysis of H&E stained pancreatic tissue from control mice fed with regular diet, CC (A), and 5% OPP diet, CP (B). Histological sections at 10X magnification demonstrate the normal region of endocrine and exocrine of the pancreas without signs of toxicity.

Specific Aim 2: To investigate mouse pancreatic tissue for antitumor activity of OPP by histology and gene expression.

3.4 Effect of OPP on Pancreatic Intraepithelial Neoplasia (PanIN) progression

The morphological alterations in pancreas through histopathological examination confirmed the formation of pancreatic cancer precursor lesions, PanINs in all four PDAC experimental groups (KC, KP, KG and KPG) by visualization of different lesion grades. PanIN lesions were graded into three grades; PanIN-1, PanIN-2 and PanIN-3 according to published criteria [13] and their numbers were recorded. Representative observations of the three PanIN grades identified in KPC mice of this study are displayed in Fig. 13.

PanIN-1 is considered as a low-grade PanIN lesion. Among the changes that characterized PanIN-1 include the change from a cuboidal duct epithelium to elongated cells and by the abundant accumulation of mucin. Nuclei of PanIN-1 are also basally located. Fig. 13a illustrates PanIN-1 lesion from a gemcitabine treated animal (KG). Basally oriented nuclei was observed (arrow A1) together with the presence of supranuclear mucin (arrow A2). As the lesions advance from the low-grade PanIN-1 to the higher grade PanIN lesion, PanIN-2, some nuclear abnormalities have become visible microscopically. The architectural make up of mucinous epithelial lesion of PanIN-2 can either be flat or papillary. Some of the nuclear alterations that can be seen in PanIN-2 lesion include loss of polarity, nuclear crowding, enlarged nuclei, pseudo-stratification and hyperchromatism. Fig. 13b represents PanIN-2 lesion from an animal treated with gemcitabine (KG). A loss in cell polarity of papillary mucinous epithelial cells can be appreciated from the micrograph (arrow B1). The highest grade of PanIN lesions is PanIN-3. It is the pre-invasive form of adenocarcinoma. Architecturally, PanIN-3 is papillary or micropapillary, although they may also appear flat. This lesion may form budding into the

pancreatic lumen with the observance of severe nuclear atypia and some abnormal mitosis. Fig. 13c shows a PanIN-3 lesion from an animal receiving dietary OPP intervention (KP). Arrow C1 displays the “budding off” of epithelial cells into the lumen.

We investigated the effect of various diets and/or treatments given on the overall PanIN count, totaling all three different PanIN grades together. As shown in Fig. 14, the average number of PanIN lesions detected in untreated group, KC, were significantly higher than all treated groups ($p < 0.05$). We observed that, similar to gemcitabine, OPP diet regimen, KP and KPG reduced the total number precursor lesions with the greatest reduction was seen in the combination of OPP and gemcitabine group (KPG).

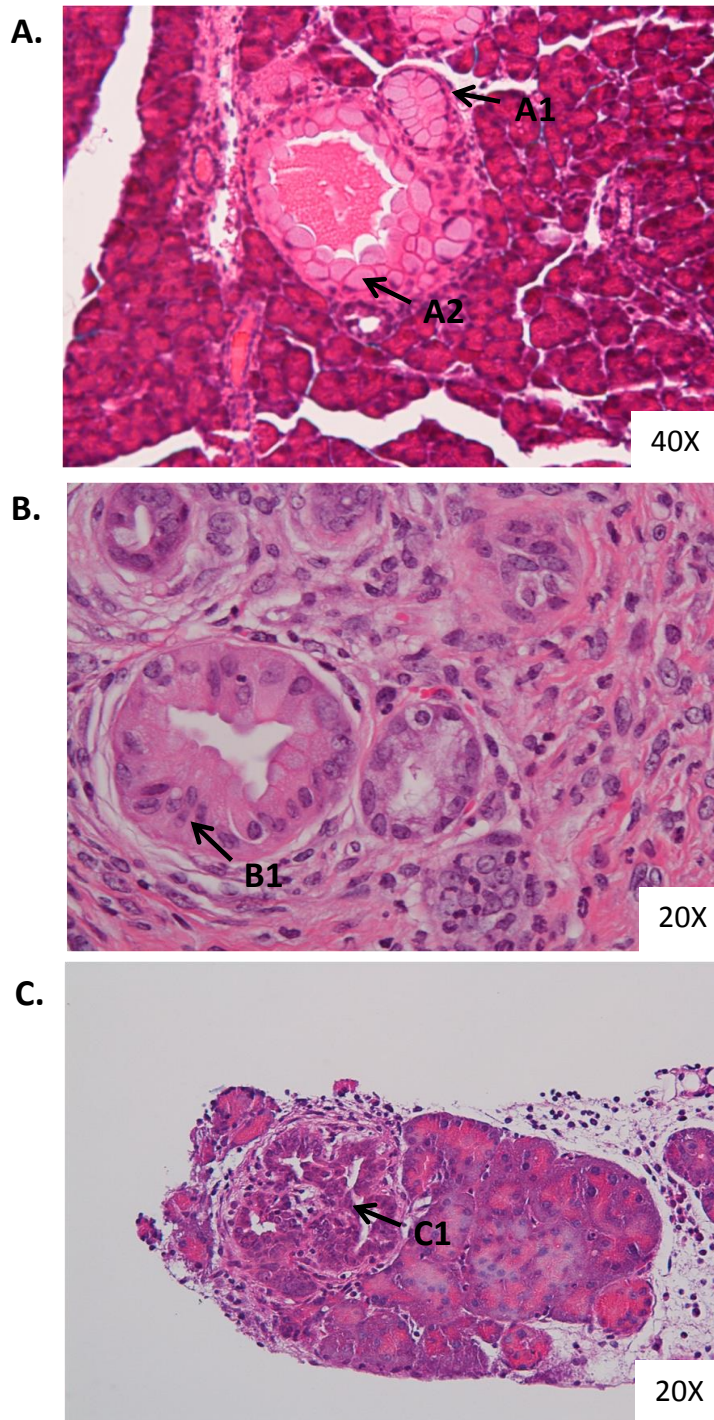


Fig. 13 Representative H&E stained pancreatic tissue the three PanIN grades in KPC mice. (A) PanIN-1 from a KG mouse. Arrow above (A1) pointing at basally located nuclei, arrow below (A2) indicates the presence of supranuclear mucin. (B) PanIN-2 from a KG mouse. Arrow B1 reveals a loss in cell polarity of papillary mucinous epithelial cells. (C) PanIN-3 from a KP mouse. Arrow C1 shows “budding off” of epithelial cells into the lumen.

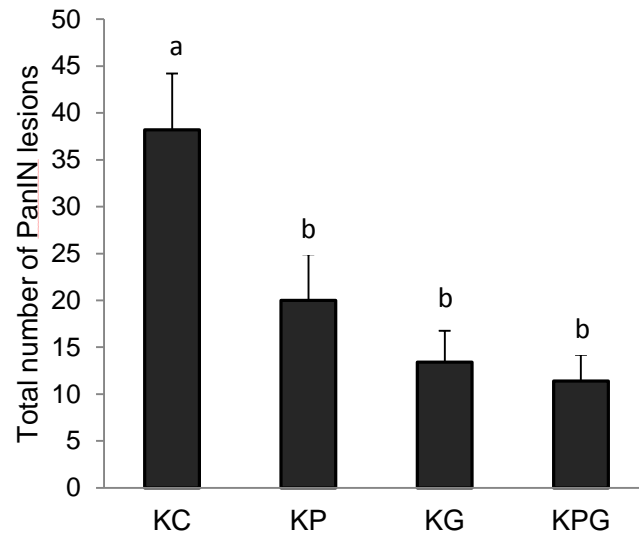


Fig. 14 Effect of dietary OPP and/or gemcitabine on total PanIN lesion count. Data are expressed as mean±SE. All three treatment groups had a significantly lower count of total PanIN ($p<0.05$) compared to untreated group, KC. The lowest count was exhibited by group receiving both 5% OPP diet and gemcitabine drug (KPG).

Further, we broke down total PanIN count into grades. As can be seen from Fig.15, there were no significant differences among groups in the average number of PanIN-1 lesions ($p>0.05$). For PanIN-2, treatment with gemcitabine drug significantly reduced the number of PanIN-2 lesion compared to the untreated group, KC ($p<0.01$). Interestingly, OPP treatment alone (KP) and its combination with gemcitabine (KPG) both demonstrated similar ability in significantly reducing PanIN-2 count as of gemcitabine drug with greater effect seen in KPG group ($p<0.05$ and $p<0.01$ respectively). For PanIN-3, gemcitabine treatment significantly reduced the number of PanIN-3 lesion compared to the untreated group, KC ($p<0.05$). Although not statistically significant, OPP treatment group was observed to have a lower count of PanIN-3 compared to the untreated group, KC. However, it is exciting to highlight that the combination of OPP with gemcitabine was able to retard PanIN progression as evident from the significant reduction of PanIN-3 lesions compared to KC group at same statistical significance as gemcitabine ($p<0.01$).

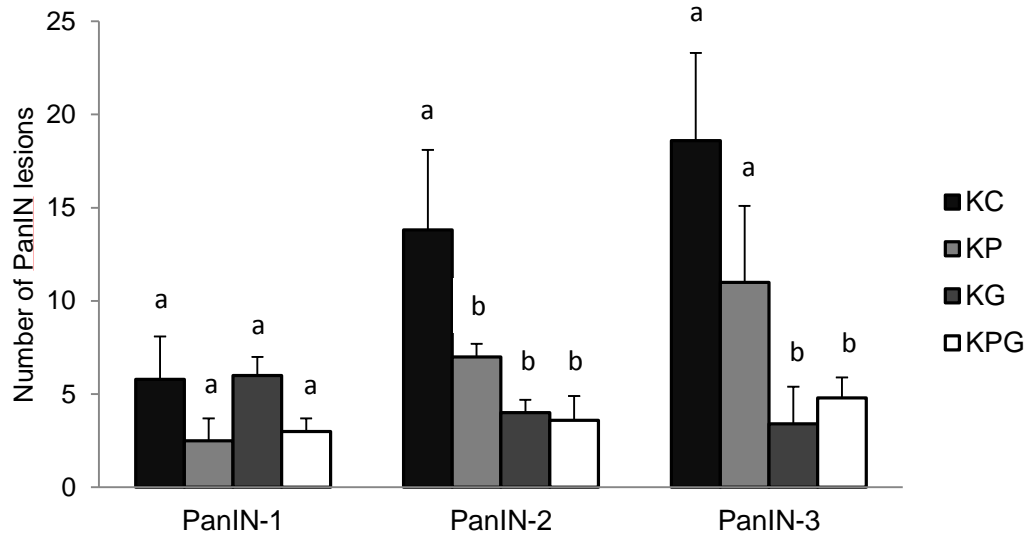


Fig. 15 Effect of dietary OPP and/or gemcitabine on different PanIN grades. Data are expressed as mean±SE. Compared to the untreated group, KC, PanIN 2 count was significantly lower in all treatment groups; KP ($p<0.05$), KG and KPG groups ($p<0.01$). PanIN 3 count was significantly lower only in KG and KPG groups ($p<0.01$).

3.5 Immunohistochemical analysis of selected tumor markers

3.5.1 S100P

In PDAC, the calcium-binding protein S100P is the most significantly up regulated protein among several other S100 proteins. It can be seen from Fig. 16 that over expression of tumor promoter gene, S100P was highly prominent in the untreated group, KC, while a satisfactory effect of gemcitabine in lowering the expression of S100P was noticeable in KG group. Remarkably, much lower expression was observed in both OPP and OPP-gemcitabine treated groups. KPG group in particular showed the least activation of S100P. Moreover, it can also be appreciated from the micrograph that the morphological structure of the pancreas in this group receiving combinatorial treatment of OPP and gemcitabine is better preserved compared to all other groups.

3.5.2 SMAD4

SMAD4 is one of the most potent tumor suppressors of PDAC. As shown in Fig. 17, the loss of expression of tumor suppressor gene, SMAD4 was clear in the group without any treatment, KC. More adhesion of staining was observed in KG group indicating less inactivation of SMAD4 with gemcitabine drug treatment. The anticancer effect following dietary treatment with OPP was evident as visualization of a strong SMAD4 protein staining in KP group. Furthermore, the combination of OPP with gemcitabine showed a positive labeling of SMAD4 protein with the strongest immunoreactivity demonstrating the most SMAD4 expression among other treatment groups.

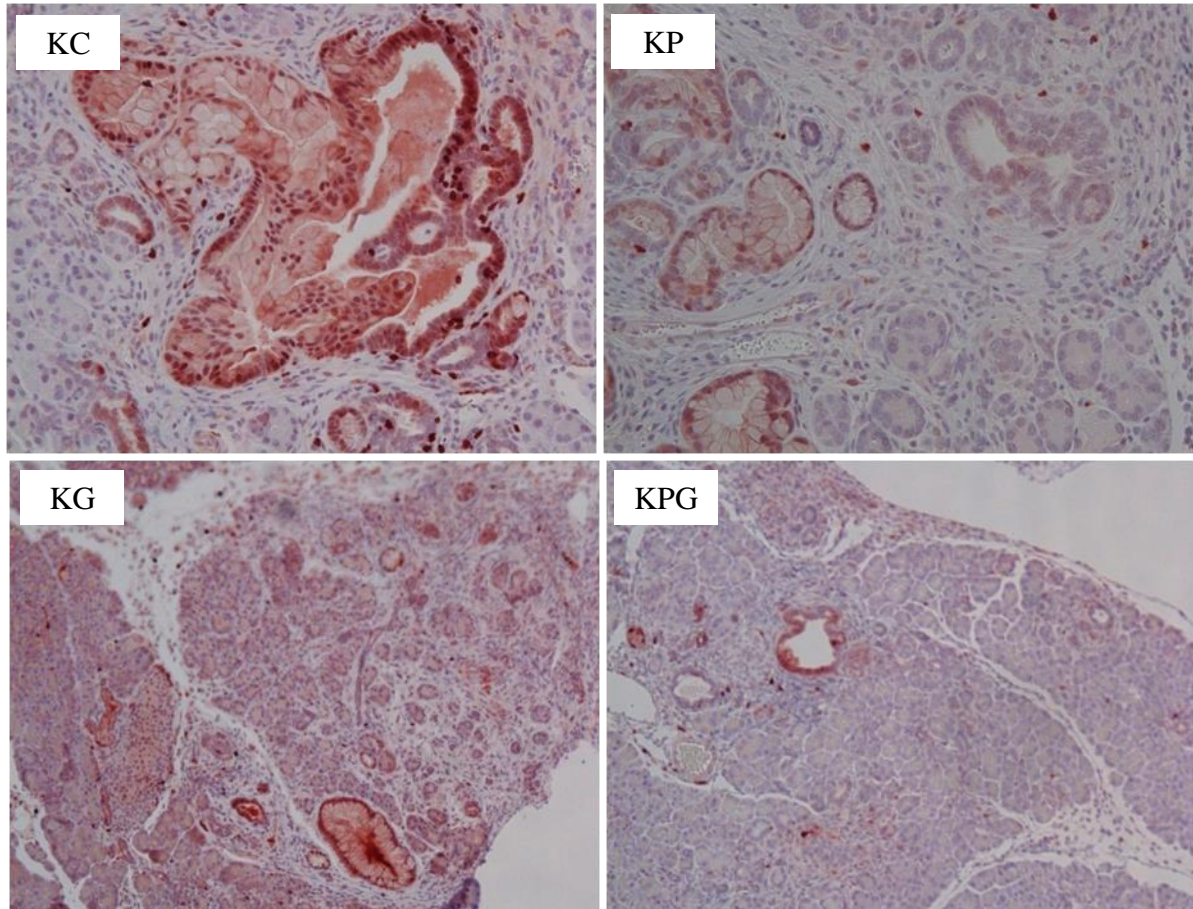


Fig. 16 Immunohistochemical analysis of the tumor promoter, S100P expression. Less expression primarily observed in KP (5% dietary OPP) and KPG (5% dietary OPP and gemcitabine) groups compared to the untreated group, KC.

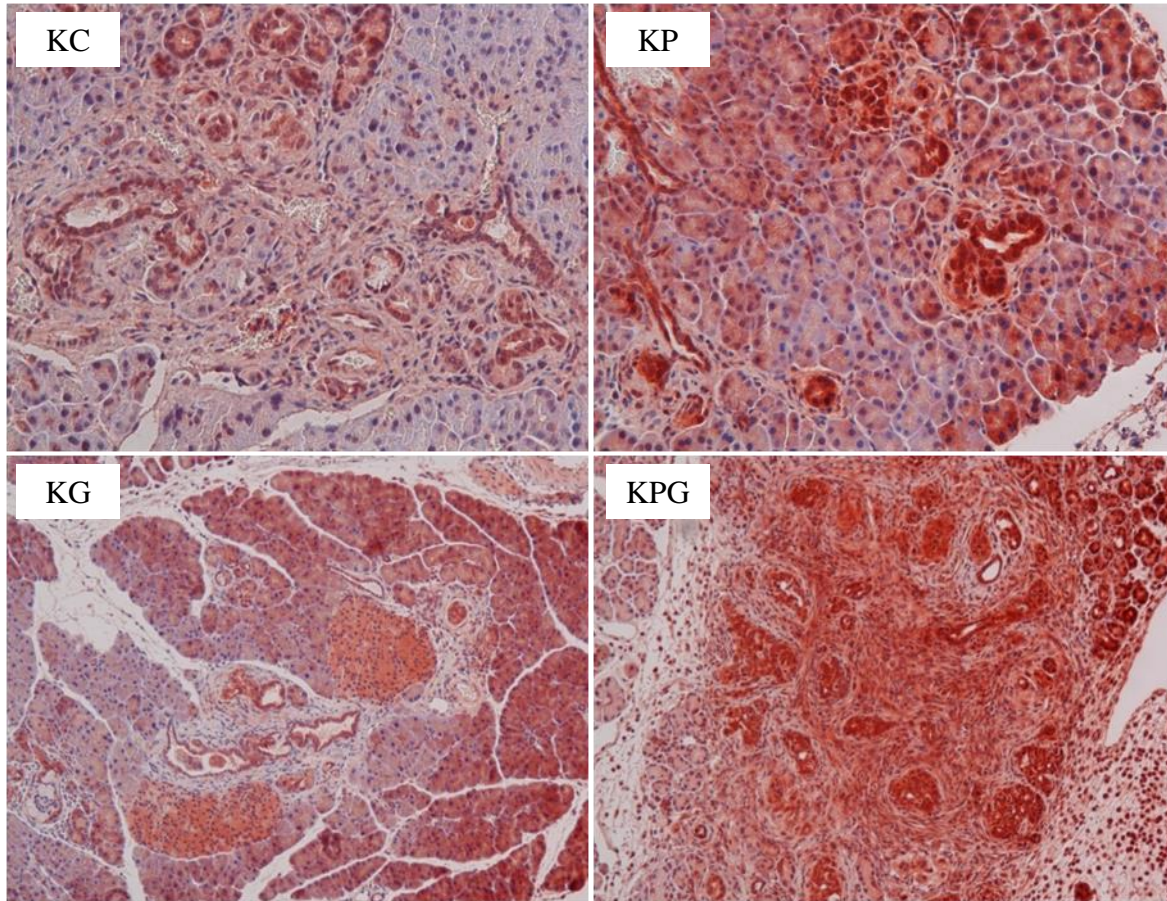


Fig. 17 Immunohistochemical analysis of the tumor suppressor, SMAD4 expression. More expression observed in KP (5% dietary OPP) and KPG (5% dietary OPP and gemcitabine) groups compared to the untreated group, KC.

3.6 Gene expression analysis of selected tumor markers

The mRNA expression of Notch1, MMP9 and CCND1 was examined in pancreatic tissues of mice from PDAC experimental groups (KC, KP, KG and KPG) by qRT-PCR. Gene expression levels are presented as ΔC_T values normalized against β -actin. Statistical significance was calculated by comparing mean ΔC_T of each treatment group (KP, KG and KPG) to the untreated PDAC group (KC). Since Cycle Threshold, C_T is in the logarithmic scale, C_T values are inversely proportional to the initial amount of target marker present in the sample. Therefore, low expression of a particular gene is represented by a high ΔC_T value while highly expressed genes have low ΔC_T values.

3.6.1 Notch1

As can be seen from Fig. 18a, compared to the untreated pancreatic cancer group, there were no significant differences in the expression of Notch1 in groups receiving OPP or gemcitabine treatment alone. However, it was remarkably observed that the OPP-gemcitabine combination had a statistically higher ΔC_T than the untreated group demonstrating a synergistic effect in lowering the pancreatic mRNA expression of Notch1 ($p < 0.05$).

From our MRI data, we observed that all animals did not respond to gemcitabine and/or OPP. Thus, we used this information to further split the gene expression results of these two groups into responders and non-responders. By separating OPP responders from non-responders, it was revealed that OPP produced a significant down regulation in responder mice compared to untreated mice ($p < 0.05$; Fig. 18b). However, the higher ΔC_T of Notch1 observed in gemcitabine treated responders was not found to be significant when compared to untreated mice (Fig. 18c).

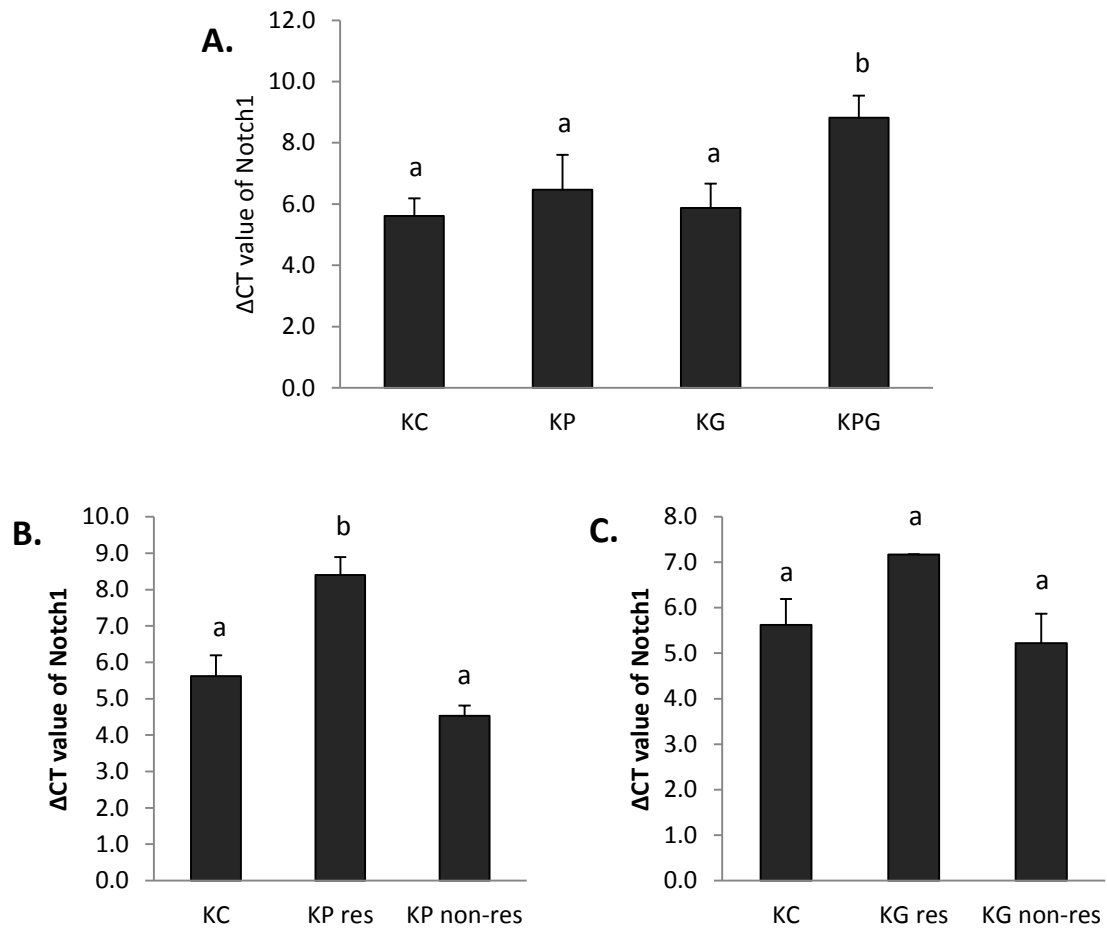


Fig. 18 Notch1 regulation by OPP treatment. OPP with gemcitabine (KPG) synergistically down regulates Notch1 expression. Data are expressed as delta C_T values normalized against β -actin (mean \pm SE). C_T values are inversely proportional to the initial amount of target marker, therefore a higher C_T value represents a lower expression level. **(A)** Notch1 expression is significantly lower in KPG group compared to untreated group, KC ($p < 0.05$). **(B)** Separating OPP treated (KP) responders from non-responders reveals a significant down regulation in responder mice compared to KC group ($p < 0.05$). **(C)** No significant differences in Notch1 expression among gemcitabine treated (KG) responders and non-responders compared to KC group ($p > 0.05$).

3.6.2 Matrix metalloproteinase-9 (MMP9)

Fig. 19 shows the pancreatic mRNA expression of MMP9 following different treatments. Treatment with OPP or gemcitabine alone was not found to alter the expression of Notch1 compared to the untreated group with no statistical differences in mean ΔC_T of these groups. Likewise to Notch1, the combination of these two agents together significantly reduced the expression of MMP9 compared to the untreated group ($p < 0.05$; Fig. 19a). Despite when taken as a whole, the levels of MMP9 in OPP treated mice were not significantly different from non-treated controls, a down-regulation was significantly pronounced when OPP responders were separated from non-responders ($p < 0.05$; Fig. 19b). On the other hand, upon separating the responders from non-responders in gemcitabine group, the up-regulation of MMP9 expression compared to untreated controls was not statistically significant (Fig. 19c).

3.6.3 Cyclin D1 (CCND1)

As shown in Fig. 20a, the group receiving combinatorial treatment of OPP with gemcitabine had a significantly higher ΔC_T than the untreated group ($p < 0.05$). But single treatment with OPP or gemcitabine did not change the expression of Notch1. Similar to both two markers presented above, this indicates a synergistic down-regulation of pancreatic CCND1 expression by OPP and gemcitabine together. Unlike the significant down-regulation of MMP9 and Notch1 observed in OPP responders, the increased mean ΔC_T of CCND1 in OPP responder group was not statistically significant compared to untreated group (Fig. 20b). The same observation was noted upon separating gemcitabine responders from non-responders (Fig. 20c).

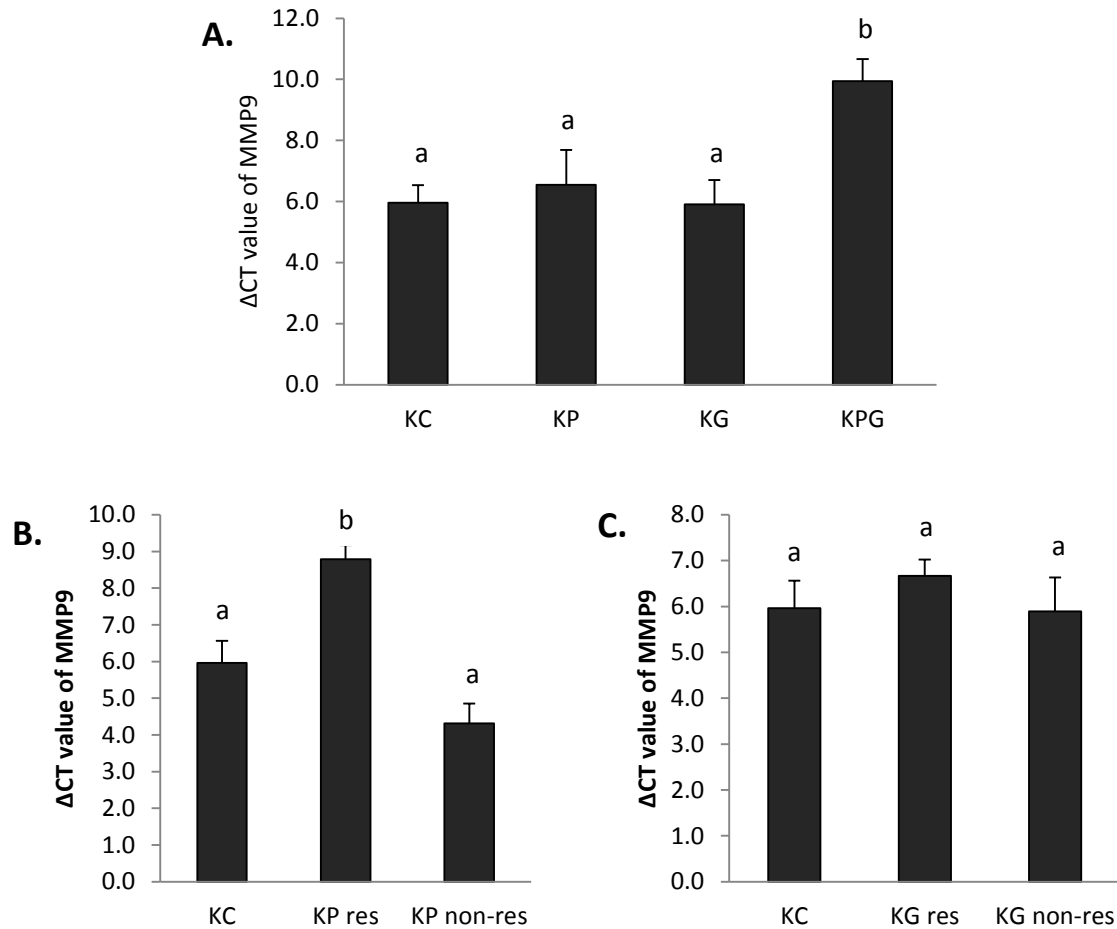


Fig. 19 MMP9 regulation by OPP treatment. OPP with gemcitabine (KPG) synergistically down regulates MMP9 expression. Data are expressed as delta C_T values, normalized against β -actin (mean \pm SE). C_T values are inversely proportional to the initial amount of target marker, therefore a higher C_T value represents a lower expression level. (A) MMP9 expression is significantly lower in KPG group compared to untreated group, KC ($p < 0.05$). (B) Separating OPP treated (KP) responders from non-responders reveals a significant down regulation in responder mice compared to KC group ($p < 0.05$). (C) No significant differences in MMP9 expression among gemcitabine treated (KG) responders and non-responders compared to KC group ($p > 0.05$).

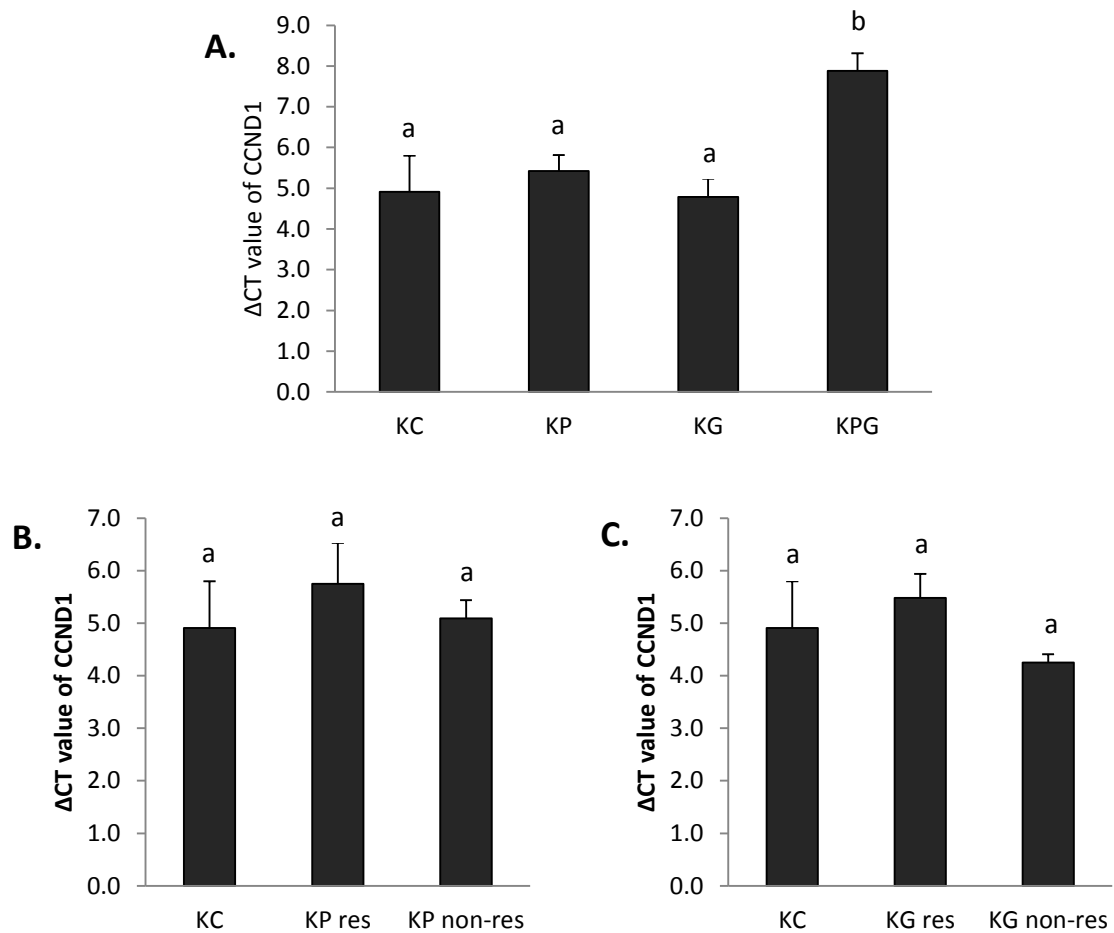


Fig. 20 CCND1 regulation by OPP treatment. OPP with gemcitabine (KPG) synergistically down regulates CCND1 expression. Data are expressed as delta C_T values normalized against β -actin (mean \pm SE). C_T values are inversely proportional to the initial amount of target marker, therefore a higher C_T value represents a lower expression level. **(A)** CCND1 expression is significantly lower in KPG group compared to untreated group, KC ($p < 0.05$). **(B)** CCND1 expression in both OPP treated (KP) responders and non-responders displays no significant difference compared to KC group ($p > 0.05$). **(C)** No significant differences in CCND1 expression among gemcitabine treated (KG) responders and non-responders compared to KC group ($p > 0.05$).

Specific Aim 3: To conduct urinary metabolomic investigation of KPC transgenic mice following dietary OPP treatment.

3.7. Exploration of urinary ^1H NMR metabolomic profiles of different groups

Differences in the metabolomic profiles of KPC transgenic mice subjected to different treatments of dietary OPP and gemcitabine drug in this study were evaluated using proton nuclear magnetic resonance spectroscopy, ^1H NMR. Spectra separation or discrimination analysis was carried out through the use of SIMCA-P+ software utilizing both unsupervised (PCA) and supervised techniques (PLS-DA and OPLS-DA). We aimed to look for possible distinction of urinary metabolomic profiles in three comparisons detailed below.

3.7.1 Discrimination analysis of metabolomic profiles between PDAC mice and non-PDAC controls

We began our analysis with unsupervised principal component analysis (PCA) which provides a basic overview for initial exploration of the data. The PCA score plot in Fig. 21a shows a good separation of the urinary NMR spectra of untreated PDAC mice (KC) and non-PDAC controls (CC) at study endpoint, week 6. The first principal component (PC1) accounts for the most variation in the data and the subsequent component (PC2) accounts for the second most variation in the data. As depicted by the diagram (Fig. 21a), the two groups are being clearly separated along the PC1. It is notable that the spectra from CC group, represented by circles on the diagram are much closer to each other than the KC group, in which the squares are slightly far from each other. This might reflect diversity in metabolomic profile among the untreated PDAC animals (KC) based on the progression of the disease. The corresponding loading plot in Fig. 21b manifests the regions in the spectra comprising metabolites that are influential in the separation of the two groups. Using the supervised technique, PLS-DA score

plot shows an even more pronounced separation between the two groups (Fig. 22a). Class discrimination for the supervised method improves the transparency and interpretability of the model. The variable importance of projection (VIP) plot reveals the 33 regions in the spectra including 1.1-2.0, 3.2-3.4, 3.6-3.8, 4.3 and 5.7-5.8 ppm as metabolites that are responsible for the clustering by PLS-DA using VIP score of more than 2 (Fig. 22b).

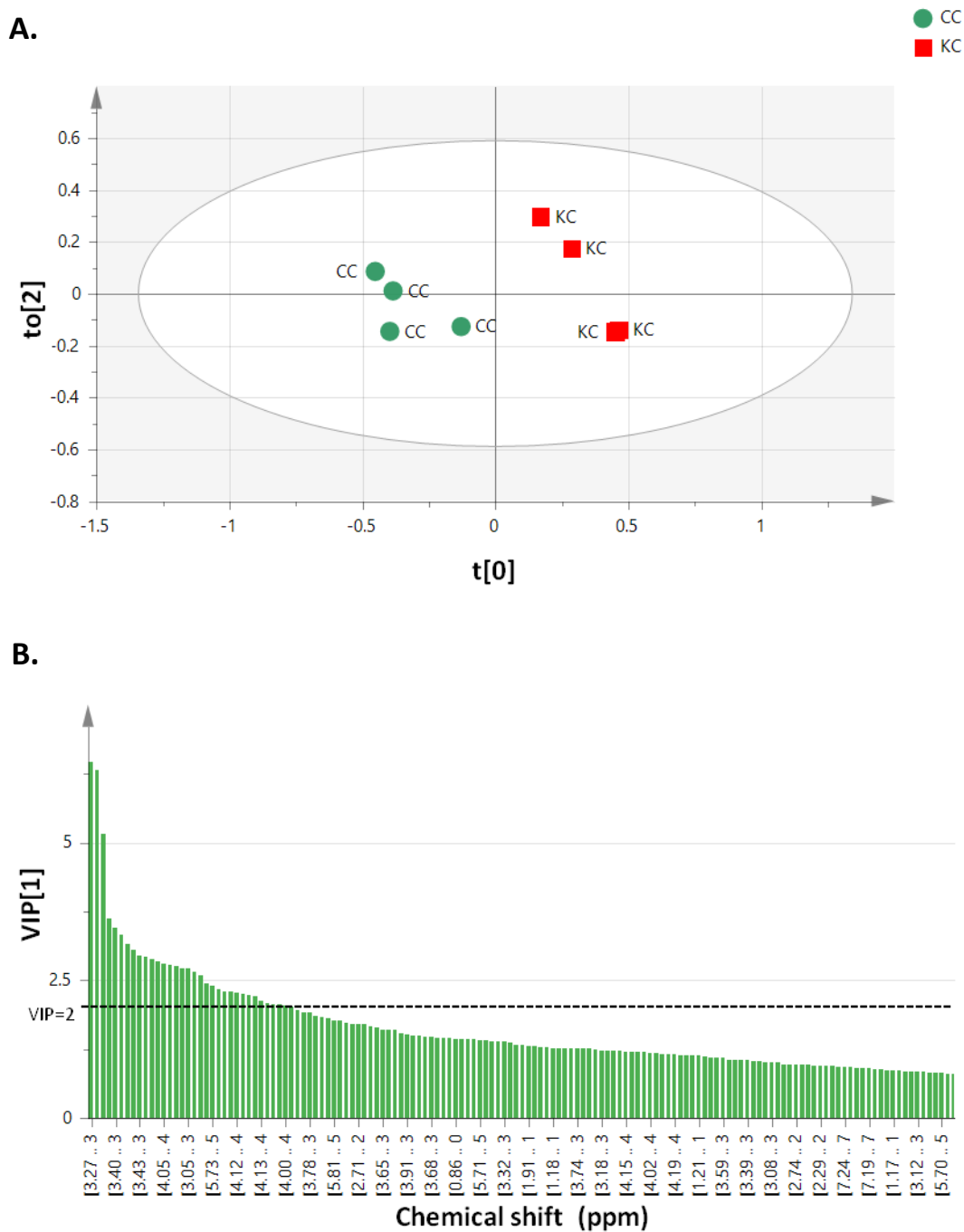


Fig. 22 Multivariate analysis of KC and CC groups utilizing the supervised method, PLS-DA. (A) Score plot based on urinary ^1H NMR spectra of mice with pancreatic cancer, PDAC (KC) and non-PDAC controls, (CC) at study endpoint using supervised method, PLS-DA. **(B)** Variable importance in the projection (VIP) plot shows the top 40 most important regions in the spectra as metabolites that are responsible for the clustering by PLS-DA.

3.7.2 Discrimination analysis of metabolomic profiles with PDAC progression

In order to understand the changes in the metabolomic profile following the progression of pancreatic cancer alone and to identify the responsible metabolites, the similar analysis as described above was performed on the NMR spectra of the untreated PDAC group (KC) at week 2 and week 6. As shown in Fig. 23a, only a certain degree of separation between the two time points was observed from the PCA score plot. By visual inspection on the loading plot (Fig. 23b), it is rather difficult to characterize the ppm regions on the below right quadrant (3.6-3.8, 4.3, 5.7-5.8 ppm) based on the two time points. Therefore, supervised classification using OPLS-DA was carried out to maximize the separation. As expected, the employment of OPLS-DA to the model improved the clustering of urinary NMR spectra of PDAC mice at study baseline and at endpoint (Fig. 24a). Fig. 24b shows the contribution plot generated from OPLS-DA score plot. The upper panel displays spectra regions containing metabolites that are present at a higher concentration at week 2 (3.6-3.8, 3.7-4.1 ppm) while lower panel is associated with week 6 (3.2-3.4, 4.3, 5.7-5.8 ppm). Upon identification, metabolites in these regions could serve as possible biomarkers of PDAC progression with potential use for early diagnosis of the disease.

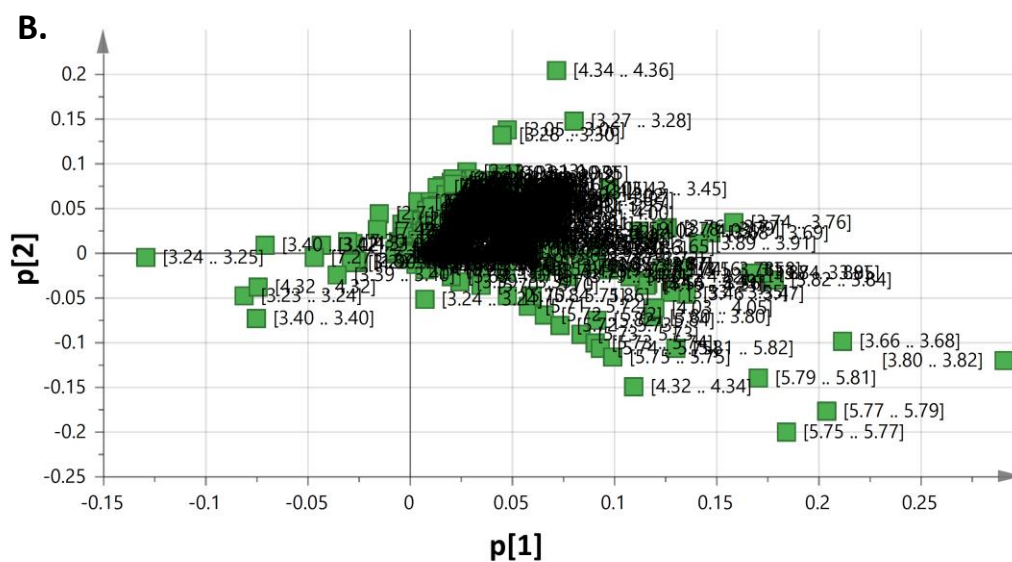
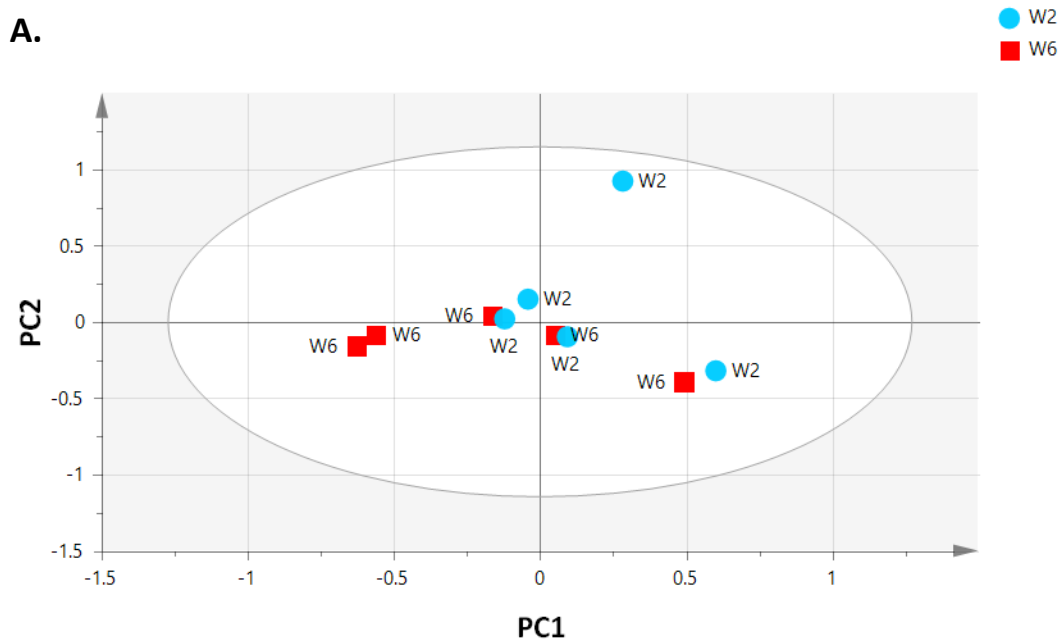


Fig. 23 Multivariate analysis of KC group at baseline and endpoint utilizing the unsupervised method, PCA. (A) PCA score plot based on urinary ^1H NMR spectra of PDAC mice at study baseline, week 2 (W2) and at endpoint, week 6 (W6). **(B)** Corresponding loading plot showing the regions in the spectra comprising metabolites that are responsible for the separation of the two time points.

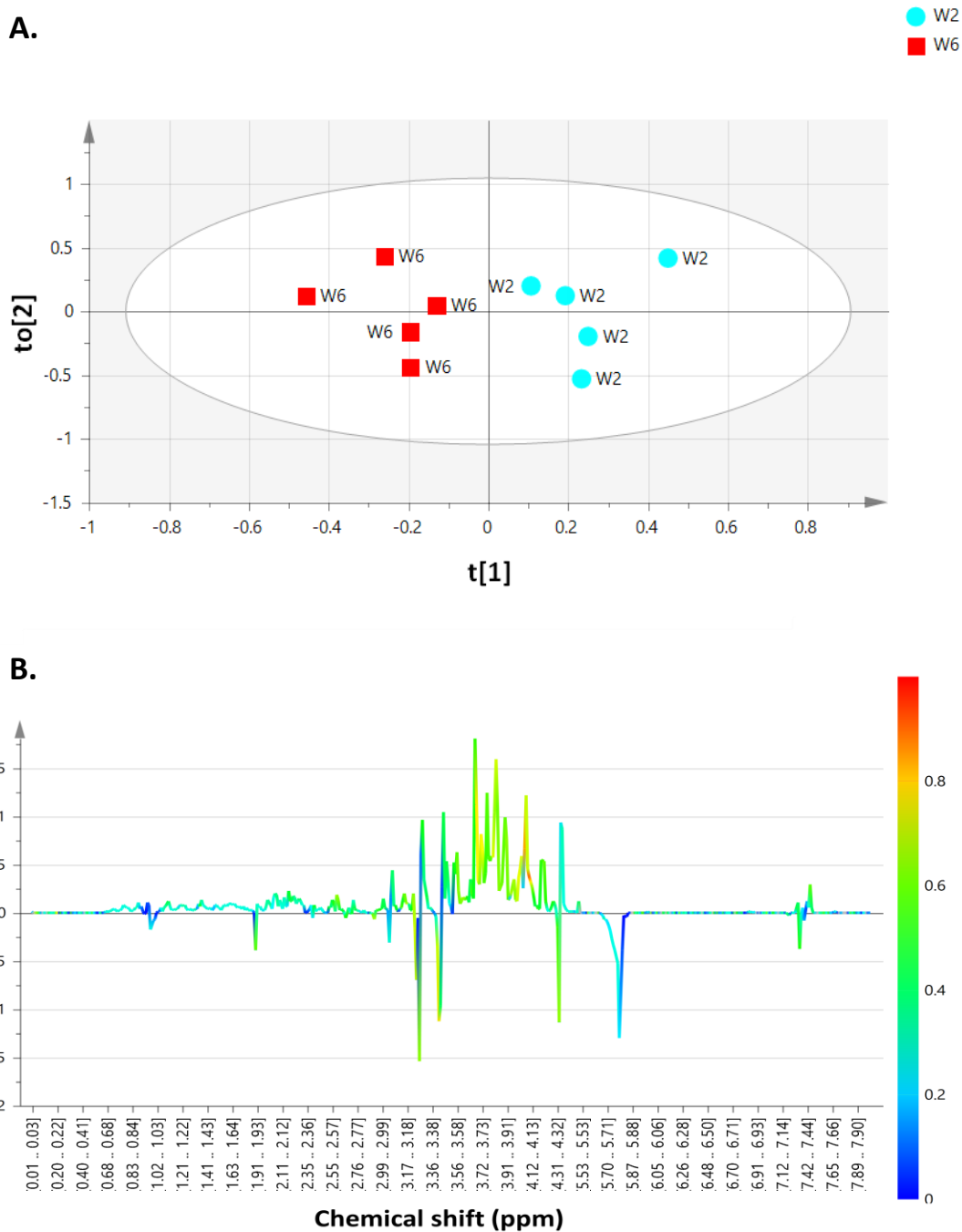


Fig. 24 Multivariate analysis of KC group at baseline and endpoint utilizing the supervised method, OPLS-DA. (A) Better clustering of urinary ^1H NMR spectra of PDAC mice at study baseline, week 2 (W2) and at endpoint, week 6 (W6) with OPLS-DA. (B) Contribution plot generated from OPLS-DA score plot. Upper panel displays spectra regions containing metabolites associated with W2 while lower panel associated with W6.

3.7.3 Discrimination analysis of metabolomic profiles following OPP treatment

To comprehend the metabolic changes following the administration of dietary OPP, the spectra from the untreated PDAC group (KC) and OPP treated group (KP) at study endpoint, week 6 were compared. In a similar manner, we first generated a PCA model for discrimination assessment. The resulting PCA plot (Fig. 25a) illustrates an obvious separation of the two groups. PCA loading plot generated from the model identifies the regions in the spectra comprising metabolites that are responsible for the clustering (Fig. 25b). Subsequently, the separation of the spectra was further enhanced when supervised PLS-DA was performed (Fig. 26a). At VIP threshold of 2, 31 regions in the spectra including 3.2-3.4, 3.6-3.8, 4.3, 5.7-5.8, 7.1-7.2 ppm were revealed as metabolites responsible for the spectra discrimination (Fig. 26b).

Furthermore, to assess the degree of separation of the urinary spectra of all the four PDAC experimental groups, principal component analysis (PCA) was performed. As shown by the score plot in Fig. 27, three clusters can generally be identified. Most animals receiving dietary OPP treatment alone (KP) and and OPP-gemcitabine combination (KPG) were clustered very close to each other away from the untreated PDAC group (KC). It is also observed that KP and KPG groups are not clustering together with the gemcitabine treated group (KG). Moreover, some spectra of KG animals were detected to be clustered near to the untreated PDAC group (KC). This supports our observations of some non-responders to the gemcitabine treatment in our MRI and mRNA expression data presented earlier under sections 3.2 and 3.6.

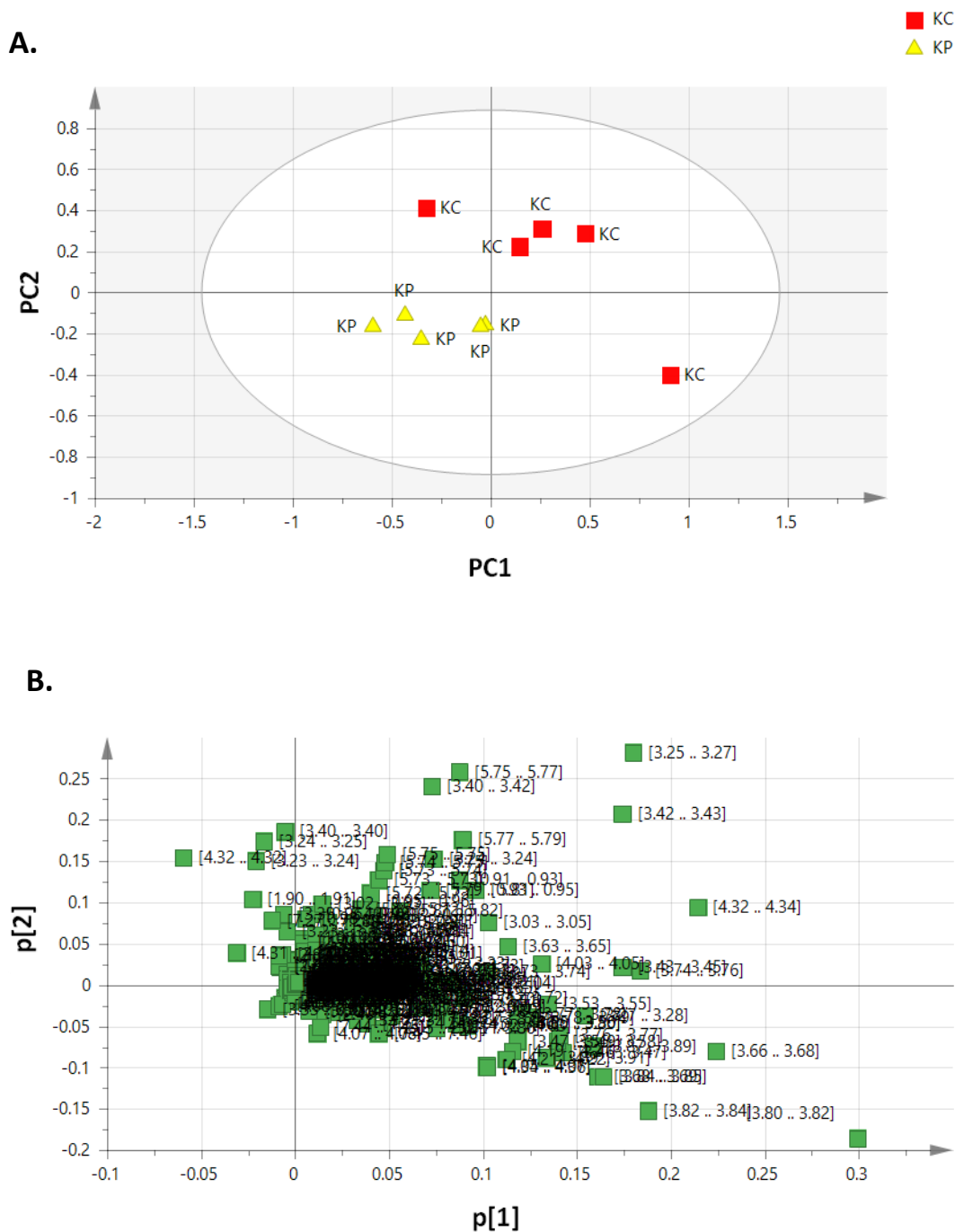


Fig. 25 Multivariate analysis of KC and KP groups utilizing the unsupervised method, PCA. (A) PCA score plot based on urinary ^1H NMR spectra of mice with pancreatic cancer, PDAC (KC) and OPP treated (KP) at study endpoint. **(B)** Corresponding loading plot manifesting the regions in the spectra comprising metabolites that are influential in the separation of the two groups.

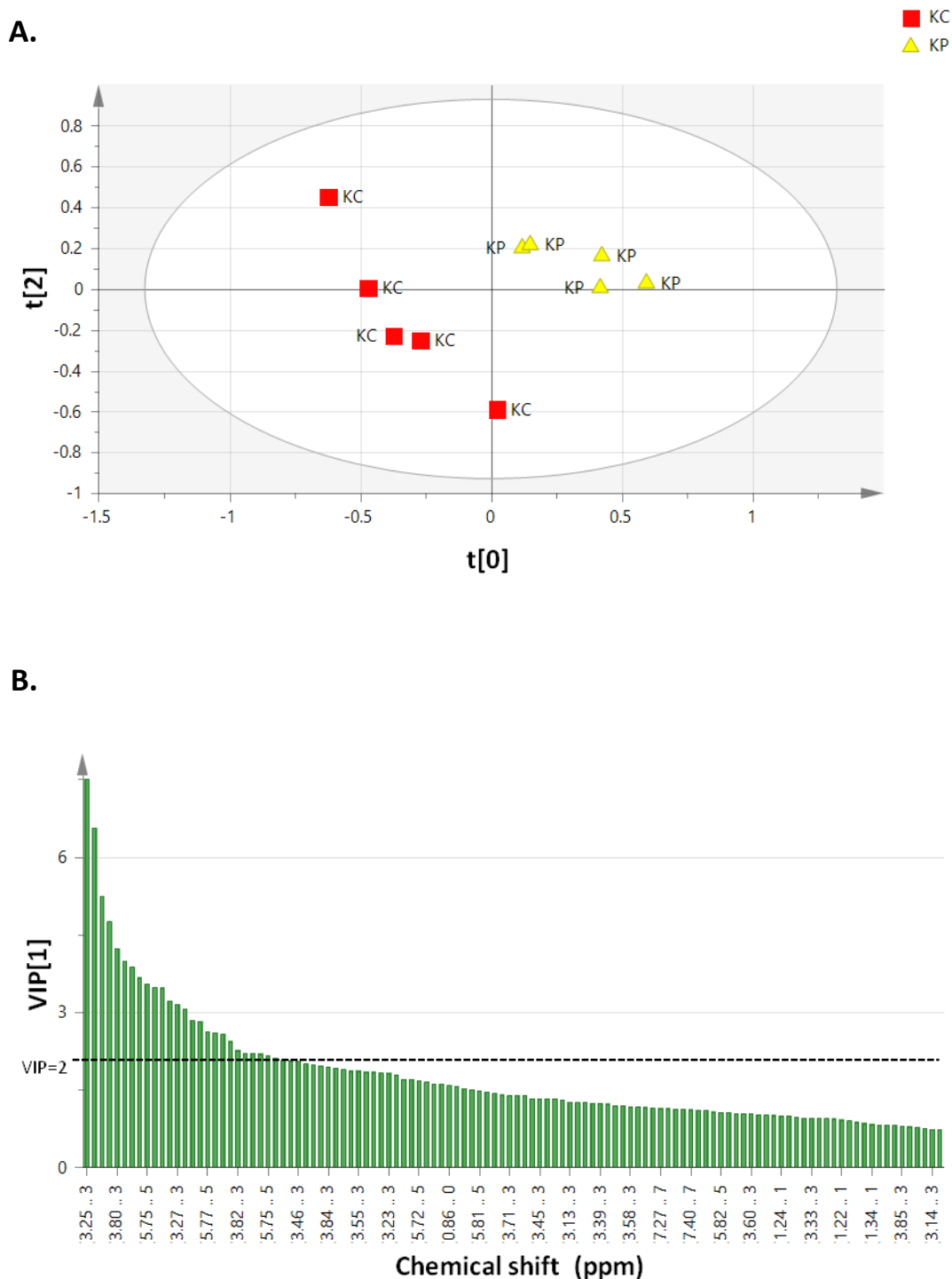


Fig. 26 Multivariate analysis of KC and KP groups utilizing the supervised method, PLS-DA. (A) Score plot based on urinary ^1H NMR spectra of mice with pancreatic cancer, PDAC (KC) and OPP treated (KP) at study endpoint. **(B)** Variable importance in the projection (VIP) plot reveals the top 40 regions in the spectra as metabolites that are responsible for the clustering by PLS-DA.

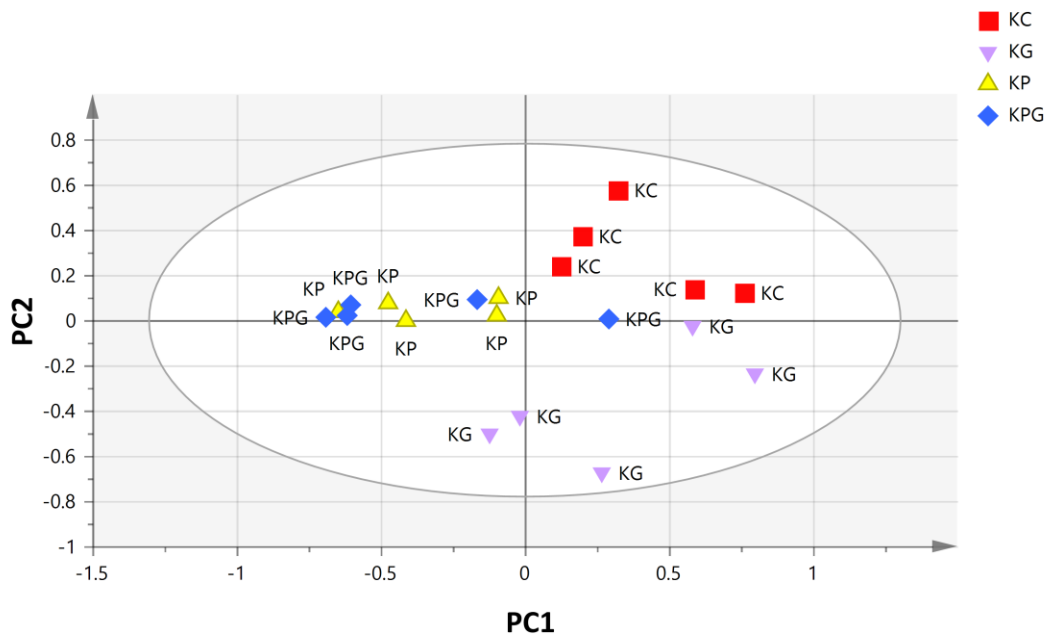


Fig. 27 Multivariate analysis of PDAC groups utilizing the unsupervised method, PCA. (A) Unsupervised, PCA score plot based on urinary ^1H NMR spectra of mice with different treatments at study endpoint. (KC = untreated PDAC mice; CC = non-PDAC control mice; KC W2 = untreated PDAC mice at study baseline, week 2; KC W6 = untreated PDAC mice at study endpoint, week 6; KG = PDAC mice treated with gemcitabine drug, KP = PDAC mice on 5% dietary OPP, KPG = PDAC mice on 5% dietary OPP and gemcitabine drug).

3.8 Identification and quantification of differential metabolites

Chenomx NMR Suite software (Chenomx Inc., Edmonton, Canada) was used to identify and quantify the metabolites responsible for separation observed in PCA, PLS-DA and OPLS-DA score plots. Metabolites were identified and measured for their concentrations by fitting the spectral peaks found for each compound in the compound library. The detail alteration trends of the profiled metabolites are shown in Table 3. The ratio above 1 indicates an increase, while the ratio below 1 indicates a decrease in metabolite concentration between groups.

Metabolites identified to be significantly changed in PDAC mice (KC) when compared to non-PDAC controls (CC) are shown in Fig. 28. Significantly decreased urinary metabolites include creatinine, formate and tartrate ($p < 0.05$) whereas the level of urea was significantly higher in KC group compared to CC group ($p < 0.01$). Urinary level of urea in untreated PDAC group (KC) was found to be significantly lowered with the progression of the disease from week 2 to week 6 (Fig. 29; $p < 0.05$).

As shown in Fig. 30., it was observed that with dietary intervention with OPP (KP), urinary concentrations of alanine, creatinine, glycerate, succinate and taurine were significantly decreased compared to untreated PDAC group (KC). Intervention with the combinatorial intervention of OPP and gemcitabine produced a significant decrease in the similar metabolites as intervention with OPP alone; alanine ($p < 0.01$), creatinine, succinate and taurine levels ($p < 0.05$).

Moreover, as given in Table 3, gemcitabine treated mice (KG) also had a significantly lower level of urinary urea compared to untreated PDAC mice (KC) ($p < 0.05$) and OPP-gemcitabine group (KPG) additionally was observed to have decreased concentrations of glucose and ethylene glycol compared to KC group ($p < 0.05$).

Metabolites	Chemical shift (ppm)	KC/CC	KC(W6)/KC(W2)	KG/KC	KP/KC	KPG/KC
Acetate	1.9	2.04	2.31	0.81	0.30	0.27
Alanine	3.8,1.5	0.55	1.36	0.68	0.28 ^a	0.15 ^b
Allantoin	8.0,7.3,6.0,5.4	0.61	1.33	0.50	0.26	0.26
Betaine	3.9,3.3	1.06	1.35	0.50	0.22	0.13
Choline	4.1,3.5,3.2	0.32	0.51	1.89	0.77	0.46
cis-Aconitate	5.7,3.1	0.26	2.06	2.16	0.77	0.48
Citrate	2.7, 2.5	0.24	1.02	1.06	0.72	0.27
Creatine	3.9,3.0	0.58	2.90	0.60	0.61	0.19
Creatinine	4.0,3.0	0.51 ^a	1.73	0.97	0.24 ^a	0.22 ^a
Dimethylamine	2.7	0.52	1.31	1.39	0.34	0.25
Ethylene glycol	3.7	0.52	0.29	1.14	0.62	0.24 ^a
Formate	8.4	0.18 ^a	0.87	2.87	1.16	0.25
Glucose	5.2,4.6,3.9,3.8,3.8,3.8,3.7, 3.7,3.5,3.5,3.5,3.4,3.4,3.2	0.53	1.03	0.98	0.39	0.21 ^a
Glycerate	4.1,3.8,3.7	2.74	1.22	2.63	0.35	0.06
Indole-3-acetate	10.0,7.6,7.5,7.2,7.2,7.2,3.6	0.98	1.53	1.14	0.33	0.20
Lactate	4.1,1.3	0.72	0.82	0.41	0.33	0.12
Methanol	3.4	0.69	1.14	1.34	1.19	0.58
Methionine	3.8,2.6,2.2,2.1,2.1	0.53	2.24	0.58	0.18	0.12
N-Isovaleroylglycine	8.0,3.7,2.2,2.0,0.9	0.56	0.92	1.54	0.39	0.28
N-Phenylacetylglycine	8.0,7.4,7.3,7.3,3.7,3.7	1.09	2.05	0.93	0.23	0.14
O-Phosphocholine	4.6,3.6,3.2	0.30	0.69	1.62	0.17	0.24
Phenylacetate	7.4,7.3,7.3,3.5	0.42	0.89	0.90	0.56	0.42
Pyruvate	2.4					
Succinate	2.4	0.43	1.00	0.34 ^a	0.44 ^a	0.28 ^a
Sucrose	5.4,4.2,4.0,3.9,3.8,3.8,3.8, 3.8,3.8,3.7,3.7,3.6,3.5	2.31	0.72	1.04	0.48	0.10
Tartrate	4.3	0.43 ^a	0.91	1.29	0.44	0.23
Taurine	3.4,3.3	0.51	1.16	1.87	0.31 ^a	0.30 ^a
Trimethylamine	2.9	0.31	0.87	1.07	0.37	0.39
Tryptophan	10.2,7.7,7.5,7.3,7.3,7.2,4.0, 3.5,3.3	0.67	1.32	1.48	0.24	0.21
Urea	5.8	6.15 ^b	2.18 ^a	0.10 ^a	0.62	1.77

KC = untreated PDAC mice; CC = non-PDAC control mice; KC W2 = untreated PDAC mice at study baseline, week 2; KC W6 = untreated PDAC mice at study endpoint, week 6; KG = PDAC mice treated with gemcitabine drug, KP = PDAC mice on 5% dietary OPP, KPG = PDAC mice on 5% dietary OPP and gemcitabine drug.

Table 3 Profiled metabolites based on urinary ¹H NMR with fold change differences of metabolite concentration between groups (numerator/denominator). The ratio above 1 indicates an increase, while the ratio below 1 indicates a decrease in metabolite concentration of the numerator's group in comparison to the denominator's group. ^ap<0.05; ^bp<0.01, statistical significance is determined using student's t-test.

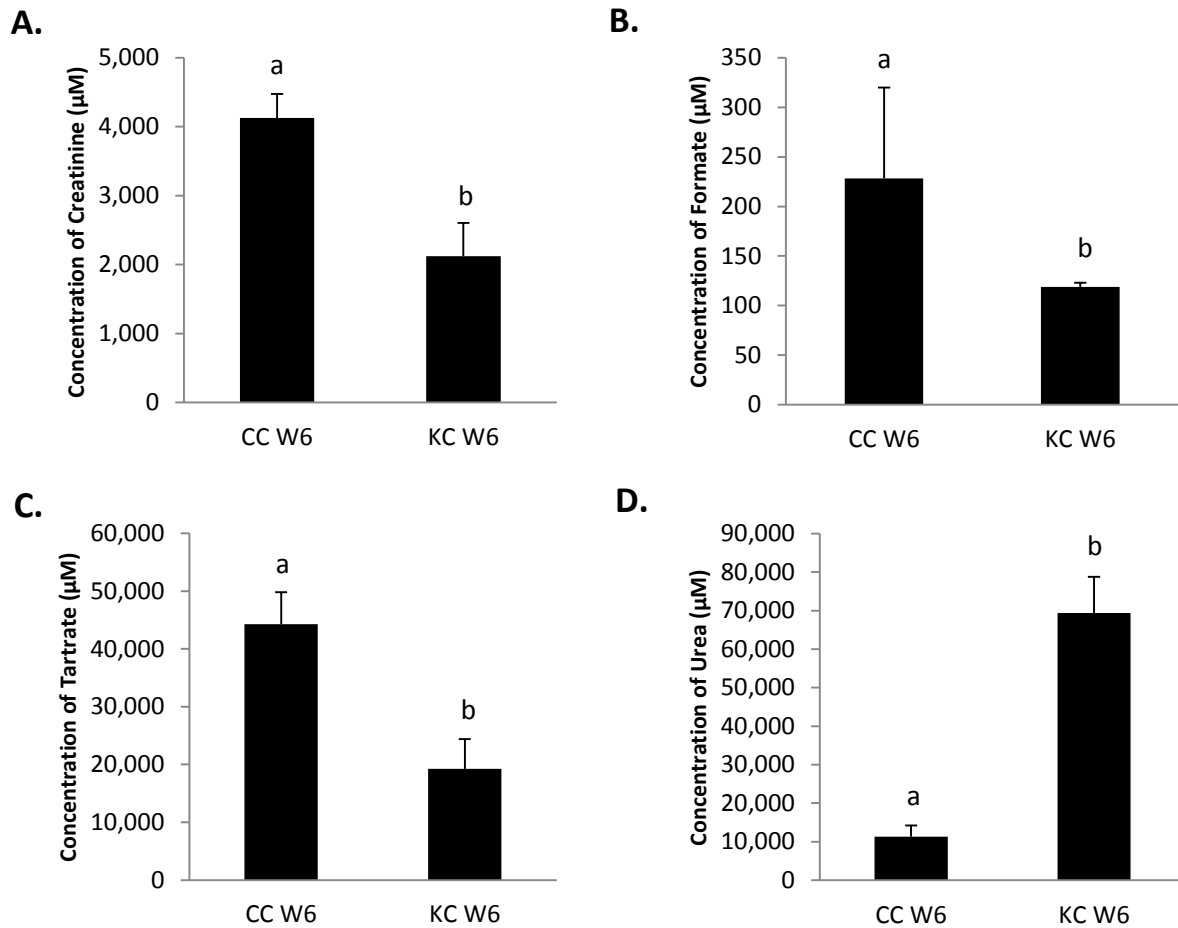


Fig. 28 Urinary metabolites associated with non-PDAC controls. Urinary metabolites identified to be significantly lowered (Table 3) comparing PDAC mice (KC) with non-PDAC controls, (CC) at study endpoint, week 6. (A) Creatinine; (B) Formate; (C) Tartrate; (D) Urea. Data are expressed as mean \pm SE. Metabolite concentrations of (A)-(C) were statistically different at $p < 0.05$, (D) at $p < 0.01$.

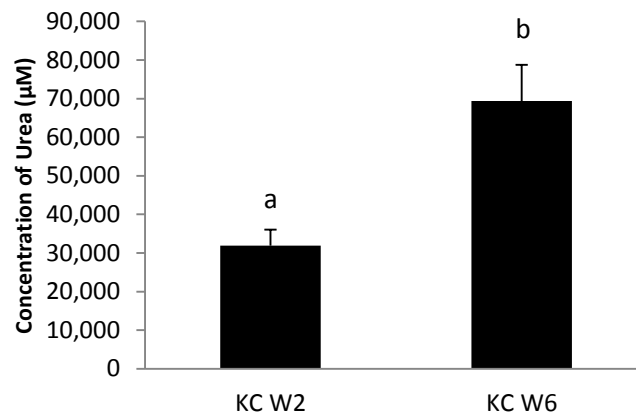


Fig. 29 Urinary metabolite associated with PDAC progression. Urinary level of urea in untreated PDAC group (KC) was identified to have changed by more than 2 folds (Table 3) with the progression of the disease from week 2 (W2) to week 6 (W6). Urea level was significantly increased with PDAC progression ($p < 0.05$). Data are expressed as mean \pm SE.

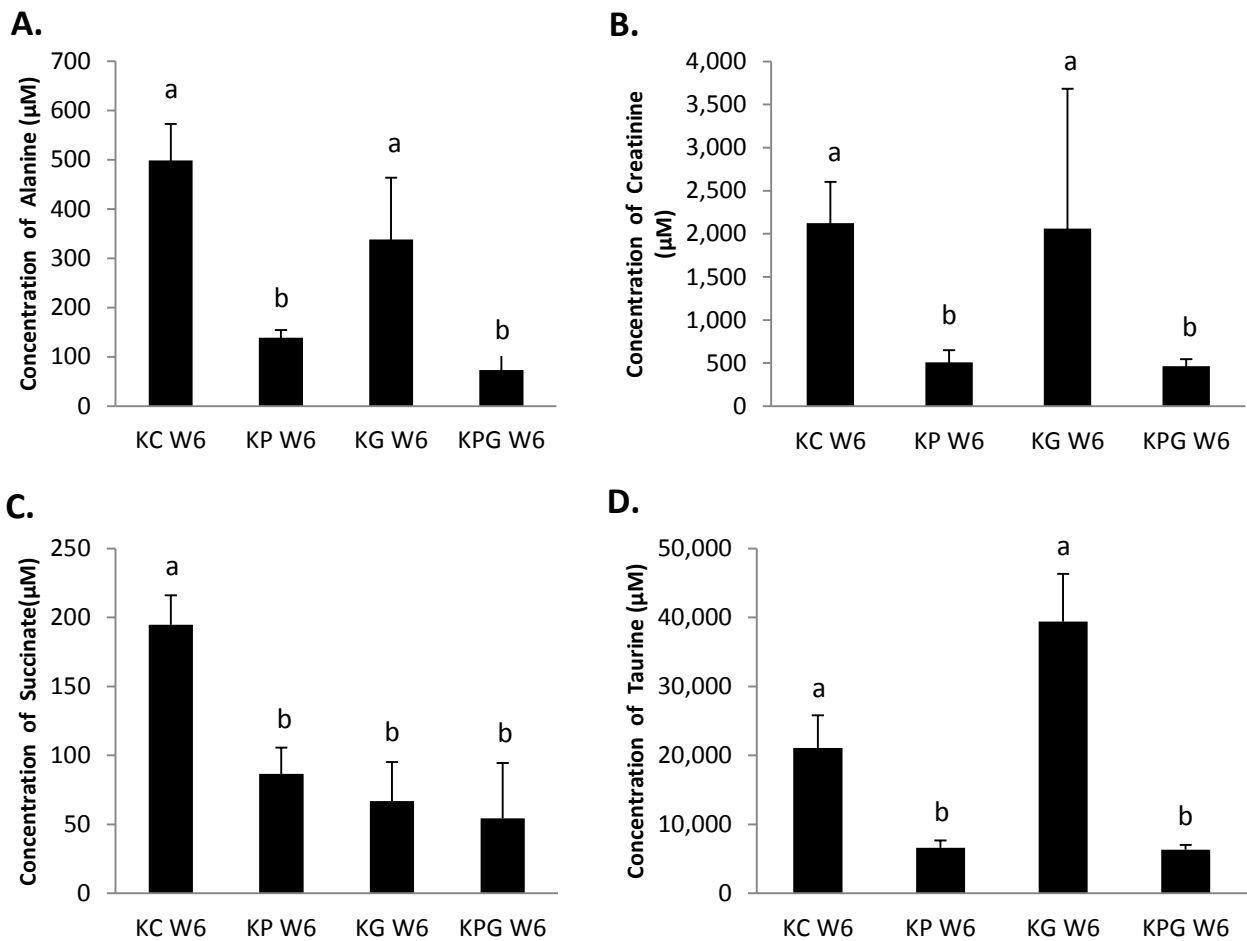


Fig. 30 Urinary metabolites associated with OPP treatment. Urinary metabolites identified to be significantly lowered at $p < 0.05$ (Table 3) comparing PDAC mice (KC) with mice on dietary OPP (KP) at study endpoint, week 6. **(A)** Alanine; **(B)** Creatinine; **(C)** Succinate; **(D)** Taurine. Data are expressed as mean \pm SE. **(A)-(D)** were also significantly lowered in mice on OPP-gemcitabine combination (KPG); **(A)** at $p < 0.01$, **(B)-(D)** at $p < 0.05$, **(C)** was also significantly lowered in gemcitabine treated (KG) mice compared to PDAC mice (KC).

3.9 Regression analysis

Additionally, we also conducted regression analysis in order to evaluate the relationship between urinary metabolite profiles with some of the variables such as PanIN lesion count and gene expression that we have investigated independently of the metabolomic profiles. As depicted by Fig. 31a, correlation resulting from OPLS regression is strong for total PanIN count ($R^2 = 0.6891$) while the association with PanIN-3 count is moderate ($R^2 = 0.5788$; Fig. 32). Similar regression analysis on gene expression data revealed a very strong correlation with Notch1 ($R^2 = 0.9417$; Fig. 33a) and MMP9 ($R^2 = 0.8636$; Fig. 34a). However, the correlation with CCND1 expression was found to be weak ($R^2 = 0.3446$; Fig. 35). Having seen that urinary metabolomic profiles of the PDAC mice are correlating very well with Notch1 expression, MMP9 expression and also total PanIN lesion count, we further decided to use these interesting observations to identify the possible pathway(s) that leads to the beneficial effect of dietary OPP on PDAC mice. S-plots are the loading plots associated with multivariate regression analysis. Information from the corresponding OPLS S-plots comparing total PanIN count (Fig. 31b), Notch1 expression (Fig. 33b) and MMP9 expression (34b) were used for pathway analyses discussed in detail in the next section.

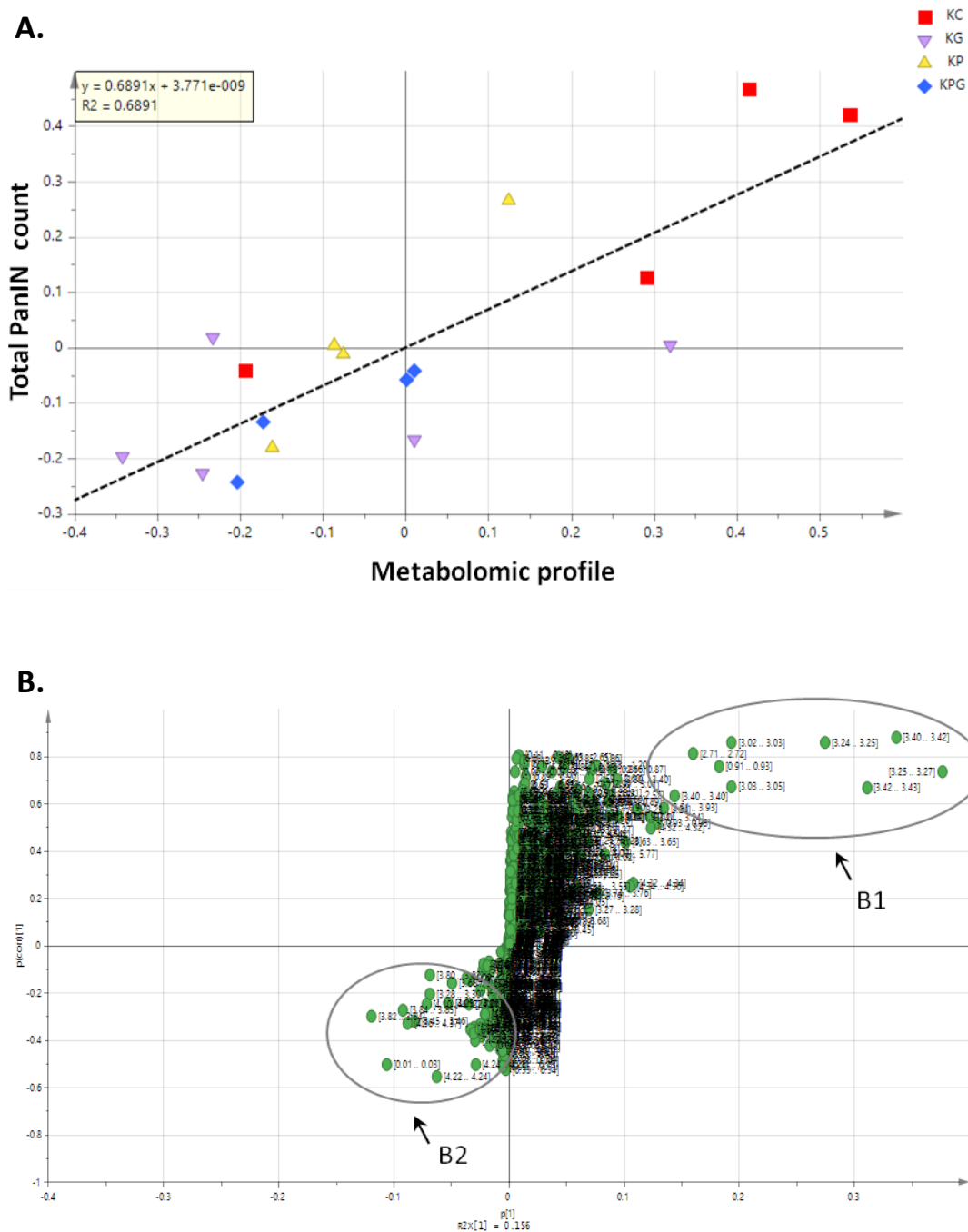


Fig. 31 OPLS regression of total PDAC lesion, PanIN count with urinary ^1H NMR profiles of the four PDAC experimental groups at end point. **(A)** OPLS score plot shows a strong correlation ($R^2=0.6891$). **(B)** S-plot obtained from OPLS model. Arrow B1 points on the regions in the spectra correlate with high number of total PanIN with metabolites identified include taurine, choline, dimethylamine, N-isovalerylglycine, creatine and creatinine. Regions containing metabolites point by arrow B2 correlate with low total PanIN count identified as lactate, glycerate, tartarate, glucose and sucrose.

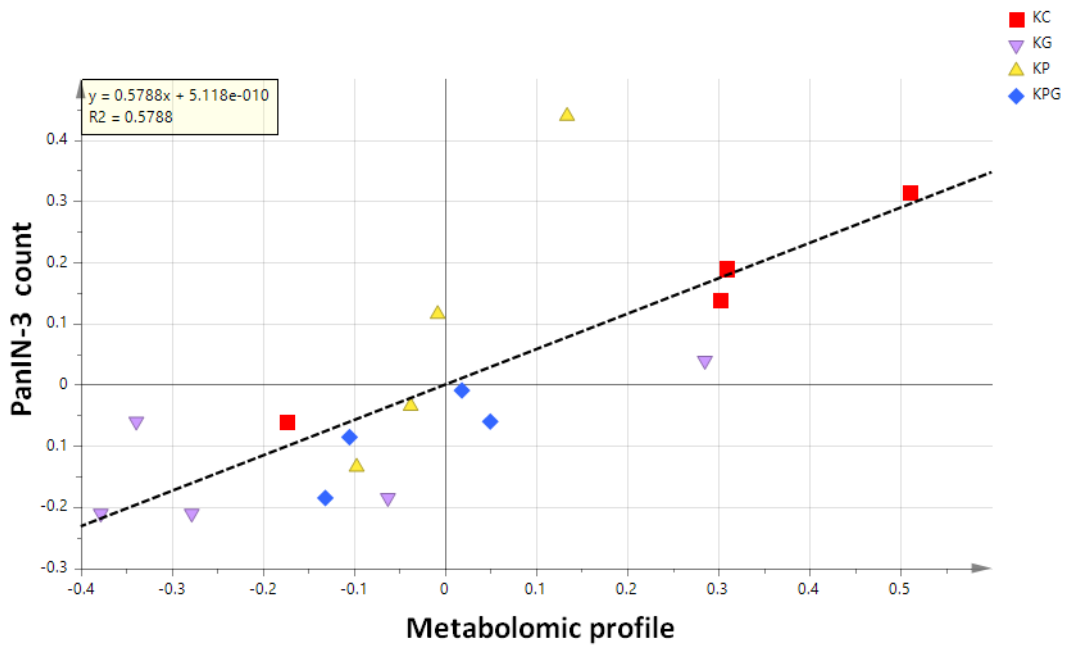


Fig. 32 OPLS regression of PanIN-3 lesion count with urinary ^1H NMR profiles of the four PDAC experimental groups at end point. OPLS score plot shows a moderate correlation ($R^2=0.5788$) between urinary profiles and PanIN-3 count.

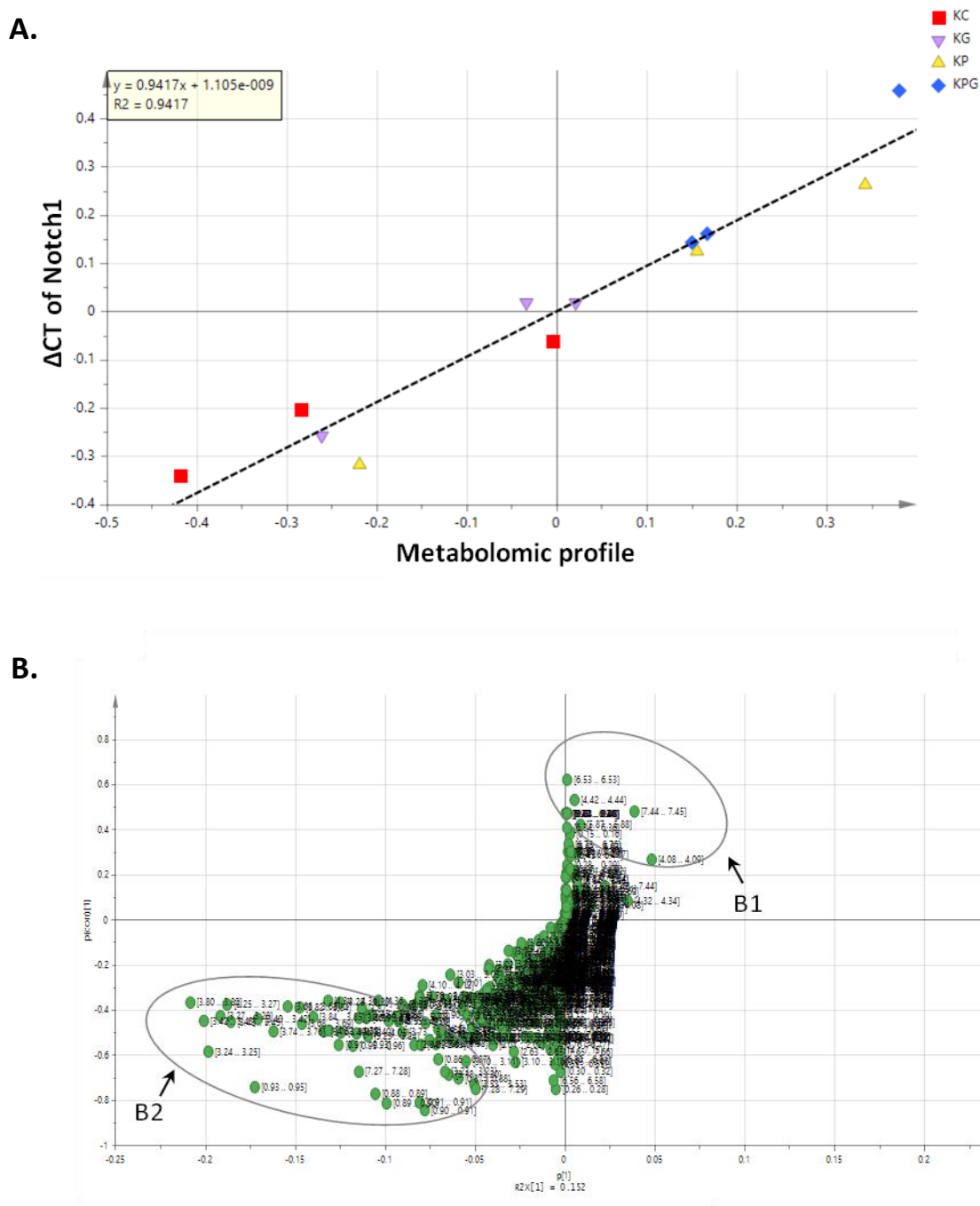


Fig. 33 OPLS regression of Notch1 expression at end point. Regression expressed as normalized C_T values with urinary ^1H NMR profiles of the four PDAC experimental groups. **(A)** OPLS score plot shows a very strong correlation ($R^2=0.9417$). **(B)** S-plot obtained from OPLS model. Arrow B1 points on the regions in the spectra correlate with high C_T values (low Notch1 expression) with metabolites identified include tartrate, phenylacetate and sucrose. Regions containing metabolites point by arrow B2 correlate with low C_T values (high Notch1 expression) identified as taurine, choline, tryptophan, glucose, sucrose and N-isovalerylglycine.

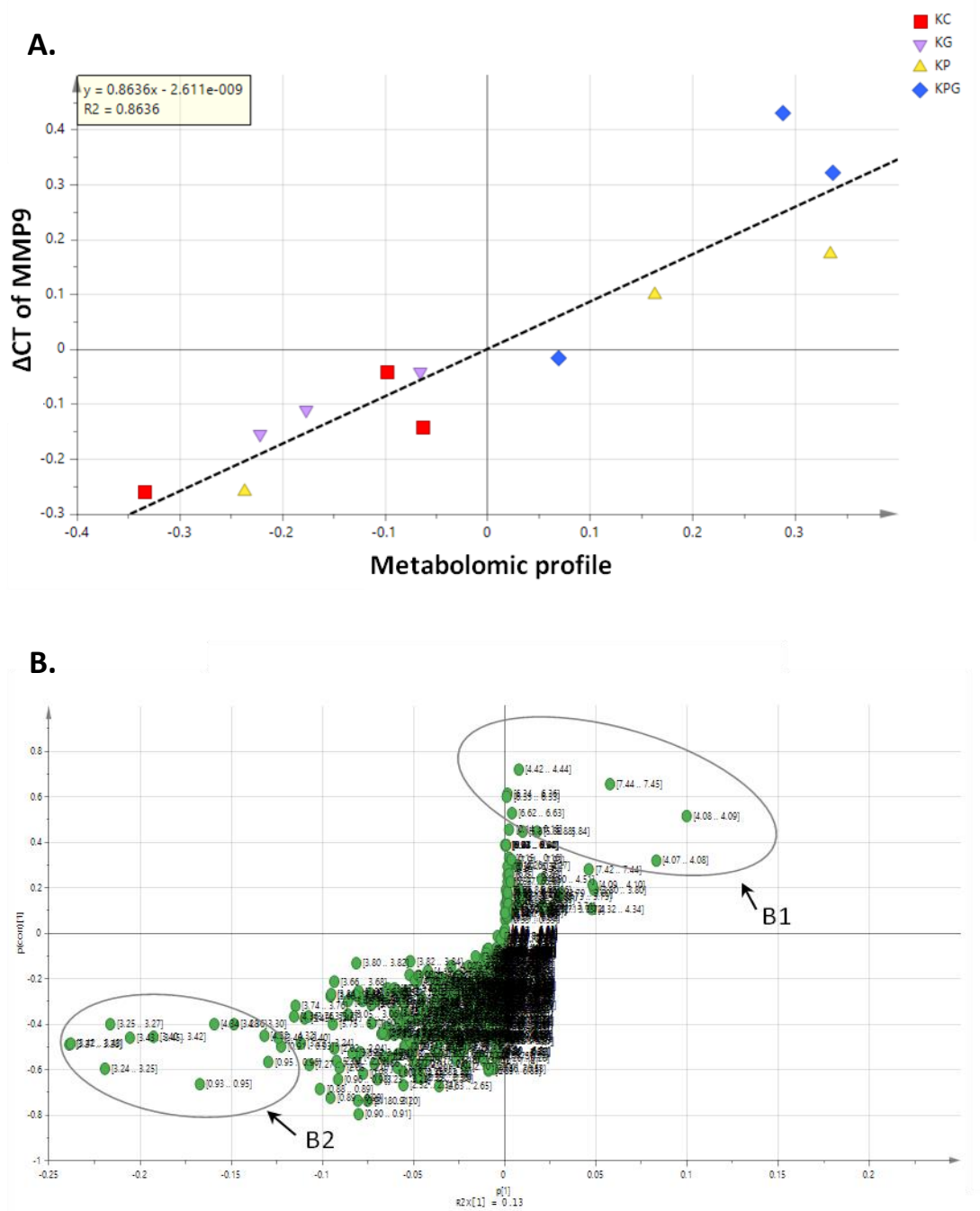


Fig. 34 OPLS regression of MMP9 expression at endpoint. Regression expressed as normalized C_T values with urinary ^1H NMR profiles of the four PDAC experimental groups. **(A)** OPLS score plot shows a very strong correlation ($R^2=0.8636$). **(B)** S-plot obtained from OPLS model. Arrow B1 points on the regions in the spectra correlate with high C_T values (low MMP9 expression) with metabolites identified include tartrate, phenylacetate and sucrose. Regions containing metabolites point by arrow B2 correlate with low C_T values (high MMP9 expression) identified as taurine, choline, tryptophan, and N-isovaleroylglycine.

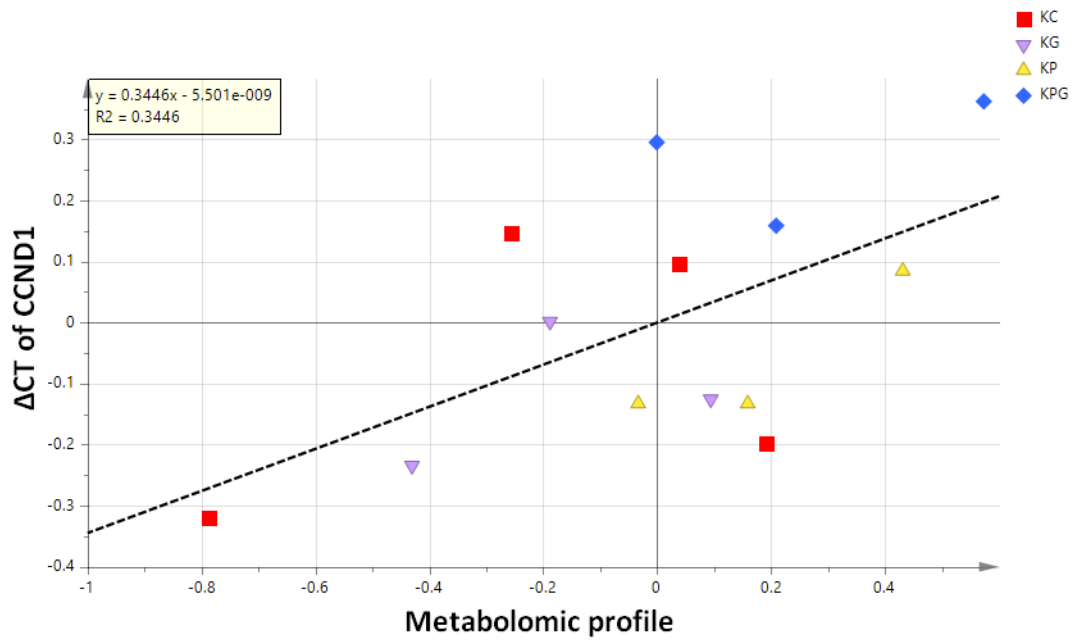


Fig. 35 OPLS regression of CCND1 expression. Regression expressed as normalized C_T values with urinary ^1H NMR profiles of the four PDAC experimental groups. OPLS score plot shows a weak correlation ($R^2=0.3446$) between urinary profiles and CCND1 expression.

3.9 Metabolic pathway analyses following dietary OPP intervention

As previously mentioned, in order to identify the metabolic pathway(s) and biological relevance of the identified metabolic changes related to Notch1 and MMP9 expression together with total PanIN lesion count due to dietary OPP intervention, the MetaboAnalyst 3.0 software and Kyoto Encyclopedia of Genes and genomes (KEGG) database were used. Metabolites identified from each S-plot that correspond to OPLS regression between urinary metabolomic profiles and Notch1 expression, MMP9 expression and total PanIN count respectively were subjected to MetaboAnalyst 3.0 for pathway analyses.

Arrow B1 on Fig. 31b points on the regions in the spectra correlate with high number of total PanIN with metabolites identified using Chenomx software include taurine, choline, dimethylamine, N-isovaleroylglycine, creatine and creatinine while regions containing metabolites pointed by arrow B2 correlate with low total PanIN count were identified as lactate, glycerate, tartarate, glucose and sucrose.

As illustrated in Fig. 33b, the regions in the spectra that correlate with high C_T values (low Notch1 expression) were identified as tartrate, phenylacetate and sucrose (arrow B1). Regions containing metabolites pointed by arrow B2 which correlate with low C_T values (high Notch1 expression) were recognized as taurine, choline, tryptophan, glucose, sucrose and N-isovaleroylglycine.

For MMP9 expression, arrow B1 on Fig. 34b points on the regions in the spectra correlate with high C_T values (low MMP9 expression) with metabolites identified include tartrate, phenylacetate and sucrose. Regions containing metabolites pointed by arrow B2 correlate with low C_T values (high MMP9 expression) were identified as taurine, choline, tryptophan, and N-isovaleroylglycine.

Next, data on the concentrations of identified metabolites quantified using Chenomx software were uploaded into the MetaboAnalyst software. MetaboAnalyst software utilizes pathway enrichment analysis and pathway topology analysis to translate metabolic trends into defined pathways relevant to the study.

Table 5 lists the significant pathways related to Notch1 expression with dietary intervention identified by the MetaboAnalyst software ($p < 0.05$). They include taurine and hypotaurine metabolism, primary bile acid biosynthesis, phenylalanine metabolism, glycerophospholipid metabolism and glycine, serine and threonine metabolism. Fig. 36 illustrates the pathway topological analysis from the software. The larger a circle and the higher its location on the y axis, the higher impact of a particular pathway. Inspection on the diagram indicates that taurine and hypotaurine metabolism has been impacted the most following dietary OPP intervention.

MMP9 expression was found to have the similar significant pathways as Notch1 (Table 6) while for total PanIN count, only taurine and hypotaurine metabolism, primary bile acid biosynthesis and glycerophospholipid metabolism was identified as significant pathways (Table 7). Interestingly, a similar observation with MMP9 expression and total PanIN count was revealed by Figs. 37 and 38 respectively in which taurine and hypotaurine metabolism was identified as the most highly impacted pathway.

Fig. 39 illustrates the taurine and hypotaurine metabolism pathway from KEGG database. Taurine which plays role in this metabolism was observed in our investigation to be significantly decreased with intervention of dietary OPP (KP) and OPP-gemcitabine combination (KPG) compared to untreated PDAC group (KC). However, taurine level in gemcitabine treated group

(KG) displayed an elevated trend compared to KC group but at a non-significant level ($p>0.05$) (Table 3;Fig. 30d).

Pathway name	Hits	p-value	$-\log(p)$	FDR
Taurine and hypotaurine metabolism	1	0.007672	4.8702	0.028972
Primary bile acid biosynthesis	1	0.007672	4.8702	0.028972
Phenylalanine metabolism	1	0.009657	4.64	0.028972
Glycerophospholipid metabolism	1	0.027769	3.5838	0.049985
Glycine, serine and threonine metabolism	1	0.027769	3.5838	0.049985

Pathway name, hits, significance, $-\log(p)$ and false discovery rate (FDR)

Table 5 Metabolites obtained from S-plot that correspond to OPLS regression between urinary metabolomic profiles and Notch1 expression were subjected to MetaboAnalyst 3.0 for pathway analysis. MetaboAnalyst 3.0 identified highly significant pathways involved.

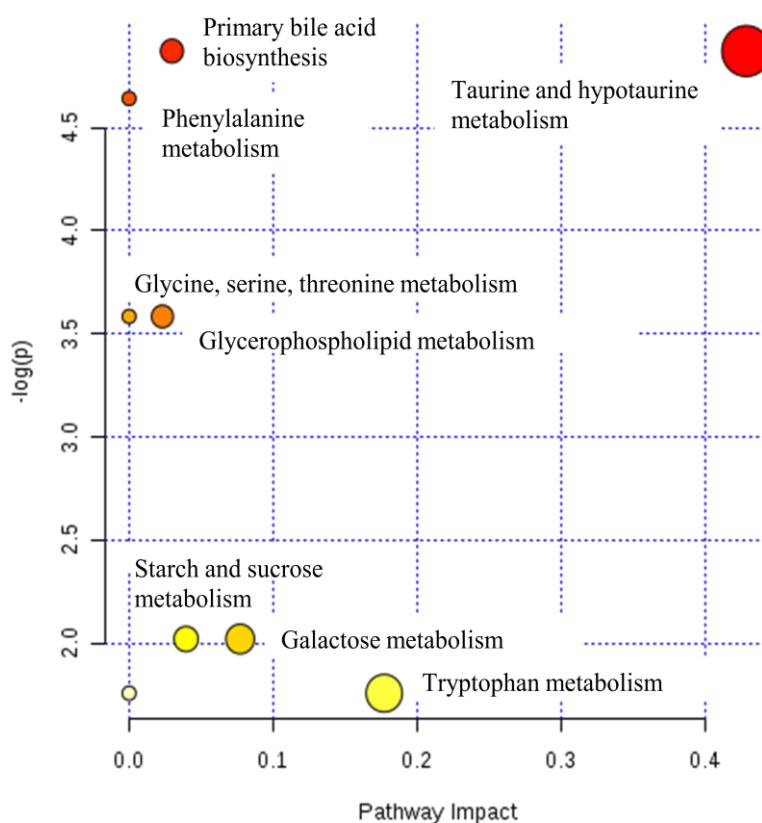


Fig. 36 MetaboAnalyst 3.0 output illustrating the most predominant metabolic pathways that correspond to OPLS regression between urinary metabolomic profiles and Notch1 expression. The larger a circle and higher on the y axis, the higher impact of pathway.

Pathway name	Hits	p-value	$-\log(p)$	FDR
Taurine and hypotaurine metabolism	1	0.007672	4.8702	0.026852
Primary bile acid biosynthesis	1	0.007672	4.8702	0.026852
Glycerophospholipid metabolism	1	0.027769	3.5838	0.04265
Glycine, serine and threonine metabolism	1	0.027769	3.5838	0.04265
Phenylalanine metabolism	2	0.030464	3.4912	0.04265

Pathway name, hits, significance, $-\log(p)$ and false discovery rate (FDR)

Table 6 Metabolites obtained from S-plot that correspond to OPLS regression between urinary metabolomic profiles and MMP9 expression were subjected to MetaboAnalyst 3.0 for pathway analysis. MetaboAnalyst 3.0 identified highly significant pathways involved.

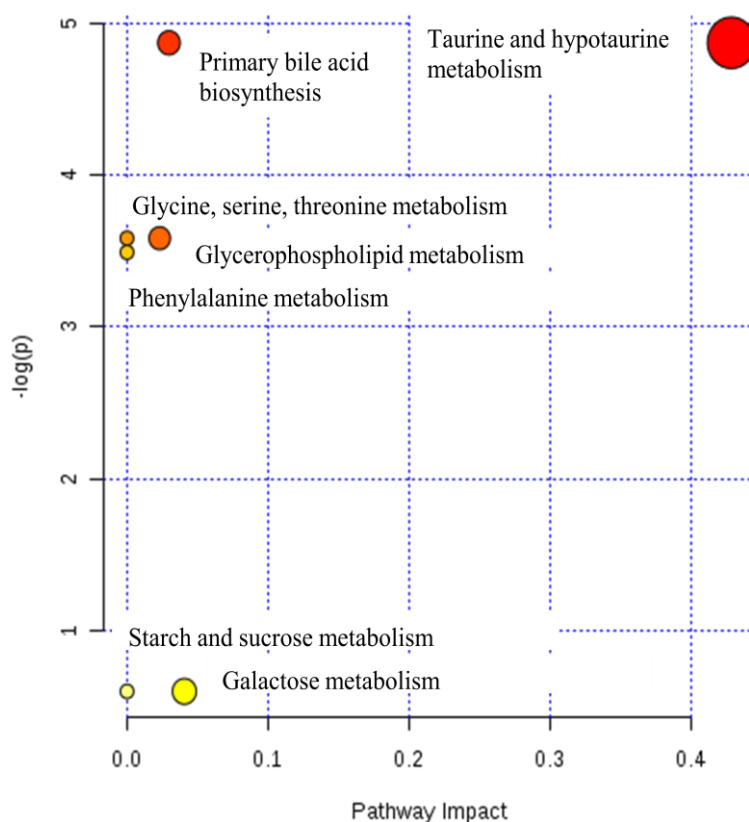


Fig. 37 MetaboAnalyst 3.0 output illustrating the most predominant metabolic pathways that correspond to OPLS regression between urinary metabolomic profiles and MMP9 expression. The larger a circle and higher on the y axis, the higher impact of pathway.

Pathway name	Hits	p-value	$-\log(p)$	FDR
Taurine and hypotaurine metabolism	1	0.007672	4.8702	0.026852
Primary bile acid biosynthesis	1	0.007672	4.8702	0.026852
Glycerophospholipid metabolism	1	0.027769	3.5838	0.064795

Pathway name, hits, significance, $-\log(p)$ and false discovery rate (FDR)

Table 7 Metabolites obtained from S-plot that correspond to OPLS regression between urinary metabolomic profiles and total PanIN lesion count were subjected to MetaboAnalyst 3.0 for pathway analysis. MetaboAnalyst 3.0 identified highly significant pathways involved.

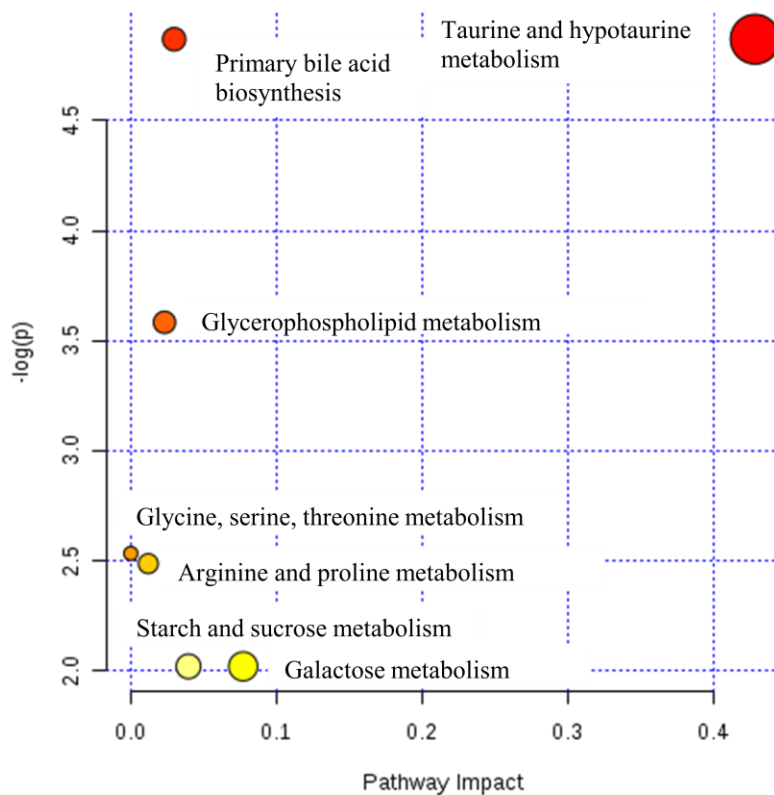


Fig. 38 MetaboAnalyst 3.0 output illustrating the most predominant metabolic pathways that correspond to OPLS regression between urinary metabolomic profiles and total PanIN lesion count. The larger a circle and higher on the y axis, the higher impact of pathway.

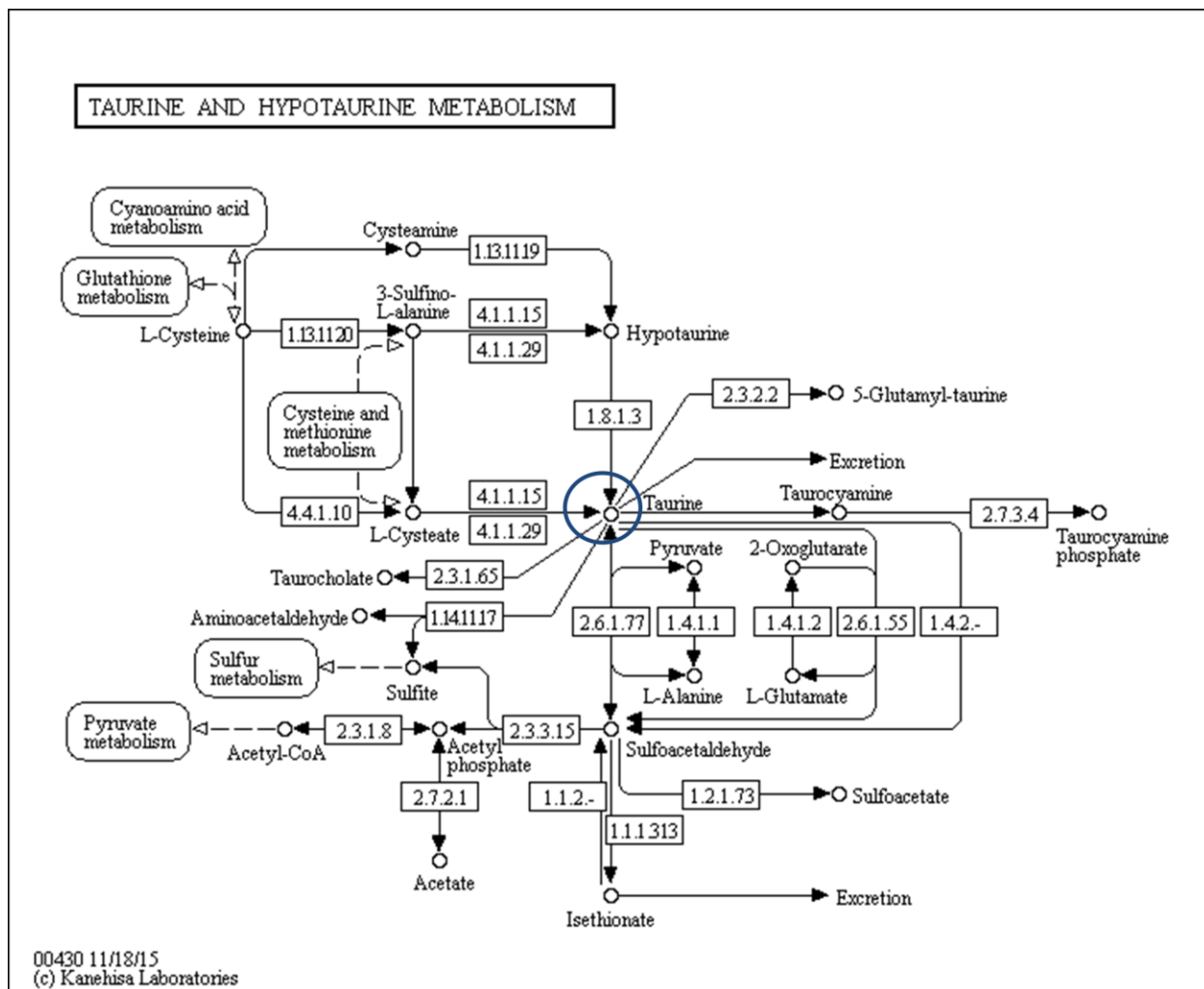


Fig. 39 The role of taurine in taurine and hypotaurine metabolism (KEGG database).

CHAPTER 4 DISCUSSION

Pancreatic cancer is currently ranked as the fourth leading cause of cancer-related deaths in the United States with the most common type being the Pancreatic Ductal Adenocarcinoma (PDAC). PDAC has a poor prognosis with only 8% of 5-year survival rate attributable to lack of early detection methods and effective treatments[1,2]. Gemcitabine, a genotoxic drug has been the treatment of choice for this lethal disease particularly for patients with nonresectable pancreatic cancer. Gemcitabine is a deoxycytidine analog and considered as an antimetabolite[50]. Antimetabolites have almost similar structure with chemicals needed for normal biochemical activity, but with some differences enabling them to interfere with normal cell function. The most significant mechanism of work for gemcitabine is by inhibiting DNA synthesis, making it a chemotherapeutic agent of choice[51]. Once being activated inside the cell, a single incorporation of deoxynucleotide will prevent chain elongation[52]. Despite being the current first line therapy for pancreatic cancer, treatment with gemcitabine remains challenging mainly due to the aggressive nature of PDAC with marked chemoresistance in addition to notable adverse side effects of the drug. Thus, development of effective treatments for pancreatic cancer that are relatively nontoxic from single agents or in combination with an established drug treatment is warranted. Several studies have documented a variety of phytochemicals with anticancer properties including curcumin, garcinol[33,34], lycopene[35,36], resveratrol[37], epigallocatechin gallate (ECGC)[38] and genistein[39,40].

Oil palm (*Elais guineesis*) is a high oil plant from the family of *Arecaceae*. The extraction of water soluble materials from the oil palm produces a class of phytochemicals including phenolics and organic acids collectively referred as Oil Palm Phenolics (OPP)[41]. OPP contains high level of antioxidants and has been shown in our recent *in vitro* work to posses

therapeutic effects against pancreatic cancer[48]. In this study, using KPC mouse-model for PDAC, we have investigated the *in vivo* effect of OPP as a single chemotherapeutic agent using a clinically relevant animal model, as well as the combinatorial effect of OPP with gemcitabine as a potential pancreatic cancer treatment.

Histological changes of the nonglandular stomach (fore stomach) such as mucosal epithelial hyperplasia with or without hyperkeratosis and inflammation are some of common findings following exposure or ingestion of toxic substance. In order to exclude any possibilities of toxicity caused by 5% dietary OPP consumption, microscopic examination of fore stomach and pancreatic tissues were conducted. We herein report that the administration of dietary OPP at 5% level was not toxic through histological analysis of fore stomach (Fig. 11) as well as pancreatic tissues (Fig. 12) in non-PDAC control animals. Hundred percent survival of non-PDAC controls on OPP diet during 6 weeks of feeding also serves as indirect toxicity assessment (Fig. 3). This confirms the earlier findings by Leow et al. on the safety of oral supplementation of OPP[46].

Fig. 40 outlines the *in vivo* effect of OPP and its combination with gemcitabine investigated in this present study. Firstly, in this study, we used tumor and cyst growth identified by the noninvasive imaging technique, MRI as our output to determine the effect of dietary OPP treatment on PDAC progression. The most striking result to emerge from this MRI data is that the OPP-gemcitabine combination showed a synergistic effect in slowing down the progression of PDAC with less than 10% of tumors and cysts increased in size following treatment (Table 2; Fig. 10). On the other hand, a mix of responders and non-responders was observed with treatment of either OPP or gemcitabine alone. This provides us with the first indicator that the combinatorial therapy of dietary OPP and gemcitabine is greater in benefit than the use of the

single agent of OPP or gemcitabine. As mentioned earlier, drug resistance in PDAC is well recognized and poor response to gemcitabine drug has been described in several publications. Previously, a number of trials including two studies in Japan and one study in Korea have reported continued disease progression despite good compliance of gemcitabine treatment in advanced pancreatic cancer[53–55].

Secondly, we also assessed the potential role of OPP as a chemopreventive agent for PDAC. Pancreatic intraepithelial neoplasms (PanINs) are known as the most common precursors to PDAC[13,56]. Upon microscopical examination of these lesions, we report that OPP was effective at lowering the number of PanIN-2, the lesser of the two kinds of higher grade PanIN lesions (Fig. 15). However, the effect was extended to both PanIN-2 and PanIN-3 in the combinatorial treatment of OPP and gemcitabine indicating the superior chemopreventive potential of this combination in prolonging the onset of invasive adenocarcinoma and in halting the progression of pancreatic cancer precursor lesions to PDAC (Fig. 15).

Moreover, we have also investigated the effect of OPP on several tumorigenesis markers in this study. Our previous *in vitro* work on OPP have elucidated the anticancer effect of OPP through the suppression of NF- κ B pathway with favorable regulation of cancer-related marker, MMP9 together with several other markers[48]. Here in this study, we started off by investigating the effect of OPP on Notch1 which is upstream of NF- κ B. The Notch signaling pathway is a fundamental signaling system used by neighboring cells to communicate with each other in order to assume their proper developmental role. Notch signaling is involved in the cellular developmental pathway including proliferation and apoptosis. As mentioned earlier, Notch1 has been described to cross-talk with other major cell growth and apoptotic pathway such as NF- κ B and its high expression has been displayed to inhibit apoptosis[57]. It has also been

reported in the study by Wang et al., that down regulation of Notch1 inhibited cell growth and induced apoptosis in pancreatic cancer cells[57]. A more recent study by Kunnimalaiyaan et al. has also demonstrated a successful suppression of pancreatic cancer cell growth was achieved through the inhibition of Notch1[58]. We observed that single agent intervention with OPP or gemcitabine alone did not produce significant down regulation of Notch1(Fig. 18a) which we expected due to different responses by responder and non-responder animals as described by our MRI data under section 3.2. Upon separating the OPP responders from the non-responders, it was revealed that OPP treatment significantly inhibited the expression of Notch1 compared to the untreated PDAC animals (Fig. 18b) but the down regulation trend of Notch1 in gemcitabine responders was not found to be significant (Fig. 18c).

Additionally, the expressions of two downstream genes of Notch1; MMP9 and CCND1 were also evaluated. MMP9 is a zinc-dependent enzyme known to be the agent to degrade extracellular matrix components. In cancer, MMP9 is responsible for angiogenesis, metastasis and tissue invasion. This current study demonstrates that in OPP responder animals, the expression of MMP9 was significantly lowered (Fig. 19b) but not in gemcitabine responder animals (Fig. 19c). Moreover, it is also demonstrated that the OPP-gemcitabine combination down regulated the level of pancreatic MMP9 comparative to untreated group significantly (Fig. 19a). This is consistent with our *in vitro* observation of the anti-invasive effect of OPP through inhibition of MMP9[48]. These results provide further support for the hypothesis that OPP is capable of arresting metastasis and cell invasion by interrupting MMP9 activity.

Dysregulation of CCND1 has been linked to the development and progression of cancer in general[59]. It is known to be frequently over expressed in PDAC. Cyclins function as cyclin-dependent kinases subunit regulators forming a complex with CDK4 or CDK6, whose activity is

required for cell cycle G1/S transition. Over expression of CCND1 increases proliferation by accelerating the cell transit through the G1 phase. Moreover, there are also present evidence that CCND1 plays a role in tumor cell migration and poses as a strong prognostic factor in the survival of pancreatic cancer patients[60,61]. In this study, we observed that OPP-gemcitabine combinatorial treatment significantly reduced the expression of CCND1(Fig.21) thus, suggesting the anti-proliferative property of OPP when use in combination with gemcitabine by its ability to arrest cell cycle. However, the down regulation trend of CCND1 in OPP responder animals and gemcitabine responder animals did not reach statistical significance (Fig. 21b & 21c).

The anticancer effect of OPP was also evident in immunohistochemical analysis. In PDAC, the calcium-binding protein S100P is the most significantly up regulated protein among several other S100 proteins. It is known to be mostly related to invasion and metastasis of tumor[62–65]. Also, its over expression has been positively correlated with poor prognosis in several other types of cancer including gastric, prostate, lung and cholangiocarcinoma[66–69]. A recent work by Dakhel et al. has demonstrated that S100P plays a role in resisting the action of gemcitabine. They have also presented that S100P induces the production of MMP9[70]. Here we showed that compared to the untreated group, treatment with OPP produced lower expression of the tumor promoter S100P and least expression was detected when OPP was combined with gemcitabine (Fig. 16). Interestingly, we have also observed the down regulation of MMP9 especially in the OPP-gemcitabine combination supporting the connection between S100P and MMP9 as reported earlier by Dakhel et al.[70]. Conversely, SMAD4 is one of the important molecules in TGF- β pathway, which serves as a tumor suppressor of PDAC. SMAD4 is exclusive in being the only member of the SMAD family that involves in the biological activity of TGF- β mainly in the inhibition of cell growth[71,72]. As reported by several researchers, the

loss of SMAD4 expression promotes the advancement of high grade PanIN lesions to PDAC and was associated with poor survival. SMAD4 has been suggested as a negative prognostic indicator and its expression marks a better survival in patients with pancreatic cancer[73–77]. In this study, we presented the chemotherapeutic potential of OPP and its combination with gemcitabine which was evident by over expression of SMAD4 in comparison with the untreated group (Fig. 17).

The final part of this report has explored the *in vivo* effect of dietary OPP on PDAC using metabolomics approach. Metabolomics is one of the ‘omics’ sciences that focuses on phenotypic features from small-molecule metabolite of biological systems[78]. Urinary metabolomics offers a non-invasive systematic analysis of potential metabolites in a biological sample allowing for biomarker and drug discoveries, identification of perturbed pathways and also serving as potential therapeutic targets in oncology generally and specifically for pancreatic cancer studies[79,80]. Apart from urine, blood serum and plasma, pancreatic tissue and saliva have also been investigated for potential metabolomic PDAC biomarkers[81–86]. In metabolomics, ¹H NMR spectroscopy is one of the main approaches for data acquisition. It provides quantitative information and is reproducible, hence suitable for multivariate analysis.

Multivariate data analysis using SIMCA P+ software revealed a good discrimination of urinary profiles between untreated PDAC animals and non-PDAC controls, and between untreated PDAC animals with animals on OPP diet using the unsupervised PCA modeling (Figs. 21a & 25a). Good discrimination of metabolomic profiles with the progression of PDAC; comparing the baseline at week 2 to the endpoint at week 6 was achieved with supervised modeling (OPLS-DA) (Fig. 24a). Several metabolites were identified to be associated with the spectral discrimination of the three comparisons using NMR Suite Chenomx software.

Comparing untreated PDAC group with non-PDAC controls, concentration of urea was found to be significantly higher in PDAC animals while the concentrations of creatinine, formate and tartrate was lowered. The progression of PDAC from week 2 to week 6 was observed to be associated with significant elevation in urinary urea level (Table 3). Out of these metabolites, urea, creatinine and formate have been previously reported as potential molecular markers for pancreatic cancer whereas tartrate has not been reported before.

Creatinine is a metabolite involves in creatine metabolism. Several studies have previously reported the change on creatinine levels in PDAC. While Napoli et al. in their study reported a lower level of creatinine in pancreatic cancer patients [81], OuYang et. al conversely reported a higher level of creatinine in pancreatic cancer subjects compared to non-PDAC controls[84]. Formate takes part in the metabolism of one-carbon compounds and is typically produced as a byproduct in the production of acetate. Metabolomics study by Bathe et. al reported higher level of formate in pancreatic cancer patients[87]. Decreased urea levels has been reported previously in the serum of pancreatic cancer patients[88]. It is also known in the clinical setting that high urinary secretion of urea can be related to nutritional status and muscle wasting. It was observed from our data that urinary level of urea is significantly higher in PDAC also with the progression of the disease. A significant reverse in urinary urea level was seen with gemcitabine treatment (Table 3). However, the analysis does not enable us to determine the correlation between urinary levels or urea with PDAC since urea is the most concentrated metabolite in urine and the protons exchange with water. Studies suggested that excretion of tartrate majorly comes from dietary sources and only 15-20% being excreted in the urine unchanged while most dietary tartrate is metabolized by bacteria especially in the large intestine[89,90]. Urinary tartrate has also been investigated as a potential inhibitor of calcium

stone formation. A decreasing trend of urinary tartrate was observed in untreated PDAC group from week 2 to week 6, also as compared to groups treated with gemcitabine and OPP as a single agent therapy (Table 3). Although not statistically significant, this might indicate that PDAC and its progression can have a lowering effect on urinary tartrate levels[91].

Gemcitabine-treated group was found to have significantly lower urinary concentrations of urea and succinate compared to untreated PDAC group. Intervention with 5% dietary OPP on PDAC animals produced a significantly decreased level of alanine, creatinine, succinate and taurine compared to untreated PDAC group. PDAC animals receiving the combination of 5% dietary OPP with gemcitabine drug had a significantly lower level of alanine, creatinine, succinate and taurine similar to dietary OPP intervention alone, with additional decreased levels of glucose and ethylene glycol compared to untreated PDAC group (Table 3).

Additionally, following OPLS regression analysis, urinary metabolomic profiles of the four PDAC groups were found to be strongly correlated with Notch1 expression, MMP9 expression and total PanIN count (Figs. 31a; 33a & 34a). These interesting observations excite us to reveal the pathway(s) associated with the favorable down regulation of the two molecular markers and also reduced amount of PDAC precursor lesion with dietary intervention of OPP. Metabolites that correspond to OPLS regression between urinary metabolomic profiles and Notch1 expression, MMP9 expression and total PanIN count respectively were then subjected to MetaboAnalyst 3.0, a web based metabolomics data analysis tool for pathway analyses. Several significant pathways were detected including taurine and hypotaurine metabolism, primary bile acid biosynthesis, and glycerophospholipid metabolism that were common for Notch1 expression, MMP9 expression and total PanIN count (Table 5-7) and interestingly, topology

analyses indicate that taurine and hypotaurine metabolism has been impacted the most in this dietary study (Figs. 31a; 33a; 34a).

Taurine is a sulfur containing amino acid derived from cysteine. It has many fundamental biological roles, such as conjugation of bile acids, antioxidation, osmoregulation, membrane stabilization, and modulation of calcium signaling. In metabolomics studies, several publications have reported an increased level of taurine in pancreatic cancer patients and also in animal models[80,82,83,92]. In this present study, compared to untreated PDAC, taurine levels were observed to be significantly decreased with intervention of dietary OPP and OPP-gemcitabine combination. This provides as an indicator that taurine plays a major role in the anticancer effect exhibited by both interventions of OPP alone and OPP-gemcitabine combination with possible action through Notch1, since we have also observed a strong correlation between taurine and hypotaurine metabolism with Notch1 and also its downstream target, MMP9. Whereas no reports to date, were found in the literature describing a connection between Taurine and Notch1, this is a future prospect worth exploring. Moreover, in addition to reduced taurine concentration, decreased levels of succinate and alanine suggest the possible involvement of energy metabolism following dietary OPP intervention. While taurine levels were significantly lowered in the OPP and OPP-gemcitabine groups, treatment with gemcitabine displayed a non-significant elevation of taurine level. This might suggest that gemcitabine is affecting a different metabolic pathway. Gemcitabine (2',2'-difluoro-2'-deoxycytidine; dFdC) is a deoxycytidine analog with multiple modes of action inside the cell. Fig. 41 depicts gemcitabine cellular metabolism and its main mechanisms of action. Once being activated inside the cell to its tri-phosphate form, dFdCTP, this will be incorporated into DNA, inhibiting the synthesis of new DNA strands resulting in apoptosis of cancer cells. An additional mechanism of action of gemcitabine is self-potential

by inhibition of enzymes related to deoxynucleotide metabolism. This leads to the lowering of dNTP pool, promotes dFdC phosphorylation to dFdCTP and increase the likeliness of dFdCTP to be incorporated into DNA[52,93]. Gemcitabine induction of cancer cell apoptosis has been reported to be associated with Bcl-2/Bax pathway[94,95].

Taken together, our work has led us to the conclusion that oil palm phenolics (OPP) exhibit mild anticancer activity when used as a single agent therapy while OPP in combination with gemcitabine displays superior therapeutic effects demonstrating potential benefit of dietary OPP as part of combinatorial therapy for Pancreatic Ductal Adenocarcinoma (PDAC). Observations from this study can be further investigated using larger scale animal studies that may lead to a pilot human study. The evidence from this study also opens up to the next stage of our research to evaluate the anticancer properties of different OPP fractions in the hope to find the effective fraction(s) as potential single agent therapy for pancreatic cancer.

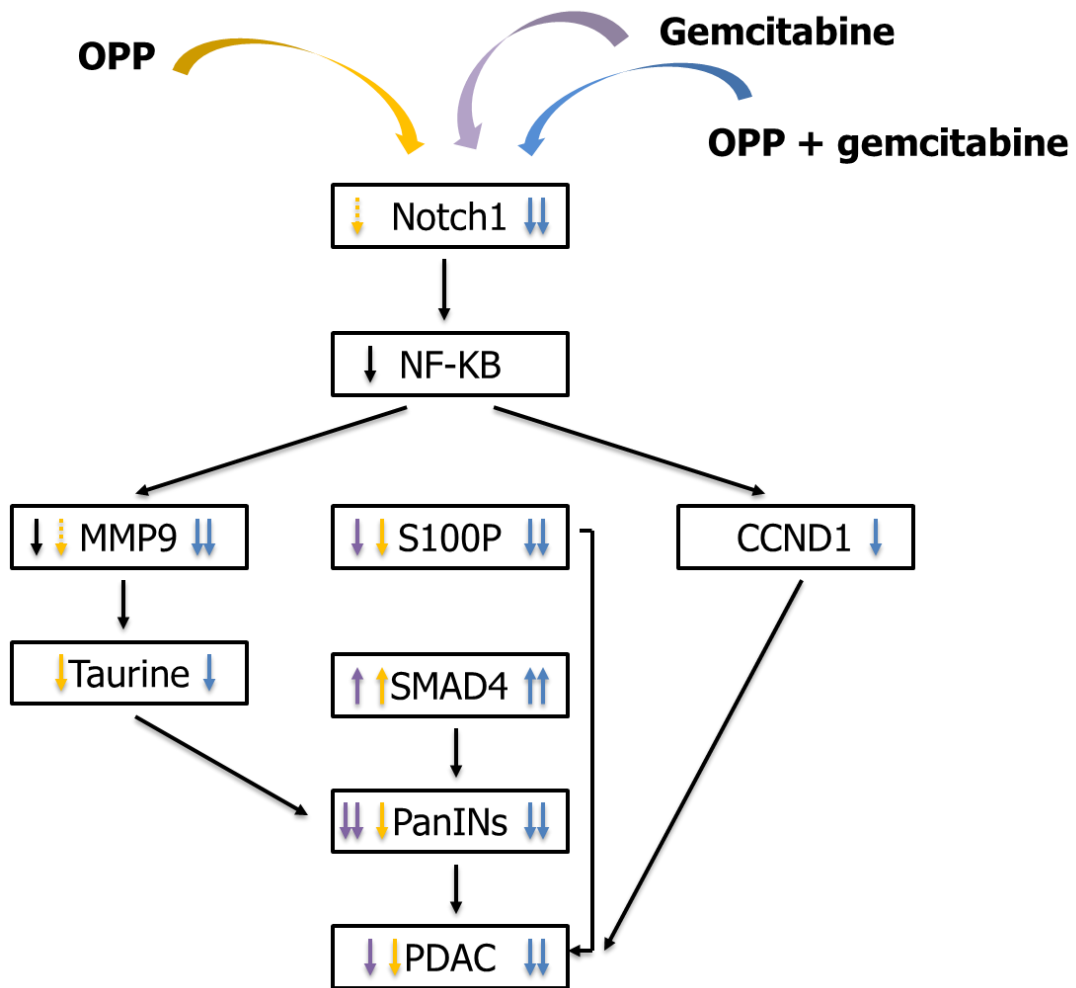


Fig. 40 Schematic diagram outlining the molecular targets and *in vivo* effect of OPP and OPP-gemcitabine combination in transgenic mouse model of PDAC. Black arrows are associated with our previous *in vitro* observations on OPP [48]. Yellow arrows are associated with *in vivo* regulations with OPP intervention alone, purple arrows are associated with gemcitabine treatment while blue arrows are associated with OPP-gemcitabine combination.

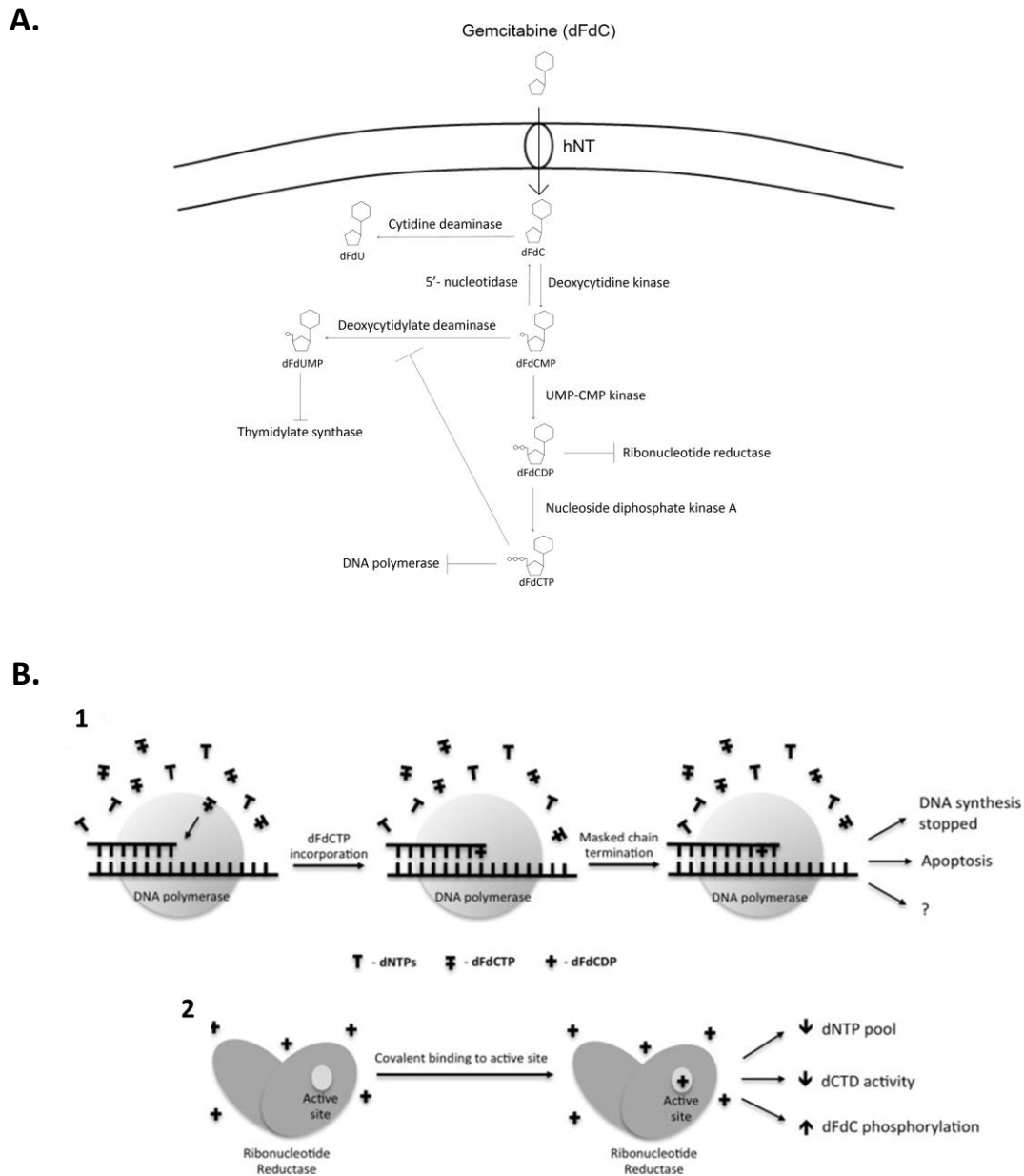


Fig. 41 Gemcitabine cellular metabolism (**A**) and main mechanisms of action (**B**)[50]. hNT: human nucleoside transporter; dFdCMP: gemcitabine monophosphate; dFdCDP: gemcitabine diphosphate; dFdCTP: gemcitabine triphosphate; dFdU: 2',2'-difluoro-2'-deoxyuridine, dFdUMP: 2',2'-difluoro-2'-deoxyuridine monophosphate; dNTP: nucleotide triphosphate.

REFERENCES

1. Data M. Cancer Statistics, 2016. 2016;66:7–30.
2. Hidalgo M. Pancreatic Cancer. *N. Engl. J. Med.* 2010;362:1605–17.
3. Seufferlein T, Bachet JB, Van cutsem E, Rougier P. Pancreatic adenocarcinoma: ESMO-ESDO clinical practice guidelines for diagnosis, treatment and follow-up. *Ann. Oncol.* 2012;23.
4. Vogelstein B, Kinzler KW. Cancer genes and the pathways they control. *Nat Med.* 2004;10:789–99.
5. Sakorafas GH, Tsiotou AG, Tsiotos GG. Molecular biology of pancreatic cancer; Oncogenes, tumour suppressor genes, growth factors, and their receptors from a clinical perspective. *Cancer Treat. Rev.* 2000. p. 29–52.
6. Bos JL. The ras gene family and human carcinogenesis. *Mutat. Res. Genet. Toxicol.* 1988;195:255–71.
7. Bos JL. ras Oncogenes in human cancer: A review. *Cancer Res.* 1989. p. 4682–9.
8. Hollstein M, Sidransky D, Vogelstein B, Harris CC. p53 mutations in human cancers. *Science* (80-.). 1991;253:49–53.
9. Jones S, Zhang X, Parsons DW, Lin JC-H, Leary RJ, Angenendt P, et al. Core Signaling Pathways in Human Pancreatic Cancers Revealed by Global Genomic Analyses. *Science* (80-.). 2008;321:1801–6.
10. Maitra A, Adsay NV, Argani P, Iacobuzio-Donahue C, De Marzo A, Cameron JL, et al. Multicomponent analysis of the pancreatic adenocarcinoma progression model using a pancreatic intraepithelial neoplasia tissue microarray. *Mod. Pathol.* 2003;16:902–12.
11. Lakshmikesari A, Radhakrishna R, Bhanumathi A, Ravi D, Srinivas G, Nair M, et al. Expression of epidermal and transforming growth factors in pancreatic cancer. *Oncol Rep.*

1996;3:963–6.

12. Friess H, Berberat P, Schilling M, Kunz J, Korc M, Buchler MW. Pancreatic cancer: the potential clinical relevance of alterations in growth factors and their receptors. *J Mol Med.* 1996;74:35–42.

13. Hruban RH, Adsay N V, Albores-Saavedra J, Compton C, Garrett ES, Goodman SN, et al. Pancreatic intraepithelial neoplasia: a new nomenclature and classification system for pancreatic duct lesions. *Am. J. Surg. Pathol.* 2001;25:579–86.

14. Bardeesy N, DePinho R a. Pancreatic cancer biology and genetics. *Nat. Rev. Cancer.* 2002;2:897–909.

15. Hruban RH, Maitra A, Goggins M. Update on pancreatic intraepithelial neoplasia. *Int. J. Clin. Exp. Pathol.* 2008;1:306–16.

16. Harsha HC, Kandasamy K, Ranganathan P, Rani S, Ramabadran S, Gollapudi S, et al. A compendium of potential biomarkers of pancreatic cancer. *PLoS Med.* 2009;6.

17. Ko a H, Hwang J, Venook a P, Abbruzzese JL, Bergsland EK, Tempero M a. Serum CA19-9 response as a surrogate for clinical outcome in patients receiving fixed-dose rate gemcitabine for advanced pancreatic cancer. *Br. J. Cancer.* 2005;93:195–9.

18. Ren YQ, Zhang HY, Su T, Wang XH, Zhang L. Clinical significance of serum survivin in patients with pancreatic ductal adenocarcinoma. *Eur Rev Med Pharmacol Sci.* 2014;18:3063–8.

19. Dong H, Qian D, Wang Y, Meng L, Chen D, Ji X, et al. Survivin expression and serum levels in pancreatic cancer. *World J. Surg. Oncol. World Journal of Surgical Oncology;* 2015;13:189.

20. Edge SB, Compton CC. The American Joint Committee on Cancer: the 7th edition of the AJCC cancer staging manual and the future of TNM. *Ann. Surg. Oncol.* 2010;17:1471–4.

21. Sun V. Update on pancreatic cancer treatment. *Nurse Pract.* 2010;35:16–23.
22. Hernandez YG, Lucas AL. MicroRNA in pancreatic ductal adenocarcinoma and its precursor lesions. *World J. Gastrointest. Oncol.* 2016;8:18–29.
23. Slidell MB, Chang DC, Cameron JL, Wolfgang C, Herman JM, Schulick RD, et al. Impact of total lymph node count and lymph node ratio on staging and survival after pancreatectomy for pancreatic adenocarcinoma: a large, population-based analysis. *Ann. Surg. Oncol.* 2008;15:165–74.
24. Neoptolemos JP, Stocken DD, Friess H, Bassi C, Dunn J a, Hickey H, et al. A randomized trial of chemoradiotherapy and chemotherapy after resection of pancreatic cancer. *N. Engl. J. Med.* 2004;350:1200–10.
25. Oettle H, Post S, Neuhaus P, Gellert K, Langrehr J, Ridwelski K, et al. Adjuvant chemotherapy with gemcitabine vs observation in patients undergoing curative-intent resection of pancreatic cancer: a randomized controlled trial. *JAMA. American Medical Association;* 2007;297:267–77.
26. Regine WF, Winter K a, Abrams R a, Safran H, Hoffman JP, Konski A, et al. Fluorouracil vs gemcitabine chemotherapy before and after fluorouracil-based chemoradiation following resection of pancreatic adenocarcinoma: a randomized controlled trial. *JAMA.* 2008;299:1019–2
27. Evans DB, Varadhachary GR, Crane CH, Sun CC, Lee JE, Pisters PWT, et al. Preoperative gemcitabine-based chemoradiation for patients with resectable adenocarcinoma of the pancreatic head. *J. Clin. Oncol.* 2008;26:3496–502.
28. Huguet F, André T, Hammel P, Artru P, Balosso J, Selle F, et al. Impact of chemoradiotherapy after disease control with chemotherapy in locally advanced pancreatic adenocarcinoma in GERCOR phase II and III studies. *J. Clin. Oncol.* 2007;25:326–31.

29. Sultana A, Smith CT, Cunningham D, Starling N, Neoptolemos JP, Ghaneh P. Meta-analyses of chemotherapy for locally advanced and metastatic pancreatic cancer. *J Clin Oncol.* 2007;25:2607–15.
30. Olive KP, Tuveson DA. The use of targeted mouse models for preclinical testing of novel cancer therapeutics. *Clin Cancer Res.* American Association for Cancer Research; 2006;12:5277–87.
31. Heinemann V, Boeck S, Hinke A, Labianca R, Louvet C. Meta-analysis of randomized trials: evaluation of benefit from gemcitabine-based combination chemotherapy applied in advanced pancreatic cancer. *BMC Cancer.* 2008;8:82.
32. Moore MJ, Goldstein D, Hamm J, Figer A, Hecht JR, Gallinger S, et al. Erlotinib plus gemcitabine compared with gemcitabine alone in patients with advanced pancreatic cancer: A phase III trial of the National Cancer Institute of Canada Clinical Trials Group. *J. Clin. Oncol.* 2007;25:1960–6.
33. Parasramka MA, Gupta SV. Synergistic effect of garcinol and curcumin on antiproliferative and apoptotic activity in pancreatic cancer cells. *J. Oncol.* 2012;2012.
34. Wang Y, Tsai ML, Chiou LY, Ho CT, Pan MH. Antitumor Activity of Garcinol in Human Prostate Cancer Cells and Xenograft Mice. *J. Agric. Food Chem.* 2015;63:9047–52.
35. Ip BC, Liu C, Ausman LM, Von Lintig J, Wang XD. Lycopene attenuated hepatic tumorigenesis via differential mechanisms depending on carotenoid cleavage enzyme in mice. *Cancer Prev. Res.* 2014;7:1219–27.
36. Bhatia N, Gupta P, Singh B, Koul A. Lycopene Enriched Tomato Extract Inhibits Hypoxia, Angiogenesis, and Metastatic Markers in early Stage N-Nitrosodiethylamine Induced Hepatocellular Carcinoma. *Nutr. Cancer.* 2015;5581:1–8.

37. Marques FZ, Markus MA, Morris BJ. Resveratrol: Cellular actions of a potent natural chemical that confers a diversity of health benefits. *Int. J. Biochem. Cell Biol.* 2009;41:2125–8.
38. Kim J, Shin D. Chemoprevention of Head and Neck Cancer with Green Tea Polyphenols. *Cancer Prev Res.* 2011;3:900–9.
39. Gu Y, Zhu C-F, Iwamoto H, Chen J-S. Genistein inhibits invasive potential of human hepatocellular carcinoma by altering cell cycle, apoptosis, and angiogenesis. *World J. Gastroenterol.* 2005;11:6512–7.
40. Gossner G, Choi M, Tan L, Fogoros S, Griffith KA, Kuenker M, et al. Genistein-induced apoptosis and autophagocytosis in ovarian cancer cells. *Gynecol. Oncol.* 2007;105:23–30.
41. Sambanthamurthi R, Tan YA, Sundram K. Treatment of vegetation liquors derived from oil-bearing fruit. 2008.
42. Sambandan, T G Rha CK, Sinskey AJ, Sambanthamurthi R, Tan YA, P Manikam KS, Wahid MB. Composition comprising caffeoylshikimic acids, protocatechuic acid, hydroxytyrosol, hydroxybenzoic acid and their derivatives and method of preparation thereof. 2012;
43. Sambanthamurthi R, Tan Y, Sundram K, Abeywardena M, Sambandan TG, Rha C, et al. Oil palm vegetation liquor: a new source of phenolic bioactives. *Br. J. Nutr.* 2011;106:1655–63.
44. Sambanthamurthi R, Tan Y, Sundram K, Hayes KC, Abeywardena M, Leow S-S, et al. Positive outcomes of oil palm phenolics on degenerative diseases in animal models. *Br. J. Nutr.* 2011;106:1664–75.
45. Sekaran SD, Leow S-S, Abobaker N, Tee KK, Sundram K, Sambanthamurthi R, et al. Effects of oil palm phenolics on tumor cells in vitro and in vivo. *African J. Food Sci.* 2010;4:495–502.
46. Leow S-S, Sekaran SD, Sundram K, Tan Y, Sambanthamurthi R. Differential transcriptomic profiles effected by oil palm phenolics indicate novel health outcomes. *BMC Genomics.*

2011;12:432.

47. Che Idris CA, Karupaiah T, Sundram K, Tan YA, Balasundram N, Leow S Sen, et al. Oil palm phenolics and vitamin E reduce atherosclerosis in rabbits. *J. Funct. Foods. Elsevier Ltd*; 2014;7:541–50.

48. Ji X, Usman A, Razalli NH. Oil Palm Phenolics (OPP) Inhibit Pancreatic Cancer Cell Proliferation via Suppression of NF- κ B Pathway. 2015;106:97–106.

49. Hingorani SR, Wang L, Multani AS, Combs C, Deramaudt TB, Hruban RH, et al. Trp53R172H and KrasG12D cooperate to promote chromosomal instability and widely metastatic pancreatic ductal adenocarcinoma in mice. *Cancer Cell*. 2005;7:469–83.

50. de Sousa Cavalcante L, Monteiro G. Gemcitabine: Metabolism and molecular mechanisms of action, sensitivity and chemoresistance in pancreatic cancer. *Eur. J. Pharmacol*. 2014;741:8–16.

51. Plunkett W, Grindey GB. Action of 2',2'-difluorodeoxycytidine on DNA Synthesis. *Cancer Res*. 1991;51:6110–7.

52. Gandhi V, Legha J, Chen F, Hertel LW, Plunkett W. Excision of 2',2'-difluorodeoxycytidine (gemcitabine) monophosphate residues from DNA. *Cancer Res*. 1996;56:4453–9.

53. Min YJ, Joo KR, Park NH, Yun TK, Nah YW, Nam CW, et al. Gemcitabine Therapy in Patients with Advanced Pancreatic Cancer. *Korean J. Intern. Med*. 2002;17:259–62.

54. Tendo M, Nakata B, Nishino H, Inoue M, Kosaka K, Amano R, et al. [Changes in tumor marker levels as a predictor of gemcitabine effect on patients with unresectable or recurrent pancreatic cancer]. *Gan To Kagaku Ryoho*. 2005;32:795–8.

55. Kobayashi N, Fujita K, Fujisawa T, Takahashi H, Fujisawa N, Yoneda M, et al. [Clinical features of long time survivors with unresectable pancreatic cancer treated by gemcitabine alone]. *Gan To Kagaku Ryoho*. 2006;33:207–12.

56. Feldmann G, Beaty R, Hruban RH, Maitra A. Molecular genetics of pancreatic intraepithelial neoplasia. *J. Hepatobiliary. Pancreat. Surg.* 2007;14:224–32.
57. Wang Z, Zhang Y, Li Y, Banerjee S, Liao J, Sarkar FH. Down-regulation of Notch-1 contributes to cell growth inhibition and apoptosis in pancreatic cancer cells. *Mol. Cancer Ther. Molecular Cancer Therapeutics*; 2006;5:483–93.
58. Kunnimalaiyaan S, Gamblin TC, Kunnimalaiyaan M. Glycogen synthase kinase-3 inhibitor AR-A014418 suppresses pancreatic cancer cell growth via inhibition of GSK-3-mediated Notch1 expression. *HPB. Blackwell Publishing Ltd*; 2015. p. 770–6.
59. Alao JP. The regulation of cyclin D1 degradation: roles in cancer development and the potential for therapeutic invention. *Mol. Cancer.* 2007;6:24.
60. Radulovich N, Pham N-A, Strumpf D, Leung L, Xie W, Jurisica I, et al. Differential roles of cyclin D1 and D3 in pancreatic ductal adenocarcinoma. *Mol. Cancer.* 2010;9:24.
61. Bachmann KAI, Neumann A, Hinsch A, Nentwich MF, Gammal ATEL, Vashist Y, et al. Cyclin D1 is a Strong Prognostic Factor for Survival in Pancreatic Cancer : Analysis of CD G870A Polymorphism , FISH and Immunohistochemistry Characteristics of the Patients and Survival. 2015;316–23.
62. Jiang H, Hu H, Tong X, Jiang Q, Zhu H, Zhang S. Calcium-binding protein S100P and cancer: Mechanisms and clinical relevance. *J. Cancer Res. Clin. Oncol.* 2012. p. 1–9.
63. Downen SE, Crnogorac-Jurcevic T, Gangeswaran R, Hansen M, Eloranta JJ, Bhakta V, et al. Expression of S100P and its novel binding partner S100PBPR in early pancreatic cancer. *Am. J. Pathol.* 2005;166:81–92.
64. Whiteman HJ, Weeks ME, Downen SE, Barry S, Timms JF, Lemoine NR, et al. The role of S100P in the invasion of pancreatic cancer cells is mediated through cytoskeletal changes and

regulation of cathepsin D. *Cancer Res.* 2007;67:8633–42.

65. Arumugam T, Simeone DM, Van Golen K, Logsdon CD. S100P promotes pancreatic cancer growth, survival, and invasion. *Clin. Cancer Res.* 2005;11:5356–64.

66. Shyu R-Y, Huang S-L, Jiang S-Y. Retinoic acid increases expression of the calcium-binding protein S100P in human gastric cancer cells. *J. Biomed. Sci.* 2003;10:313–9.

67. Averboukh L, Liang P, Kantoff PW, Pardee AB. Regulation of S100P expression by androgen. *Prostate.* 1996;29:350–5.

68. Beer DG, Kardia SLR, Huang C-C, Giordano TJ, Levin AM, Misek DE, et al. Gene-expression profiles predict survival of patients with lung adenocarcinoma. *Nat. Med.* 2002;8:816–24.

69. Hamada S, Satoh K, Hirota M, Kanno A, Ishida K, Umino J, et al. Calcium-binding protein S100P is a novel diagnostic marker of cholangiocarcinoma. *Cancer Sci.* 2011;102:150–6.

70. Dakhel S, Padilla L, Adan J, Masa M, Martinez JM, Roque L, et al. S100P antibody-mediated therapy as a new promising strategy for the treatment of pancreatic cancer. *Oncogenesis.* 2014;3:e92.

71. Gordon KJ, Blobel GC. Role of transforming growth factor- β superfamily signaling pathways in human disease. *Biochim. Biophys. Acta - Mol. Basis Dis.* 2008;1782:197–228.

72. Massagué J, Blain SW, Lo RS. TGF β signaling in growth control, cancer, and heritable disorders. *Cell.* 2000;103:295–309.

73. Biankin AV, Morey AL, Lee CS, Kench JG, Biankin SA, Hook HC, et al. DPC4/Smad4 expression and outcome in pancreatic ductal adenocarcinoma. *J. Clin. Oncol.* 2002;20:4531–42.

74. Javle M, Li Y, Tan D, Dong X, Chang P, Kar S, et al. Biomarkers of TGF- β signaling pathway and prognosis of pancreatic cancer. *PLoS One.* 2014;9:1–8.

75. Hua Z, Zhang YC, Hu XM, Jia ZG. Loss of DPC4 expression and its correlation with clinicopathological parameters in pancreatic carcinoma. *World J. Gastroenterol.* 2003;9:2764–7.
76. Yamada S, Fujii T, Shimoyama Y, Kanda M, Nakayama G, Sugimoto H, et al. SMAD4 expression predicts local spread and treatment failure in resected pancreatic cancer. *Pancreas.* 2015;44:660–4.
77. Shugang X, Hongfa Y, Jianpeng L, Xu Z, Jingqi F, Xiangxiang L, et al. Prognostic Value of SMAD4 in Pancreatic Cancer: A Meta-Analysis. *Transl. Oncol. The Authors;* 2016;9:1–7.
78. Fiehn O. Metabolomics - The link between genotypes and phenotypes. *Plant Mol. Biol.* 2002;48:155–71.
79. Spratlin JL, Serkova NJ, Eckhardt SG. Clinical applications of metabolomics in oncology: A review. *Clin. Cancer Res.* 2009. p. 431–40.
80. Tesiram Y a, Lerner M, Stewart C, Njoku C, Brackett DJ. Utility of nuclear magnetic resonance spectroscopy for pancreatic cancer studies. *Pancreas.* 2012;41:474–80.
81. Napoli C, Sperandio N, Lawlor RT, Scarpa A, Molinari H, Assfalg M. Urine metabolic signature of pancreatic ductal adenocarcinoma by H-1 nuclear magnetic resonance: Identification, mapping, and evolution. *J. Proteome Res.* 2012;11:1274–83.
82. Fang F, He X, Deng H, Chen Q, Lu J, Spraul M, et al. Discrimination of metabolic profiles of pancreatic cancer from chronic pancreatitis by high-resolution magic angle spinning 1H nuclear magnetic resonance and principal components analysis. *Cancer Sci.* 2007;98:1678–82.
83. Kaplan O, Kushnir T, Askenazy N, Knubovets T, Navon G. Role of nuclear magnetic resonance spectroscopy (MRS) in cancer diagnosis and treatment: 31P, 23Na, and 1H MRS studies of three models of pancreatic cancer. *Cancer Res.* 1997;57:1452–9.
84. OuYang D, Xu J, Huang H, Chen Z. Metabolomic Profiling of Serum from Human

Pancreatic Cancer Patients Using ^1H NMR Spectroscopy and Principal Component Analysis. *Appl. Biochem. Biotechnol.* 2011;1–7.

85. Urayama S, Zou W, Brooks K, Tolstikov V. Comprehensive mass spectrometry based metabolic profiling of blood plasma reveals potent discriminatory classifiers of pancreatic cancer. *Rapid Commun. Mass Spectrom.* 2010;24:613–20.

86. Sugimoto M, Wong DT, Hirayama A, Soga T, Tomita M. Capillary electrophoresis mass spectrometry-based saliva metabolomics identified oral, breast and pancreatic cancer-specific profiles. *Metabolomics.* 2010;6:78–95.

87. Bathe OF, Shaykhtudinov R, Kopciuk K, Weljie AM, McKay A, Sutherland FR, et al. Feasibility of identifying pancreatic cancer based on serum metabolomics. *Cancer Epidemiol. Biomarkers Prev.* 2011;20:140–7.

88. Nishiumi S, Shinohara M, Ikeda A, Yoshie T, Hatano N, Kakuyama S, et al. Serum metabolomics as a novel diagnostic approach for pancreatic cancer. *Metabolomics.* Springer US; 2010;6:518–28.

89. Underhill FP, Peterman FI, Jaleski TC, Leonard CS. Studies on the metabolism of tartrates. III. The behavior of tartrate in the human body. *J. Pharmacol. Exp. Ther.* 1931;381–98.

90. Chadwick V, Vince A, Killingley M, Wrong O. The metabolism of tartrate in man and the rat. *Clin Sci Mol Med.* 1978;54:273–81.

91. Petrarulo M, Marangella M, Blanco O, Linari F. Ion-chromatographic determination of L-tartrate in urine samples. *Clin. Chem.* 1991;37:90–3.

92. He X-H, Li W-T, Gu Y-J, Yang B-F, Deng H-W, Yu Y-H, et al. Metabonomic studies of pancreatic cancer response to radiotherapy in a mouse xenograft model using magnetic resonance spectroscopy and principal components analysis. *World J. Gastroenterol.*

2013;19:4200–8.

93. Huang P, Chubb S, Hertel LW, Grindey GB, Plunkett W. Action of 2',2'-difluorodeoxycytidine on DNA synthesis. *Cancer Res.* 1991;51:6110–7.

94. Hill R, Rabb M, Madureira PA, Clements D, Gujar SA, Waisman DM, et al. Gemcitabine-mediated tumour regression and p53-dependent gene expression: implications for colon and pancreatic cancer therapy. *Cell Death Dis.* Nature Publishing Group; 2013;4:e791.

95. Shen Z, Wu X, Wang L, Li B, Zhu X. Effects of gemcitabine on radiosensitization, apoptosis, and Bcl-2 and Bax protein expression in human pancreatic cancer xenografts in nude mice. *funpecrp.com.br Genet. Mol. Res. Mol. Res.* 2015;14:15587–96.

ABSTRACT**THE EFFECT OF OIL PALM PHENOLICS (OPP) ON PANCREATIC DUCTAL ADENOCARCINOMA (PDAC) IN TRANSGENIC MOUSE MODEL**

by

NURUL HUDA RAZALLI**May 2017****Advisor:** Dr. Smiti Gupta**Major:** Nutrition and Food Science**Degree:** Doctor of Philosophy

Pancreatic ductal adenocarcinoma (PDAC) is an extremely aggressive form of pancreatic cancer with low survival rates partly due to late diagnosis and poor treatment outcomes. The use of chemotherapy drug, gemcitabine alone often provides minimal benefits. This study explored the *in vivo* effect of oil palm phenolics (OPP), a water-soluble extract from oil palm in transgenic mouse model of PDAC and its combination with gemcitabine. Administration of 5% dietary OPP was found to be non-toxic in non-PDAC controls. Compared to single agent therapy with either OPP or gemcitabine, OPP-gemcitabine combination showed a superior benefit with profound synergistic effect both as chemotherapeutic and chemopreventive agent evident in halted tumor and cyst growth, as well as lowered high grade precursor lesion count. Favorable regulation of several tumorigenesis markers through immunohistochemistry (S100P and SMAD4) and real-time PCR (Notch1, MMP9 and CCND1) that was partially displayed by OPP but was more significant with the combinatorial therapy has provided an insight on the molecular targets responsible for the anticancer effect of OPP and OPP-gemcitabine combination. Using multivariate analysis software, SIMCA-P+, discrimination in urinary ¹H NMR metabolomic profiles between groups was revealed. Metabolite profiling has identified decreased levels of

alanine, creatinine, succinate and taurine following intervention with OPP and its combination with gemcitabine. Metabolomic profiles were shown to be strongly correlated with Notch1 and MMP9 expression, also with total precursor lesion count following regression analyses. Finally, pathway analyses by MetaboAnalyst software, based on the information from regression analyses revealed that taurine, which involved in taurine and hypotaurine metabolism plays a major role in the anticancer effect exhibited by both interventions of OPP alone and OPP-gemcitabine combination. Collectively, OPP as a single agent exhibited a milder therapeutic effect than the use of OPP in combination with gemcitabine which displayed superior advantage. This demonstrates the potential benefit of dietary OPP as part of combinatorial therapy against progression of PDAC.

AUTOBIOGRAPHICAL STATEMENT

NURUL HUDA RAZALLI

EDUCATION:

B.S in Dietetics, Universiti Kebangsaan Malaysia, Kuala Lumpur (2009)
M.S in Nutrition and Food Science, Wayne State University, Detroit (2013)
Post-bachelor certificate in Dietetics, Wayne State University, Detroit (2014)

PROFESSIONAL APPOINTMENTS:

Dietitian, BESTA Food Services Sdn. Bhd., Malaysia (2009)
Research Assistant, Universiti Kebangsaan Malaysia, Kuala Lumpur (2009)
Tutor, Universiti Kebangsaan Malaysia, Kuala Lumpur (2010)
Lecturer, Universiti Kebangsaan Malaysia, Kuala Lumpur (2014 – present)

PROFESSIONAL AWARDS:

The Higher Education Public Institution Training Scheme (SLAI) Scholarship, Ministry of Higher Education, Malaysia (2011)

PROFESSIONAL ASSOCIATIONS:

United States Registered Dietitian (RD), (2014 – present)
The Academy of Nutrition and Dietetics (AND)
Southeastern Michigan Dietetic Association (SEMDA)
American Society for Nutrition (ASN)
Malaysian Dietitian Association (MDA)
Malaysian Association for the Study of Obesity (MASO)

PUBLICATIONS AND PRESENTATIONS:

1. **Razalli, N. H.**, Gowthaman, P., Saadat, N., Vemuri, S., Goja, A., Sambanthamurthi, R., & Gupta, S. V. (2016). The effect of Oil Palm Phenolics (OPP) on Pancreatic Ductal Adenocarcinoma (PDAC) in transgenic mouse model. *FASEB J.* 30,147.2
2. Ji, X., Usman, A., **Razalli, N. H.**, Sambanthamurthi, R., & Gupta, S. V. (2015). Oil palm phenolics (OPP) inhibit pancreatic cancer cell proliferation via suppression of NF-κB pathway. *Anticancer research*, 35(1), 97-106.
3. Abdul Manaf, Z., Kassim, N., Hamzaid, N. H., & **Razali, N. H.** (2013). Delivery of enteral nutrition for critically ill children. *Nutrition & Dietetics*, 70(2), 120-125.